Master's thesis

NTNU
Norwegian University of Science and Technology
Faculty of Natural Sciences
Department of Chemistry

Jostein Lund

Preparation of Novel N-Heterocyclic Carbene Au(III)-complexes

Master's thesis in MTKJ

Supervisor: Anne Fiksdahl

June 2020

NTNU
Kunnskap for en bedre verden

Jostein Lund

Preparation of Novel N-Heterocyclic Carbene Au(III)-complexes

Master's thesis in MTKJ
Supervisor: Anne Fiksdahl
June 2020

Norwegian University of Science and Technology
Faculty of Natural Sciences
Department of Chemistry

NTNU
Norwegian University of
Science and Technology

Preface

I would like to extend my gratitude to my supervisor, Anne Fiksdahl, for giving me the opportunity to work within this new and exiting field as a part of such a welcoming and dedicated group. Furhtermore I want to thank my co-supervisor, Helgi Freyr Jonsson, for invaluable advice and guidance this last year. I am impressed by the patience he has displayed in the face of my continuous stream of questions. A big thanks also goes to Melanie Siah, Ann-Christin Reiersølmoen, and Thomas Solvi, for good company during my hours spent in the lab, and for every piece of advice they have offered along the way. I am also grateful for the support provided by the staff at NTNU. Including Susanna V. Gonzales and Julie Asmussen for MS assistance, Tournn M. Mælø for help with NMR, and Roger Aarvik for providing crucial chemicals.
Finally i would like to thank my fellow students at Demokrit, for their good company by the coffee-maker during the late nights spent working towards the end of this project.

> ***It is better not to attempt the art of alchemy at all than to practise it casually.***
>
> -Splendor Solis, 16th century alchemical manuscript.[1]

Jostein Lund
Trondheim, June, 2020

Summary

In this project, two unique imidazolium N-benzyl, N-methylene-(C_4-substitued)-oxazoline imidazolium NHC precursors **7a** (*i*Pr-C_4) and **7b** (*t*Bu-C_4) NHC precursors have been prepared in three steps.

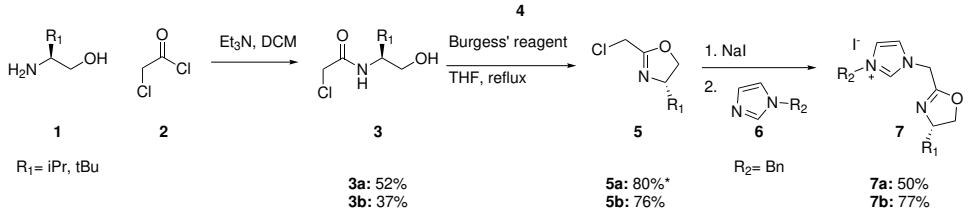

Synthetic route leading to the NHC precursor imidazolium salts **7a,b**.

A condensation of the chiral amino alcohols **1a,b** with 2-chloroacetyl chloride (**2**) yielded the corresponding chiral amides **3a,b**. The amides **3a,b** were then subjected to an intramolecular dehydration facilitated by Burgess' reagent, and produced the chloromethyl oxazolines **5a,b**. The oxazolines **5a,b** underwent a halogen exchange to their iodized counterparts, utilizing the Finkelstein protocol, before final N-alkylation with 1-benzyl imidazole **6** to afford the imidazolium salts **7a,b** (50%, 77%), with an overall yield of 21 and 22% for imidazolium salt **7a** and **7b** respectively.

The imidazolium salts (**7a,b**) were coordinated to a gold(I) atom centre by transmetallation from a silver intermediate, which yielded the novel Au(I)NHC-complexes **8a** (69%) and **8b** (18%).

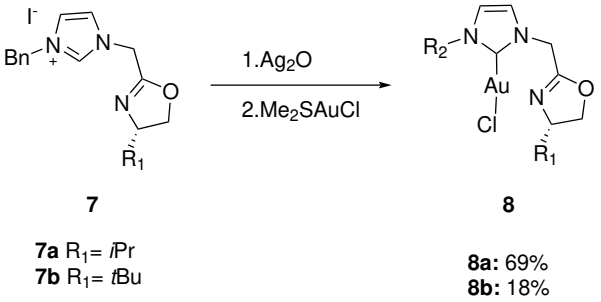

A summary of the coordination of imidazolium salts ***7a,b*** *to gold, yielding the Au(I)-complexes* **8a,b**

The large difference in obtained yields of the Au(I)NHC-complexes **8a,b** suggests that the preparation of the Au(I)-complex **8b** is obstructed by a more sterically hindered ligand (*t*Bu) than the Au(I)-complex **8a** (*i*Pr).

The novel Au(I)NHC-complexes (**8a,b** were oxidised to their corresponding Au(III)NHC[Cl_3]-complexes **10a,b** by dichloro-iodobenzene and subsequent anion exchange to give the bidentate C,N-Au(III)NHC[oxazoline] complexes **11a,b**.

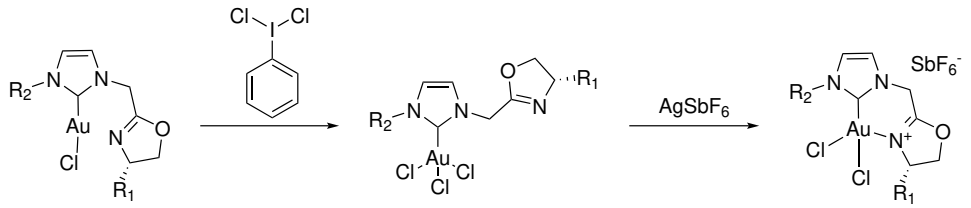

8 **10** **11**

Preparation of the Au(III)NHC[Cl_3]-complexes ***10a,b*** *and the bidentate C,N-Au(III)NHC[oxazoline] complexes* **11a,b**

While neither of the four Au(III)-complexes were isolated nor fully characterised, their crude reaction mixtures were analysed by ^{1}H-NMR and ^{1}H,^{15}N-HMBC . The changes in δ^{15}N-shifts ($\Delta\delta N^{ox}$, $\Delta\delta N^{AE}$) for the nitrogens atoms by oxidation and anion exchange coordination strongly indicate the formation of the Au(III)NHC[Cl_3]complexes **10a,b** and the bidentate C,N-Au(III)NHC[Oxazoline] complex **11a**.

Sammendrag

I dette prosjektet har to unike imidazolium N-benzyl, N-metylene - (C_4-substituerte) -oxazoline imidazolium NHC-forløpere **7a** (*i*Pr-C_4) og **7b** (*t*BuC4) utarbeidet i tre trinn.

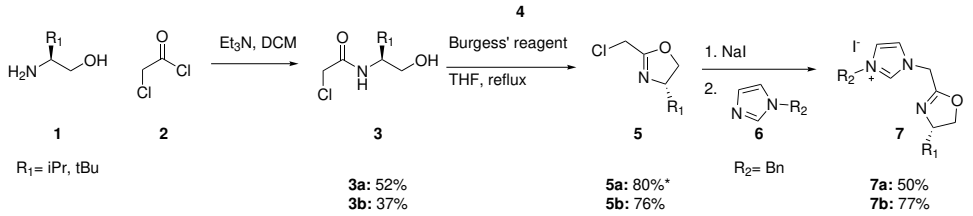

Syntese veien til NHC imidazolium saltene 7a,b.

En kondensasjon av de chirale amino alkoholene **1a, b** med 2-kloroacetylklorid (**2**) ga de tilsvarende chirale amidene **3a, b**. Amidene **3a, b** ble deretter utsatt for en intramolekylær dehydrering i nærvær av Burgess 'reagens, og produserte klormetyloxsazolinene **5a, b**. Oxazolinene **5a, b** gjennomgikk en halogenutveksling til sine joderte motparter, ved Finkelstein-protokollen, før den endelige N-alkyleringen med 1-benzylimidazol **6** ga imidazoliumsaltene **7a, b** (50 %, 77 %), med et samlet utbytte på henholdsvis 21 og 22 % for imidazolium salt **7a** og **7b**.

Imidazolium-saltene (**7a, b**) ble koordinert til et gullsenter (I) ved transmetallering fra et sølvintermediat, som ga de nye Au (I) NHC-kompleksene **8a** (69 %) og **8b** (18 %).

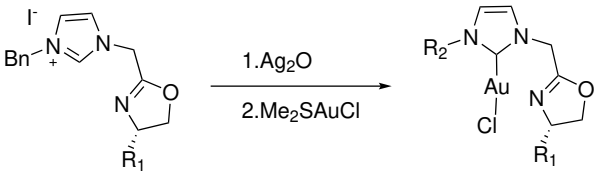

Koordinasjon av imidazoliumsaltene ***7a, b*** *til gull, for å framstille Au(I)-kompleksene* **8a, b**

Variasjonen i oppnådde utbytter av Au(I)NHC-kompleksene **8a, b** antyder at fremstillingen av Au I)-komplekset **8b** er heftet av en mer sterisk hindret ligand (*t*Bu) enn Au (I)-komplekset **8a** (*i*Pr).

De nye Au (I) NHC-kompleksene (**8a, b** ble oksidert til deres tilsvarende Au (III)NHC[Cl_3] - komplekser **10a, b** med diklor-jodbenzen og et påfølgende anion-bytte for å gi bidentate C, N- Au(III)NHC[oxazoline]-kompleksene **11a, b**.

Mens ingen av de fire Au(III)-kompleksene ble isolert eller fullstendig karakterisert, ble deres urensede reaksjonsblandinger analysert med ^{1}H-NMR og ^{1}H,^{15}N-HMBC . Endringene i δ^{15}N- skift ($\Delta\delta N^{ox}$, $\Delta\delta N^{AE}$) for nitrogenatomene ved oksidasjon og anionebyttekoordinasjon indikerer sterkt dannelsen av Au (III) NHC [Cl_3]-kompleksene **10a, b** og bidentatet C, N-Au(III)NHC[Oxazoline] complex **11a**.

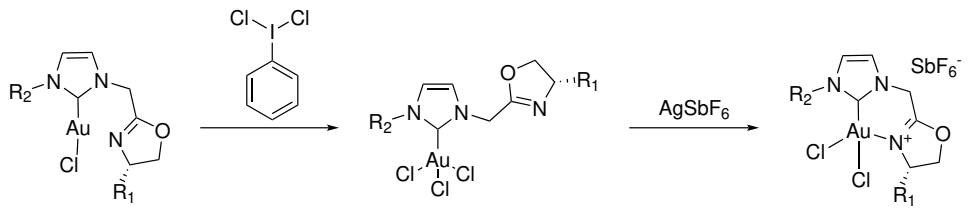

8 **10** **11**

Framstilling av Au(III)NHC[Cl_3]-komplekser ***10a, b*** *og bidentate C, N-Au(III)NHC[oxazoline]-komplekser* **11a, b**

List of Numbered Compounds

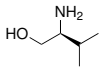

1a

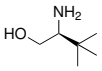

1b

2

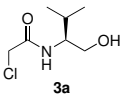

3a

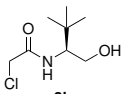

3b

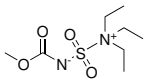

4

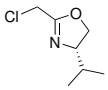

5a

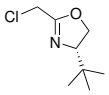

5b

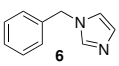

6

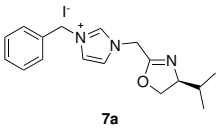

7a

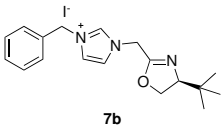

7b

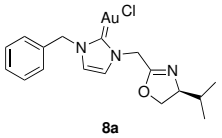

8a

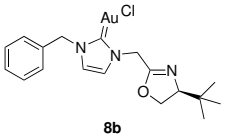

8b

9

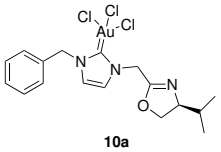

10a

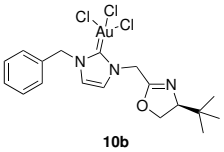

10b

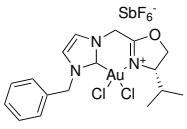

11a

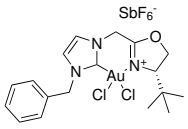

11b

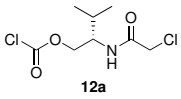

12a

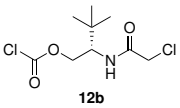

12b

13a

13b

Contents

1 Introduction **1**
1.1 Outline . . . 2

2 Theory **2**
2.1 On the Stability of Gold . . . 2
2.2 Gold Catalysis . . . 3
2.3 Heterogeneous catalysis . . . 3
2.4 Homogeneous catalysis . . . 5
2.4.1 Gold salts (AuX/AuX_3) . . . 6
2.4.2 Gold(I) . . . 6
2.4.3 Dual-gold . . . 7
2.4.4 Gold(III) . . . 8
2.5 Enantioselective Gold Catalysis . . . 9
2.5.1 Au(I) Strategies . . . 9
2.5.2 Au(III) Strategies . . . 9
2.6 N-Heterocyclic Carbenes . . . 10
2.7 Oxazolines as Ligands . . . 12
2.8 Synthesis of Imidazolium Salt Based NHC Precursors . . . 13
2.8.1 Amidation of an acyl chloride . . . 13
2.8.2 Cyclodehydration of Hydroxy Amides . . . 14
2.8.3 Burgess Reagent . . . 14
2.8.4 Finkelstein reaction . . . 15
2.9 Coordination of NHC precursor to Au . . . 15
2.10 Oxidation of Au(I) complexes . . . 16

3 Results and Discussion **17**
3.1 Synthesis of Imidazolium Salt Based NHC Precursors . . . 17
3.1.1 Motivation . . . 17
3.1.2 Synthesis of 1-Benzyl-3-Oxazolineimidazoles. . . . 17
3.1.3 Synthesis of Chiral Amides . . . 18
3.1.4 Condensation Complications . . . 20
3.1.5 The Oxazoline Obstacle . . . 21
3.1.6 Synthesis of Oxazolines . . . 22
3.1.7 Imdiazolium Salt Synthesis . . . 25
3.2 Synthesis of AuNHC-Complexes . . . 26
3.2.1 Synthesis of Au(I)NHC-Complexes . . . 26
3.2.2 Synthesis of Au(III)NHC-complexes from Au(I)NHC-complexes . . . 29
3.2.3 Coordination Effects on Nitrogen . . . 30

4 Conclusion **36**

5 Experimental **37**
5.1 Synthesis of Amides . . . 37
5.1.1 General procedure A . . . 37
5.2 Synthesis of Oxazolines . . . 38
5.2.1 General procedure B . . . 38
5.2.2 (R)-2-(Chloromethyl)-4-isopropyl-4,5-dihydrooxazole (**5a**) . . . 38

5.2.3 (R)-4-(*tert*-Butyl)-2-(chloromethyl)-4,5-dihydrooxazole (**5b**) . . . 38
5.3 Synthesis of Iodized Oxazolines . . . 39
5.4 Synthesis of Imidazolium Salts . . . 39
5.4.1 General procedure C . . . 39
5.4.2 (R)-1-Benzyl-3-((4-isopropyl-4,5-dihydrooxazol-2-yl)methyl)-1H-imidazol-3-ium iodide (**7a**) . . . 39
5.4.3 (R)-1-Benzyl-3-((4-(tert-butyl)-4,5-dihydrooxazol-2-yl)methyl)-1H-imidazol-3-ium iodide (**7b**) . . . 40
5.5 Synthesis of Au(I)-NHC complexes . . . 40
5.5.1 General Procedure D . . . 40
5.5.2 (1-Benzyl-3-(((S)-4-isopropyl-4,5-dihydrooxazol-2-yl)methyl)-2,3-dihydro-1H-imidazol-2-yl)gold(I) chloride (**8a**) . . . 40
5.5.3 (1-Benzyl-3-(((S)-4-(tert-butyl)-4,5-dihydrooxazol-2-yl)methyl)-2,3-dihydro-1H-imidazol-2-yl)gold(I) chloride (**8b**) . . . 41
5.6 Synthesis of Au(III)NHC[Cl_3] complexes . . . 41
5.6.1 General Procedure E . . . 41
5.6.2 (S)-(1-Benzyl-3-((4-isopropyl-4,5-dihydrooxazol-2-yl)methyl)-1,3-dihydro-2H-imidazol-2-ylidene)gold(III) chloride (**10a**) . . . 42
5.6.3 (S)-(1-Benzyl-3-((4-(tert-butyl)-4,5-dihydrooxazol-2-yl)methyl)-1,3-dihydro-2H-imidazol-2-ylidene)gold(III) chloride (**10b**) . . . 42
5.7 Synthesis of Bidentate C,N-Au(III)NHC[Oxazoline] complexes . . . 42
5.7.1 (S)-(1-Benzyl-3-((4-isopropyl-4,5-dihydrooxazol-2-yl)methyl)-1,3-dihydro-2H-imidazol-2-ylidene) bidentate C,N-gold(III) dichloride-antimony hexafluoride (**11a**) . . . 42
5.7.2 (S)-(1-Benzyl-3-((4-(tert-butyl)-4,5-dihydrooxazol-2-yl)methyl)-1,3-dihydro-2H-imidazol-2-ylidene) bidentate C,N-gold(III) dichloride-antimony hexafluoride (**11b**) . . . 43

A Spectra of Amides 3a, 3b **52**

B Spectra of Oxazolines 5a, 5b **66**

C Spectra of Imidazollium salts 7a, 7b **80**

D SPectra of Au(I)-complexes 8a, 8b **94**

E Spectra of Au(III)[C_3]-complexes 10a, 10b **110**

F Spectra of Bidentate C,N-Au(III)NHC[Cl_3 complexes 11a, 11b **114**

1 Introduction

Few other metals have had the same impact on human history as gold. This soft, yellow, gleaming bit of rock has been valued by humanity on all continents for thousands of years for its appearance and rarity. In early history, gold occupied a spiritual position. Findings in Egypt and western Africa have linked the spiritual value of gold to its imitation of the sun, a highly worshipped deity in ancient times.[2,3]
It has also made appearances in the earliest stories of the monotheistic religions, as Moses descended mount Sinai and found his followers worshipping a calf made of gold.

Throughout history, gold has shared this spiritual position with its monetary and scientific value. This monetary value which drove the conquistadors to south America[4] and fueled a slave trade along the western shore of Africa for use in the mines owned by the Asante king.[5] While the European and African kings traded slaves and fared wars to fill their treasure chambers, Arabic alchemists attempted the much more difficult, and much less successful, transmutation. While the scientific reputation of alchemy is dubious at best, it is the origin of modern chemistry, pharmacology, and medicine. With its name rooting back to the Egyptian word "khem" which constitutes the primordial soup in which the god Ra was created,[6] alchemists have always sought the knowledge necessary to create divinity from nothing. To the alchemist this divinity was, of course, gold the purest and most perfect of all matter.[3] The alchemical symbol of gold is the circumpunct. A simple, yet significant symbol, representing god in Christianity and earlier a symbol for the sun, which rose from the khem in Egyptian mythology.[6]

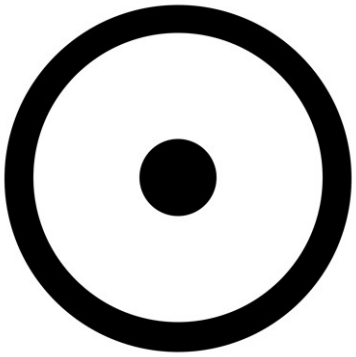

Figure 1.1: The circumpunct is represented by a circled dot, which can represent a multitude of things. One of which is gold.

In modern times, gold is still highly priced for its monetary value, and is highly used in jewelries, but it has also found extraordinary use in the production of electronics due to its excellent conductive properties.[7] While the chemical interest for gold slightly faded after the decline of alchemy in the 19th century, it has experienced a surge in interest the last 40 years. While no credible scientist is publishing articles on the miracles of transmutation, gold is now researched for its ability to "transmute" other compounds, in the modern science of catalysis.

1.1 Outline

The goal of this project was to synthesise and charactherise a range of bidentate C,N-Au(III)NHC[Oxazoline]-complexes (fig. 1.2), and all intermediate products.

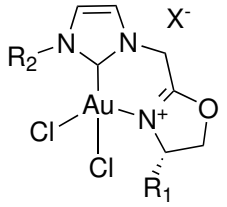

Figure 1.2: The target compounds of this project.

In addition to the synthetic route leading to these complexes, the theory surrounding gold catalysis and N-heterocyclic carbene ligands will be presented, along with a brief overview of the theory necessary for preparing both the NHC-ligands, gold(I),- and gold(III)-complexes, and all related intermediates.

2 Theory

Elemental gold (Au^0) is remarkably resistant to both air and moisture and is virtually immune to oxidation. Only by the use of a mixture of hydrochloric,- and nitric acid, or by oxidation in the presence of cyanide is it oxidised and dissolved. These properties combined with the ability to catalyse a wide variety of reactions will be presented and discussed further in the following section.

2.1 On the Stability of Gold

Gold will only dissolve in oxidising solutions containing certain species that can stabilise the cationic gold atoms. In aqua regia, the nitric acid (HNO_3) is the oxidising species, and hydrochloric acid (HCl) contributes the Cl^- counterion which donates electrons to stabilise the positively charged ion.[8] Resulting in eq. (2.1)

$$\mathrm{Au\,(s) + 4\,Cl^- + NO_3{}^- + 4\,H_3O^+ \longleftrightarrow AuCl_4{}^- + NO\,(g) + 6\,H_2O} \tag{2.1}$$

While the use of aqua regia might be the most famous way of dissolving gold, it is not the only method available. The MacArthur-Forrest process utilises cyanide to dissolve and stabilise gold complexes in the presence of oxygen as represented by the Elsner equation[9] eq. (2.2). This method was developed for the mining industry, and is still used to extract gold from low grade ores.

$$\mathrm{2\,Au + 4\,KCN + \frac{1}{2}\,O_2 + H_2O \longleftrightarrow 2\,AuK(CN)_2 + 2\,KOH} \tag{2.2}$$

Depending on the complexing ligand, the oxidation state may vary, due to the different stability constants. Electron donors like cyanide are what is called soft electron donors, and prefer the Au(I) oxidation state. Other donors like chlorine and other halides prefer the Au(III) state.

Despite the stability of these complexes, they are however susceptible to reduction in the presence of a more preferred reaction. This is again exemplified by the MacArthur-Forrest process, as the recovery of the gold from solution is done by the addition of zinc powder.[10] This method works due to the electrochemical reaction that occurs between zinc (Zn) and the gold-cyano complex ($Au(CN)_2^-$) as shown in eq. (2.3). The reaction has a positive electron potential, but a negative free Gibbs energy, which results in the spontaneous precipitation of Au^0.[9]

$$2\,Au(CN)_2^- + Zn \longleftrightarrow 2\,Au + Zn(CN)_4^{2-}\,[9] \tag{2.3}$$

The required reduction agent is depending on the stability of the gold complex, a more stable complex requires a stronger reduction agent than an unstable one. In the field of homogeneous gold catalysis, an important considertation for the choice of ligand is its ability to form stable complexes that are highly resistant to reduction.

2.2 Gold Catalysis

The long lasting belief that gold was completely inert[11] led to it being used as the inner layer of various reactors designed to prevent unwanted catalysis of reactions. This led to a surprising result when Meyer and Meijere (1976) decided to study the thermal [2+2+2]-cycloreversion of diademane to triquinacene, but instead, they observed a 50% conversion to snoutene scheme 1. The latter reaction was found to be catalysed by both the walls of the gold reactor and gold(I)-dicyclopentadiene-chloride ($Au(C_{10}H_{12})Cl$) complexes.[12] Since then gold catalysis as a field has exploded, and numerous new applications have been discovered within both homogeneous and heterogeneous catalysis.

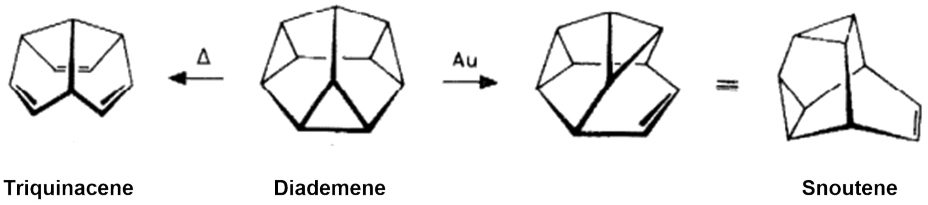

Scheme 1: Reaction scheme for the expected thermal cycloreversion to triquinacene(left) alongside the gold catalysed conversion to snoutene (right)

2.3 Heterogeneous catalysis

The field of heterogeneous gold catalysis gained substantial traction in the mid 80s after two simultaneous and independent discoveries were made by Haruta and Hutchings. They discovered that gold had exceptional abilities to catalyse both the oxidation of CO at low temperatures[13] and the hydrochlorination of acetylene.[14]
Since this discovery, publications on heterogeneous gold catalysis saw an exponential increase and several new applications and transformations have been discovered[15]. Due to its ability to oxidise CO, it was a natural step to study its possible applications in the water-gas shift.[16] These studies revealed that Au/α-Fe_2O_3 had a much greater catalytic ability than the most active catalyst already in use[17]. The ability to oxidise CO at low temperatures also has applications outside the industrial perspective. There are

potentials for it to be used in respirators[15] and hydrogen fuel cells,[18] as a gold catalyst is active in much lower temperature ranges compared to catalysts such as Pt, Pd, and Rh. Gold based catalysis is also much more active than copper oxides which exhibit catalytic activity at the same temperatures.[15]

Despite being a huge field of research and even having commercialised applications, there has been an intense discussion amongst scientist regarding the active sites of the catalyst. In 2004, Lopez *et al.* observed that an increased concentration of low-coordinated Au atoms lowered the O and CO adsorption energies.[19] Lower adsorption energies correlates closely to lower activation barriers for surface reactions[20] and thus it can be concluded that the availability of low coordinated gold atoms contributes to the catalytic ability of gold. Such an increased availability is achieved by a reduced particle size of gold.

In 2008 Coquet*et. al*[21] published a review in which the gold catalysed oxidation of CO was compared to theoretical calculations in an attempt to explain the mechanism behind it.[21] The review elaborates upon the conclusion made by Lopez *et al.*[19], considering the added effects of the support structure and its electronic effects. While CO is adsorbed at low-coordinated Au-atoms in Au_{n0} and Au_{n+} particles, the adsorption of O_2 requires a negative charge. This is where the support structure becomes relevant. A reducible support structure creates a negatively charged cluster upon the adsorption of Au. These anionic clusters facilitate the adsorption of molecular O_2, but because the charge is localised, the top of the Au-particle maintains a neutral charge, which allows for the adsorption of CO.
This explanation does however leave out the effects of cationic species which is often observed in experimental data. There is suggested that the formation of gold oxides that are stable at the reaction conditions may provide a cationic species which will impact the oxidation, but such a theory is still in need of further study. Other models also assume dissociative adsorption of oxygen[22], or O_2 adsorption at oxide lattice defects.[23] The various mechanisms theorised by the review is summarised in fig. 2.1.

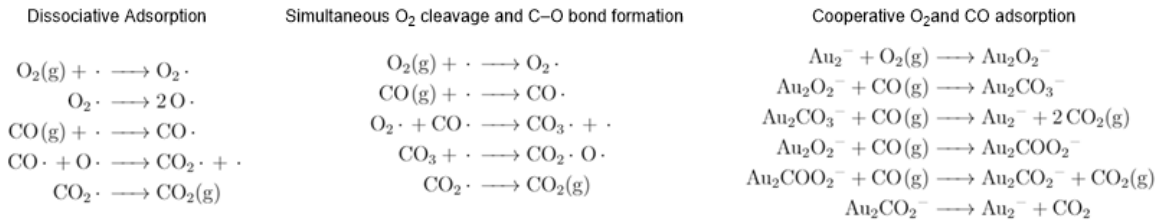

$$O_2(g) + \cdot \longrightarrow O_2\cdot$$
$$O_2\cdot \longrightarrow 2\,O\cdot$$
$$CO(g) + \cdot \longrightarrow CO\cdot$$
$$CO\cdot + O\cdot \longrightarrow CO_2\cdot + \cdot$$
$$CO_2\cdot \longrightarrow CO_2(g)$$

$$O_2(g) + \cdot \longrightarrow O_2\cdot$$
$$CO(g) + \cdot \longrightarrow CO\cdot$$
$$O_2\cdot + CO\cdot \longrightarrow CO_3\cdot + \cdot$$
$$CO_3 + \cdot \longrightarrow CO_2\cdot O\cdot$$
$$CO_2\cdot \longrightarrow CO_2(g)$$

$$Au_2^- + O_2(g) \longrightarrow Au_2O_2^-$$
$$Au_2O_2^- + CO(g) \longrightarrow Au_2CO_3^-$$
$$Au_2CO_3^- + CO(g) \longrightarrow Au_2^- + 2\,CO_2(g)$$
$$Au_2O_2^- + CO(g) \longrightarrow Au_2COO_2^-$$
$$Au_2COO_2^- + CO(g) \longrightarrow Au_2CO_2^- + CO_2(g)$$
$$Au_2CO_2^- \longrightarrow Au_2^- + CO_2$$

Figure 2.1: The three different mechanisms for CO oxidation investigated by Coquet *et al.* For the first two mechanisms $\cdot$ indicates a single Au-particle site.

As per 2012, there has yet to be published a definitive study concerning the active sites for the catalytic reactions of gold nano-particles (NPs), despite an abundance of attention from a multitude of surface scientists.[24] Instead, the takeaway from all the studies performed is that the catalysts needs to be custom made for their intended reaction. This reaffirms Harutas point from his lecture the previous year, where he presents the concept of a hierarchy of activity for gold species.[25] In 2018, Hutchings published an article in

where the activity of gold species were compared for both the oxidation of CO and the hydrochlorination of acetylenes.[26] While the active species for the hydrochlorination of acetylenes is the highly dispersed Au(I) cations, the CO oxidation is catalysed by a hierarchy of active species, among which small clusters contribute the most when performed on an iron oxide support.

2.4 Homogeneous catalysis

Gold complexes used in homogeneous catalysis have shown to be remarkably strong, yet air,- and moisture resistant carbophilic Lewis acids.[27] Au(I) and Au(III) complexes' ability to activate π-bonds presents an attractive option to synthetic chemists, as these bonds previously have been approached using Hg(II) and Ti(III)[27]. While the first reported experiments on homogeneous gold catalysis appeared as early as 1935, where $AuCl_3$ was found to catalyse the chlorination of naphthalene[28] the real start of the gold rush in organic chemistry[29] began in 1986 with the discovery of a chiral gold(I) complexes' ability to catalyse the asymmetric aldol reaction of an isocyanoacetate with various aldehydes to enantioselectively produce 5-alkyl-2-oxazoline-4-carboxylates.[30] This discovery presented a milestone in homogeneous gold catalysis and sparked a rise in publications on the topic. A second milestone came with Teles *et al.* and their presentation of monoligated Au(I) complexes as catalysts for the addition of heteronucleophiles to alkynes.[31] This reaction is representative for golds' ability to activate π-alkyne systems to give incorporation of a range of nucleophiles via the vinyl-gold intermediate. A representative mechanism is shown in scheme 2.

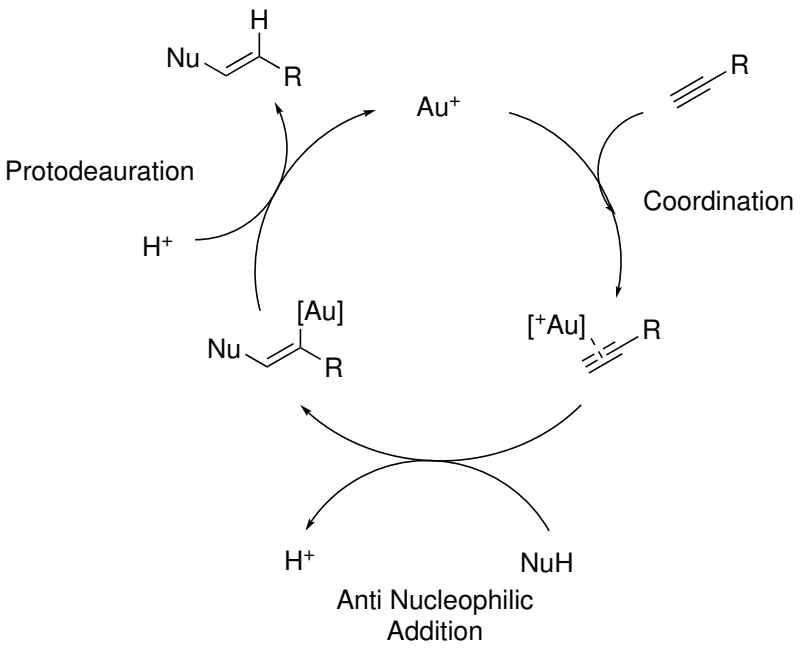

Scheme 2: Mechanistic scheme for gold-catalysed nucleophillic addition to alkynes.

Since the turn of the millennium, homogeneous gold catalysis has seen a massive surge in publications and applications, and afforded a wide array of new transformations,[32] catalyzed by various species of gold. These species range from simple gold salts, AuX/AuX_3, and ligated gold(I)/gold(III) species, to dual gold activated reactions, and bifunctional ligand effects.

2.4.1 Gold salts (AuX/AuX_3)

The first use of gold as a homogeneous catalyst naturally used simple gold salts, such as $AuCl_3$, AuI_3 etc, as they are the most easily available catalytic species. $AuCl_3$ has shown to be exceptionally effective in reactions involving both carbon-carbon multiple bonds and a heteroatom like oxygen or nitrogen. It has proven its usefulness in reactions such as cyclizations of allenyl azetidiones[33] and provided a way of making substituted polyaromatics by catalysing a [4+2] benzannulation between *o*-alkenylbenzaldehydes and alkynes.[34] It has also seen use in the field of biochemistry, where a catalytic system of $AuCl_3$ and phenylacetylene proved to be excellent at the glycosylation of both armed and disarmed trichloroacetamide-based glycosol donors.[35]
While gold salts, $AuCl_3$ especially, have shown remarkable versatility, the field in which it has received the most attention, is the chemistry of furanes. In 2000 Hashmi *et al.* reported a novel gold-catalysed cycloisomerizations of alkenyl and allenyl ketones which previously had been impossible using Ag(I), and at much lower temperatures than that utilising Pd.[36]

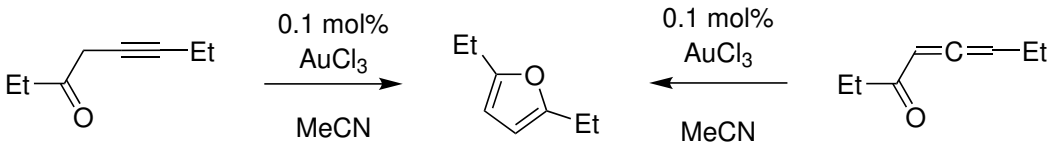

Scheme 3: Example of gold-catalyzed cycloisomerization reported by Hashmi *et al*[36]

The need for highly substituted furanes[37,38] led to further research into the use of $AuCl_3$ as a catalyst. In 2004, Larock *et al.* reported that highly substituted furans were available through the transition-metal catalysed addition of a nucleophile to an alkenynone, in which $AuCl_3$ displayed the greatest activity.[39] In 2011, this work was supplemented by a DFT study performed by Fang *et al.* which confirms the theory presented by Larock *et al.*, that the reaction occurs due to $AuCl_3$ activating the triple bond, to facilitate the cyclization of the carbonyl oxygen.

In addition to allow new ways of synthesising furanes, use of $AuCl_3$ has also paved the way for new utilisations of furanes in further synthesis. The gold-catalysed synthesis of phenols from furanes presented by Hashmi *et al.*[40] transferred the regioselective introduction of substituents on a phenol, from an arene to a furane. In 2006, Rabbaâ *et al.* showed that this reaction proceeds by an intramolecular Au(III)-catalysed [4+2] Diels-Alder process in which the furane attacks the alkyne, rather than by a Au(I)-catalysed exo-vinylidene complex, despite it being kinetically favoured.[41]

2.4.2 Gold(I)

Probably the most researched area of gold catalysis, Au(I) catalysts have been widely studied, and several transformations reported. A large number of these transformations consider various cyclization reactions.[32] Examples of such transformations include carboxylative cyclization of propargylamines to oxazolidinones[42], the preparation of polyfunctionalized carbazoles from indole-linked alkynoles,[43], synthesis of indoles from alkynylated anilines,[44] and dehydrative spirocyclization of triols.[45] Another class of compounds gold has proven quite appllicable is in the chemistry of pyrroles. With the ability to

catalyse both inter,- and intramolecular reactions of pyrroles and alkynes,[46] and the tandem synthesis of substituted pyrroles, gold(I) has shown remarkable applicability in the synthesis of pharmaceuticals and natural products[47].

The Fiksdahl-group has also devoted considerable resources to the study of Au(I)-catalysed transformations. Working with various propargyl acetals, a multitude of papers have been published covering cycloproanations[48], [2+3] cycloadditions,[49] [2+5] cycloadditions,[50] [3+3] cycloadditions,[51] [2+2+2] cyclotrimerization,[52] and tandem cyclizations.[53,54]

2.4.3 Dual-gold

In 2012, two publications independently reported the dual gold-catalysed reaction of diynes.[55,56] Up until this point all gold catalysed reactions were based on the activation of the substrate, using just one gold nucleus. The newly observed activation mode of two independent gold centres, in which one gold-atom is π bonded to a triple-bond while the second gold atom is σ-bonded to either the same, or more commonly, a different triple bond, is fascinating. Not just for the field of gold catalysis, but for all transition-metal based catalysis.[57]
This field of gold chemistry is still young and so far it only has two rough applications: Intramolecular activation and intermolecular activation. Intramolecular activation of conjugated[58] and non-conjugated diyne systems has proven useful for the construction of polycycles.[57] A suggested mechanism for such an intramolecular reaction is shown in scheme 4.

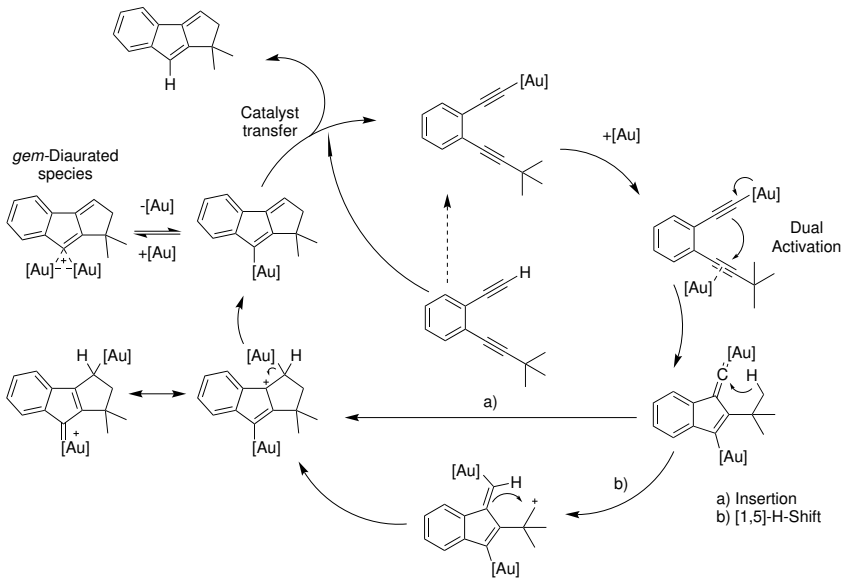

Scheme 4: A suggested catalytic cycle for the dual gold-catalysed formation of benzofulvenes.[55]

The intermolecular reactions are limited to haloalkynes in which two gold atoms coordinate to the same triple-bond in both a σ and π fashion. A transfer of one gold species to a second molecule activates it and enables a nucleophilic attack by the gold acetylide. This is followed by a final catalyst transfer with a new haloalkyne which yields the product and completes the catalytic cycle,[59] (scheme 5). The Fiksdahl group has also performed work on dual gold with the study of its ability to catalyse the trifluoromethylation of terminal aromatic alkynes[60], and the cyclopropanation and cyclopentenylation of propargyl -esters and -acetals (ee up to 65%).[61]

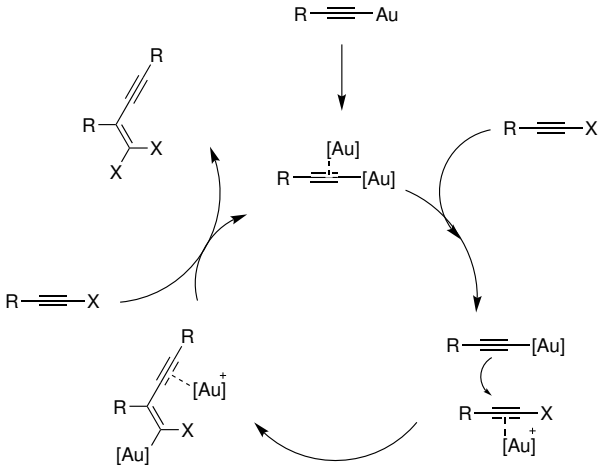

Scheme 5: The catalytic cycle for a dual gold catalysed coupling of haloalkyne.[59]

2.4.4 Gold(III)

Gold(III) complexes have received less attention by the catalytic chemist than their Au(I) counterparts, instead, most research conducted on Au(III) complexes have focused on their ability to form cyclometalated complexes, and the preparation and ligand-exchange reactivity of these.[62] This ability for cyclometallation stems from the geometry of Au(III) complexes, which prefer a square planar geometry over the linear geometry seen in Au(I) complexes. A square planar geometry allows for more tuning of the spatial environment of the gold centre by ligand design.[63] This was first explored using pyridine derivatives with chelating oxygen functionalities ($PicAuCl_2$) (fig. 2.2).

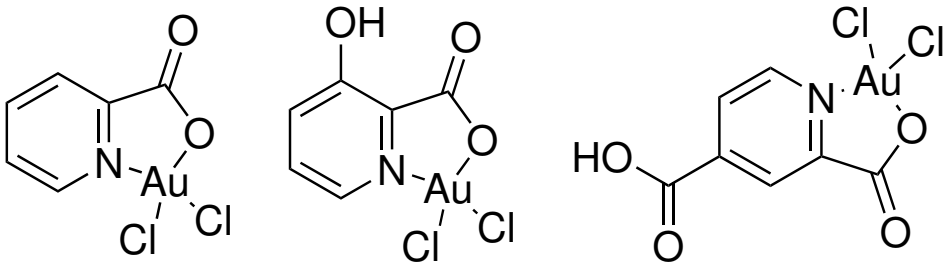

Figure 2.2: Different PicAu(III)Cl_2 compounds prepared and tested by Hashmi *et al.*[64]

Hasmi *et al* reported that these complexes surpassed their respective Au(I) derivatives for the synthesis of tetrahydroisoquinolines with respect to selectivity (scheme 6).[64]

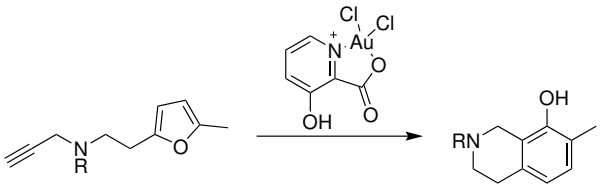

Scheme 6: Synthesis of tetrahydroisoquinolines using PicAu(III)Cl_2 as a precatalyst.

Continuing with the development of $PicAuCl_2$ catalyst, Toste et al. described the synthesis of azepines via an intermolecular [4+3]-annulation reaction.[65] and Waser et al

developed the selective synthesis of 2- and 3-alkynylated furans based on a domino cyclization/alkynylation process in 2013.[66]

In recent years however, gold(III) complexes have been more widely studied for the ability of their geometry to facilitate enantioselective catalysis.

2.5 Enantioselective Gold Catalysis

In parallel with the development of gold catalysed transformations, there has been a similar development of enantioselective transformations.[67]
Several different strategies have been developed to achieve this for both Au(I),- and Au(III)-catalysts.

2.5.1 Au(I) Strategies

The linear geometry of Au(I)-complexes requires complex ligand structures in order for the chiral effect of the ligand to affect the active site.[67] There are three main systems that have seen success in enantioselective gold catalysed transformations. The use of bimetallic gold, chiral counterions, and monodentate phosphoramidite-type ligands.[27,29,68] The latter strategy has especially proven effective for intramolecular [4+2] cycloadditions of allene-dienes.[69] and the [3+2] cycloaddition of propargyl acetals with aldehydes.[70]

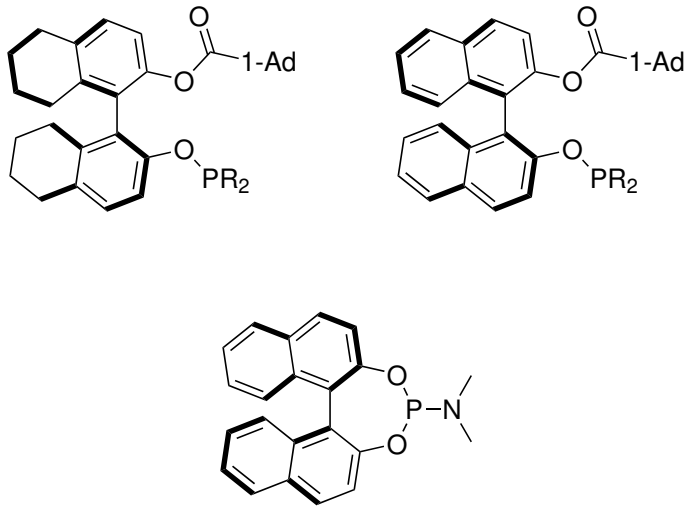

Figure 2.3: Some phosphite ligands developed by Toste *et al* for enantioselective Au(I) catalysis.[69]

2.5.2 Au(III) Strategies

While monoligated Au(I)-complexes exhibit a linear geometry, Au(III)-complexes prefer a square planar geometry which should provide alternative solutions for enantioselective catalysis[71,27]. Examples of this is the gold catalyzed asymmetric epoxidation of alkenes where molecular oxygen is incorporated directly onto to alkene via a gold-oxo, or -peroxo species (7).[72]

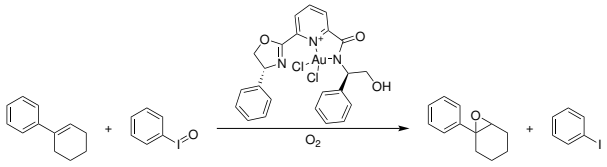

Scheme 7: The enantioselective epoxidation of 1-phenyl cyclohexene with a chiral bidentate Au(III) catalyst and stochiometric amounts of oxidant.

The Fiksdahl group has also reported cases where a chiral butyl-bisoxazoline-Au(III) complex catalyse the formation and *cis*-to-*trans* isomerization of cyclopropanes (scheme 8).[73]

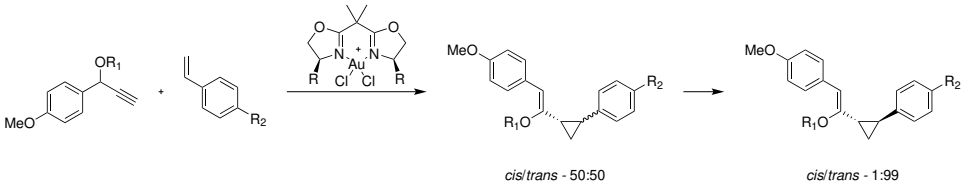

-catalysed cyclopropanation with subsequent *cis*-to-*trans* isomerization.

Scheme 8: The Au(III

The challenge such complexes face is the intrinsic instability of Au(III), which is readily reduced to Au^0 or Au(I) in the presence of electron-rich reagents.[74] A straightforward strategy for overcoming these challenges is by the coordination of σ-donating ligands which stabilise the complex. A type of ligands that accomplishes this are N-heterocyclic carbenes (NHCs).[75]

2.6 N-Heterocyclic Carbenes

N-Heterocyclic Carbenes (NHCs) belong to a class of compounds defined as heterocyclic species containing a carbene carbon and at least one nitrogen atom within the ring structure.[76] A complete overview of the history, properties, and synthetic applications of carbenes would be far to extensive, and outside the scope of this thesis, to be adequately covered. In brief, they are a highly reactive species of compounds consisting of a neutral divalent carbon with a six electron valence shell.[77] This leaves two valence electrons to occupy to empty orbitals. The electronics can occupy these orbitals in two different ways, which is differentiated by the spin state of the electron. If the spins are aligned, the electrons will occupy two each their orbital with an overall spin state of $S = (\frac{1}{2})+(\frac{1}{2}) = 1$, giving a multiplicity of $m_s = 2S + 1 = 3$, in other words, a triplet state. If the spins are opposed to each other, this results in a spin state of $S = (\frac{1}{2}) + (-\frac{1}{2}) = 0$ with a corresponding multiplicity of $m_s = 2S + 1 = 1$, a singlet state. Two states which distinctive in their own reactivity and geometry,[78] and will be touched upon later in this section.

The high reactivity of carbenes is what drove the development of NHCs as a tool to stabilise carbenes sufficiently enough to isolate them. This was first accomplished by Arduengo *et al.* who presented the first crystalline carbene, 1,3-di-1-adamantyl-imidazol-2-ylidene, which exhibited both kinetic and thermodynamic stability in the presence of both oxygen and moisture.[79]

The most common NHCs are based on the imidazole structure, saturated or unsaturated,

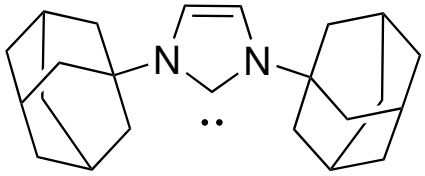

Figure 2.4: The first crystalline carbene, 1,3-di-1-adamantyl-imidazol-2-ylidene, prepared by Arduengo *et al.* in 1991.[79]

with various N and C4-C5 substituents. Some of the most common NHCs reported are presented in fig. 2.5. There have also been reported several other NHCs that have other heteroatoms in the cyclic structure, or different numbers of heteroatoms altogether, as well as *abnormal* NHCs in which the carbene isn't situated on the C_2-carbon.[75]

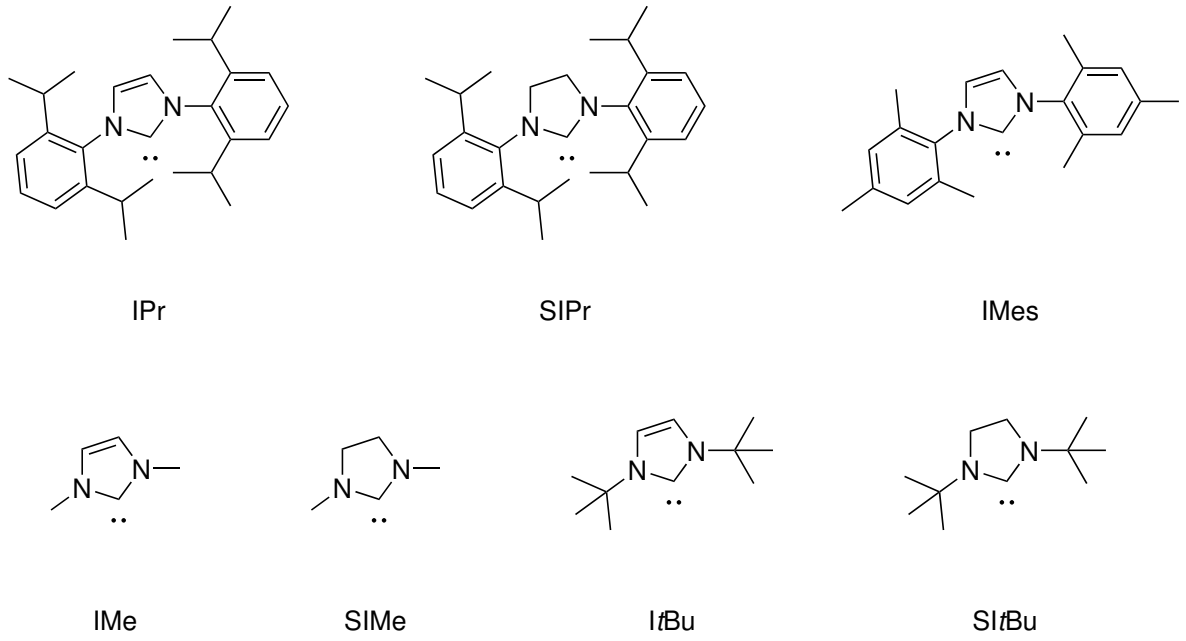

Figure 2.5: An overview of some of the most common NHCs

There are two overarching aspects that explain NHCs ability to stabilise carbenes, and are important to keep in mind when designing new NHCs. Their electronic effects, and their kinetic effects. Calculations have shown that the nitrogen atoms positioned next to the carbene carbon stabilise it both *via* their inductive electron-withdrawing ability, and their π-donation to the empty p-orbital of the carbene.[80] This effect is visualised in fig. 2.6. There are several additional electronic effects that contribute to the stability of the carbenes, such as the aromaticity of the imidazoles and π-donating/σ-withdrawing N-substituents. However, Arduengo *et al.* proved that the π-donating carbene substituents (i.e N, S, P.. etc) are the critical components when they synthesised the saturated 1,3-dimesitylimidazoliin-2-ylidene.[81]

The use of sterically large substituents on the nitrogen atoms helps kinetically stabilise the species by sterically disfavouring dimerization. This effect is illustrated by the Wanzlick equilibrium (9) which states that the tetraaminoethylene and its corresponding carbenes exist in an equilibrium, where sterically demanding substituents push the equilibrium

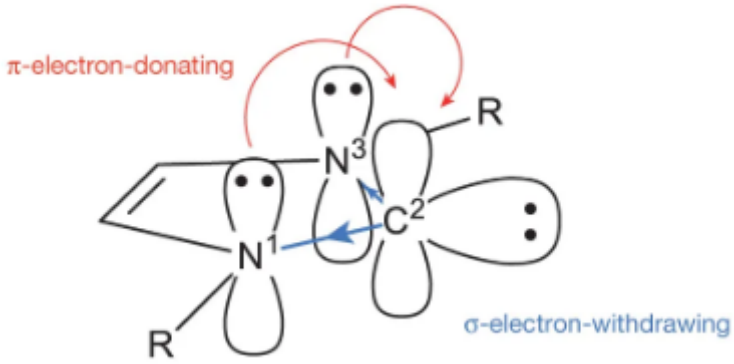

Figure 2.6: Electronic stabilisation effects of nitrogen on a sp^2-hybridised carbene. Used with permission from the authors[71].

towards the carbene, whereas less sterically demanding substituents push the equilibrium towards the olefin.[82]

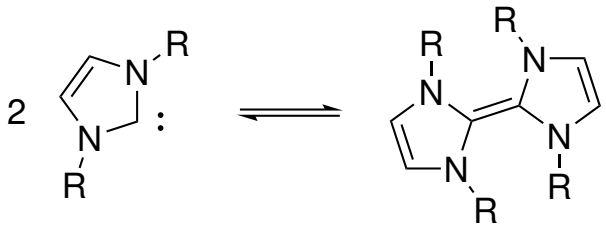

Scheme 9: The carbene-olefin equilibrium described by the Wanzlick equilibrium.

A third aspect which defines the electronic configuration of the carbene is the ring size. Most NHCs are five-membered rings which create a N-C-N bond angle of 108^o. Such an angle creates an sp^2-like arrangement which favours the carbene singlet state. However, larger rings produce a greater N-C-N bond angle, which effectively pushes the nitrogen substituents closer to the catalytic site, increasing the steric effect.

NHCs are exceptionallly suited for transition metal coordination due to their strong σ donation and π back-bonding ability. NHCs exhibit an even larger electron-donating ability than, the more historically used, phosphines. A greater σ-donating ability creates a more thermodynamically stable metal-ligand complex, and is reflected in the greater bond-dissociation energies and shorter metal ligand bonds observed for NHC complexes compared to their phosphine counterparts.
Several basic NHC-ligands are available for purchase. Particularly on the form 1R-imidazole. Such imidazoles are primed to undergo N-alkylation on the non-substituted nitrogen through either a S_N1 or a S_N2 reaction. Tuning of the ligand properties is then left to the choice of N-substituent, which will act as an auxiliary ligand.

2.7 Oxazolines as Ligands

Oxazolines have been utilised as versatile chiral auxiliaries for a long time[83], however, Brunner *et al.* (1988) were the first to report the use of pyridinyloxazolines as a cocatalayst to enantioselectively catalyse the monophenylation of meso-diols, with %ee up to 50.4% (scheme 10).[84]

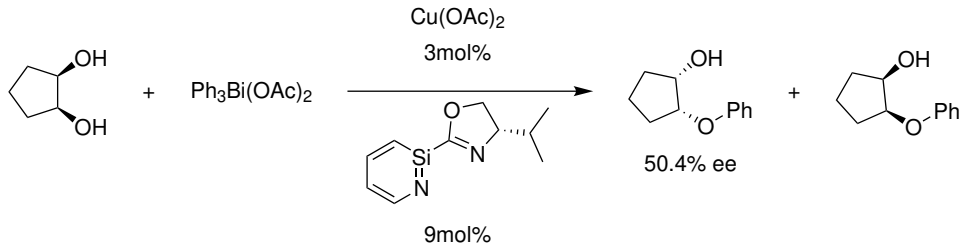

Scheme 10: The enantioselective monophenylation of (*1R,2S*)-cyclopentane-1,2-diol with $Cu(OAc)_2$/pyridinyloxazoline catalyst.[84]

Continuing this work Bolm *et al.* synthesised a series of oxazoline-metal complexes for use in catalytic testing.[85]

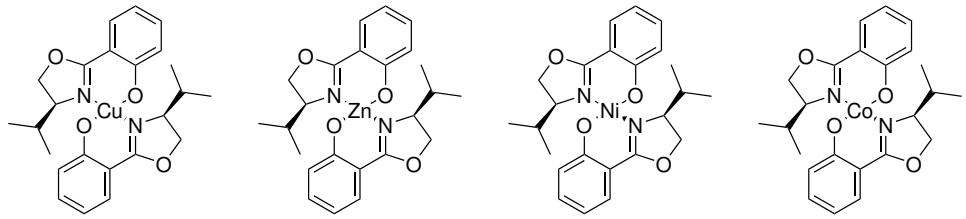

Scheme 11: A series of oxazoline–metal complexes prepared by Bolm *et al.*[85]

Andreas Pfaltz has also reported his success using bis-oxazoline for both enantioselective cyclopropanations and allylic alkylations.[86] As previously demonstrated (scheme 8), these ligands have also been utilised effectively in enantioselective gold catalysis by the Fiksdahl group.[73]

2.8 Synthesis of Imidazolium Salt Based NHC Precursors

The following section will elucidate the theory relevant to the preparation of an imidazole-based NHC ligand with an oxazoline structure as an auxiliary ligand.

2.8.1 Amidation of an acyl chloride

Amides are a class of compounds defined by a carbonyl group connected to a nitrogen atom with or without substituents. They most commonly exist as the product of the condensation reaction that occur between amines and carboxylic acids. In biology, amides are most commonly found in proteins, as part of the polymer structure formed by amino acids. Amides are also widely present in synthetic polymer chemistry, nylon is a great example of how synthetic amides can be of great commercial value.

Amides can be prepared in a range of different ways, however, what all of them have in common, is that they involve nucleophilic addition-elimination at at an acyl carbon. And as such, acid chlorides are the most reactive reagent. Amines and ammonia quickly react with acid chlorides to form amides, with an excess amine or different tertiary amine to neutralise the formed hydrochloric acid.[87] The mechanism for the addition-elimination between a primary amine and am acid chloride is shown in scheme 12

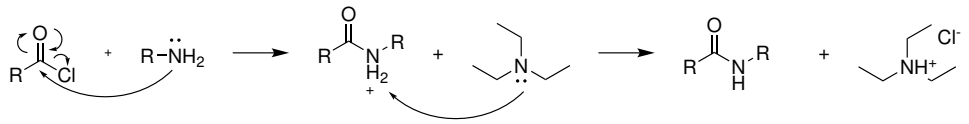

Scheme 12: Mechanism for the nucleophilic addition-elimination of acid chlorides with a primary amine and a tertiary amine acting as a base.

Due to the carbonyl group, amides are susceptible to hydrolysis in the presence of an aqueous acid or base. They are however less susceptible to this kind of hydrolysis than a corresponding ester would, and as so requires harsher conditions as heat or strong acids or bases.

2.8.2 Cyclodehydration of Hydroxy Amides

Oxazolines are five-membered heterocycles containing an oxygen atom in the 1-position, and an imine nitrogen atom in the 3-position. This class of compounds has been known to chemists for more than a century[88] and numerous methods for their preparation have been developed. The simplest of these methods is the direct formation through the cyclodehydration between a carboxylic acid and a β-amino alcohol[89] as shown in scheme 13.

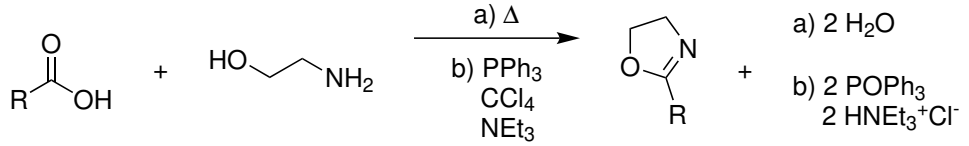

Scheme 13: Reaction scheme for the formation of 2-oxazoline from a carboxylic acid and a β-amino alcohol under various conditions.[89]

Cyclodehydration of hydroxy amides to oxazolines has been achieved by the use heat, sulfuric acid and phosphorus pentoxide or pentachloride.[90] Bergmann *et al.* developed the use thionyl chloride to activate the hydroxy group.[91] However, this reagent is too reactive, and as such a number of milder alternatives were developed.[89] A turning point came when Wipf and Miller reported the effectiveness of Burgess reagent exceeding that of the results achieved under Mitsunobu conditions.[92]

2.8.3 Burgess Reagent

Developed bu Peter Burgess in 1968, methyl N-(triethylammonioumsulfonyl)carbamate is a mild and powerful dehydrating agent. While the reagent has applications for a wide array of transformations, such as the formation of alkenes from second and tertiary alcohols[93] and the formation of nitriles from primary amines,[94] the most noteworthy application is its ability to cyclodehydrate hydroxy amides and hydroxy thioamides to afford the corresponding oxazolines and thiazolines.[95]

The structure of the Burgess reagent and a suggested mechanism for the cyclodehydration of an hydroxy amide to afford the five-mebered heterocycle is shown in scheme 14.

The applications of the Burgess reagent is not only limited to the fomration of five-membered heterocycles, it is also useful for the formation of 6-membered oxazines and thiazines[96] as well as the seven-membered oxazepines and thiazepines.[97]

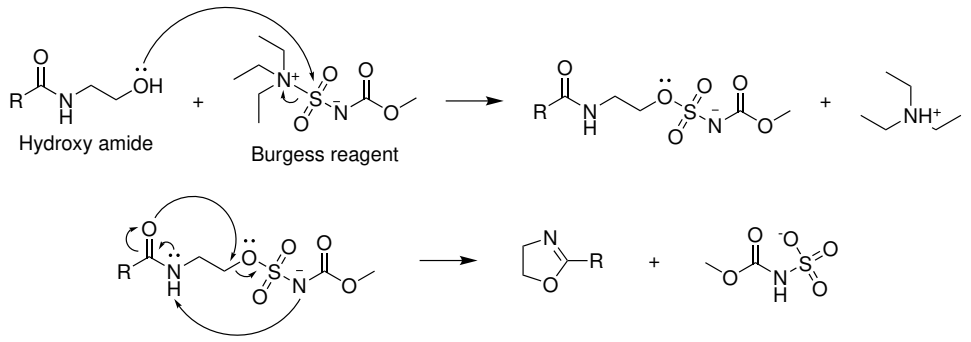

Scheme 14: A suggested mechanism for the cyclodehydration reaction that occurs between a hydroxy amide and the Burgess reagent.

In 1996, Wipf and Venkatraman developed a polyethyleneglycol-linked version of the Burgess reagent, and applied it in the synthesis of five,- and sixmembered heterocycles to great effect.[96,98]. However in the case of seven membered thiazepine, the use of (PEG)-linked Burgess resulted in a greatly reduced yield compared to the standard Burgess reagent.[97]

2.8.4 Finkelstein reaction

The N-alkylation of alkyl halides progress through a common S_N2 reaction where the nitrogen atom acts as a nucleophile with the subsequent elimination the leaving group. Due to the good nucleophility of the chloride anions,[87] the S_N2 reactions where it acts as the leaving group, progress slowly (scheme 16). Therefore, it is beneficial to substitute it with a better leaving group when it's possible. This is accomplished by the Finkelstein reaction. The Finkelstein reaction is a S_N2 reaction with the iodine ion acting as a nucleophile. Whilst KI is soluble in acetone, other halogen salts are not. Therefore, as the transhalogenation progresses, KX precipitates, and this drives the reaction in accordance with Le Châteliers principle.[99]

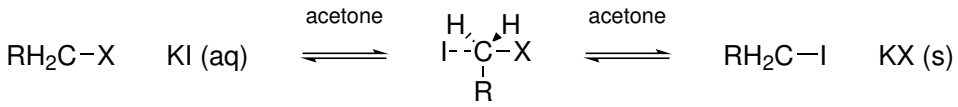

Scheme 15: Finkelstein reaction scheme (X=Cl, Br)

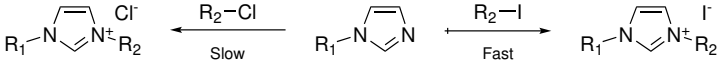

Scheme 16: Compartive reaction schemes for the N-alkylation of alkyl halides.

2.9 Coordination of NHC precursor to Au

Historically there have only been two commonly used methods of coordinating NHCs to transition metals such as gold. One being the generation of a free carbene which coordinates directly, but since this method requires the use of a glove box and an argon atmosphere,[100] most work is done utilising the second method. This method generates a silver complex which undergoes transmetallation to the corresponding gold complex. The

most common way of generating this silver complex is by reacting the NHC precursor with Ag_2O as shown in scheme 17.

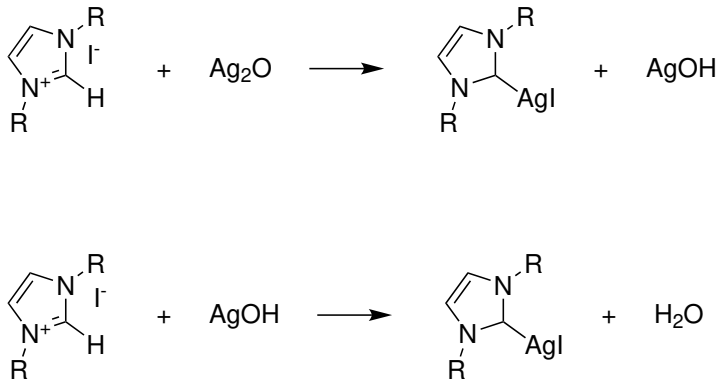

Scheme 17: The reaction scheme for the coordination of a NHC to silver via Ag_2O as a mild base and silver source.

The reaction occurs in two steps, where the first step occurs rapidly due to the pKa difference between the imidazolium cation and the protonated Ag_2O. The second deprotonation of an imidazolium cation by AgOH is not energetically favourable, but the exothermic formation of the NHC-Ag(I) drives the reaction.[101]
Some of the drawbacks to this method of Au-coordination lies in the atomic economy, as it requires one mole of Ag, for each mole of Au, and it is unfit for the synthesis of gold complexes bearing very large, sterically demanding, ligands.[102]

In 2013, Gimeno *et al.* reported a new and simple method of directly coordinating an NHC to a gold atom in a one pot synthesis. Utilising a mild base such as K_2CO_3 Alternatively it may be coordinated directly to gold by first forming a $[NHC-H]^+[AuCl_2]^-$ salt, followed by deprotonation of the imidazolium salt to form the Au(I)-NHC complex[103] (scheme 18).

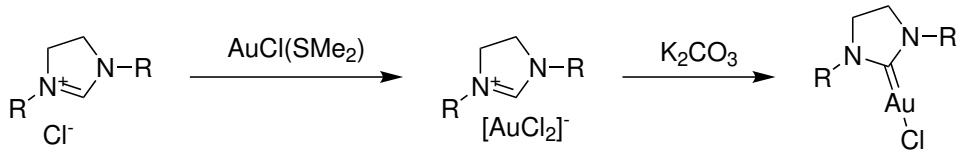

Scheme 18: Reaction scheme for the coordination of a NHC precursor to gold via deprotonation of a $[NHC-H]^+[AuCl_2]^-$ intermediate.

2.10 Oxidation of Au(I) complexes

In 2010, Nolan *et al.*, described a fast and effective method of preparing Au(III)-complexes from their corresponding Au(I)-complexes by oxidative addition of chloride using dichloroiodobenzene.[104] This method is superior to the previously conventional way of preparing the $AuCl_3$(NHC) which utilised Cl_2 (g) in several aspects like reactivity, selectivity, usability, and sustainability. Traits like these is also why hypervalent iodine compounds is gaining increasing interest among synthetic chemists.[105,106]

3 Results and Discussion

This section is divided into two main parts. The first section will describe the synthetic work that produced the chiral NHC precursors discussed in this paper, and the challenges that this work faced.
The second section will describe the synthetic work conducted as a means of coordinating the aforementioned NHC precursor, and the auxillary oxazolineligand to a central gold atom. After this, an evaluation of the changes in ^{15}N-NMR shifts will presented along with their implications on the geometry and structure of the Au(III)-complexes.

3.1 Synthesis of Imidazolium Salt Based NHC Precursors

3.1.1 Motivation

As previously described in section 2.5.2, the square-planar geometry of Au(III) provides new possibilities for enantioselective gold-catalysis as it allows the ligands to be closer to the catalytic cite. Despite the new geometry of the gold atom, it will still be energetically favourable for the substrate and ligand to be on opposite sides of the gold atom. It is therefore of interest to develop NHC ligands which have a secondary ligand that can also coordinate to the central gold atom, and force the substrate into a more sterically controlled environment (scheme 19)

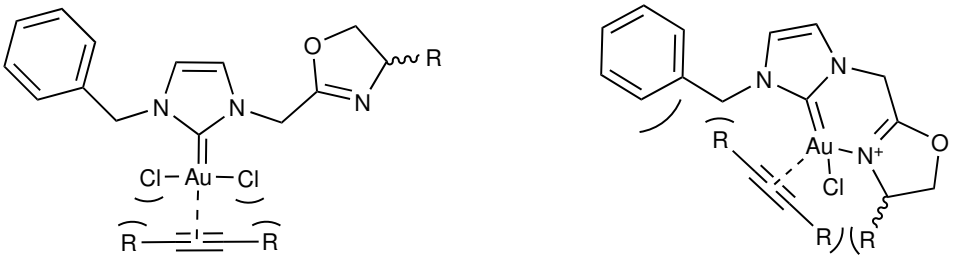

Scheme 19: Left: Monodentate Au(III)NHC coordinated ligand; **Right**: Bidentate C,N-coordinated Au(III)NHC ligand

3.1.2 Synthesis of 1-Benzyl-3-Oxazolineimidazoles.

Previously in this text, several different types of NHCs have been presented. Herein, the synthetic route to a range of imidazole-based precursor will be presented.

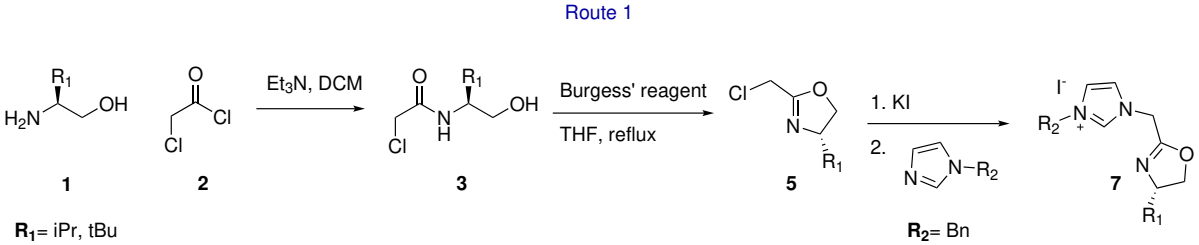

Scheme 20: The synthetic route towards the target 1-benzyl-3-oxazolinimidazole.

Structural variations in the C-4 position of the oxazoline will affect the steric and chemical environment of the catalytic site, and control of this is achieved by starting from the 1,2-

amino-alcohols **1**, following a documented route[107] giving **7** in three steps (scheme 20). The reactions in route 1 resulted in mediocre to good yields in step 2 and 3 (42-80%), but surprisingly only afforded poor to mediocre yields in step 1 (22-52%).

3.1.3 Synthesis of Chiral Amides

Through the condensation of the 1,2-amino alcohols **1a,b** on chloroacetyl chloride **2** (scheme 21) amides **3a,b** were prepared as white wax-like solids in poor to mediocre yields (22-52%).

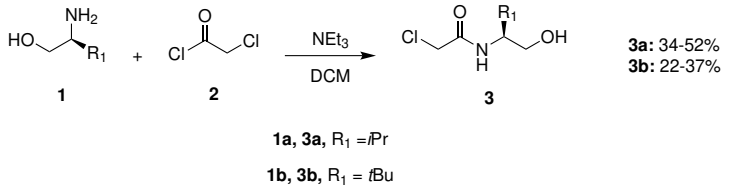

Scheme 21: General reaction scheme for the preparation of Amide **3a-b**

The reaction was initiated by dissolving amino alcohols **1a,b** and NEt_3 in DCM. This mixture was cooled to 0^oCusing an ice-bath, before 2-chloro acetylchloride was added dropwise using a syringe. Upon injection of the syringe into the closed system there was visible oozing of white smoke from the needle, which visually demonstrates the reactivity of **2**. During addition of acetylchloride **2** the reaction mixture displayed different behaviour in different iterations of the experiment. Most commonly the solution obtained a dim yellow shade during the addition, which remained throughout the entire reaction. There were also iterations where the entire mixture turned bright red, before spontaneous boiling with an instant colour shift to the common yellow, and iterations where the mixture remained completely clear throughout.
After the reactions were terminated, DCM was removed under reduced pressure, which prompted the precipitation of $[HNEt_3]^+Cl^-$ as a white solid alongside the formed amide. The residue was diluted in EtOAc and filtered through celite. The insoluble amine salt was washed repeatedly to prevent mechanical loss of product trapped in the insoluble matrix. The mixture was concentrated under reduced pressure and purified by flash column chromatography, eluting with EtOAc. This yielded amides **3a,b** as a dark or clear oil at 40^oC. Cooling to room temperature caused the oil to solidify, and form a light brown or white wax. Despite the variations in colour, all ^{1}H-NMR spectra showed that the amides **3a,b** contained no organic impurities.
The compounds were characterised by HRMS, ^{1}H-NMR , ^{13}C-NMR , COSY, HSQC, ^{1}H,^{13}C-HMBC and IR. The results of the NMR analysis' are summarised in fig. 3.1 and fig. 3.2. The shifts are readily assigned by their integrals, multiplicity, coupling constants and 2D-NMR spectra.

An interesting structural observation found in these ^{1}H-NMR spectra is the revelation of amide **3b** as a diastereotope as evidenced by the splitting of the methylene ^{1}H-NMR signals. (fig. 3.3). This is caused by a locking of the $NCH-CH_2OH$ bond for the amide **3b**, whilst the same bond in amide **3a** Can rotate freely. An explanation to this might be the formation of an intramolecular five-membered ring through hydrogen interaction between the amide and hydroxy group, but if this was the case it should be affect the C=O bond of the amide. Partial bonding between the amide proton and the hydroxy oxygen would increase the electron density donated to the carbonyl carbon by the nitrogen, resulting

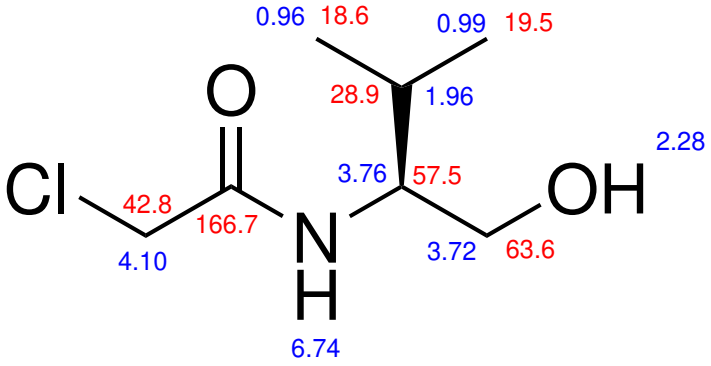

Figure 3.1: Compound **3a** with assigned ^{1}H-NMR and ^{13}C-NMR shifts.

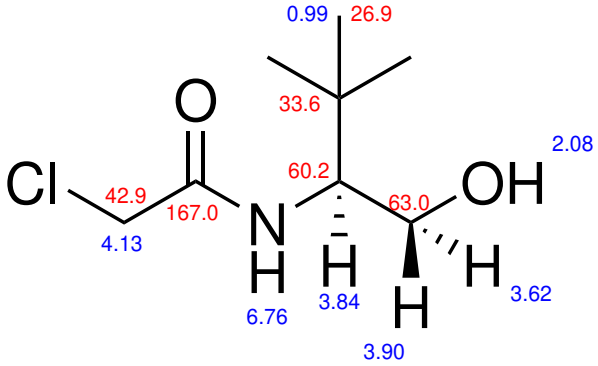

Figure 3.2: Compound **3b** with assigned ^{1}H-NMR and ^{13}C-NMR shifts.

in a C=O stretch a lower wavenumbers. The observed IR signals of the carbonyl stretch for **3a** and **3b** occur at 1650.7 and 1658.2 respectively. This observation excludes the possibility of amide-hydroxy interactions as the reason for amide **3b** appearing as a diastereotope. It is therefore suggested that the free rotation of the NCH-CH_2OH bond is hindered by steric interactions from the *tert*-butyl group. This indicates that the *tert*-butyl substituent is far more sterically demanding than the *iso*-propyl group, since the NCH-CH_2OH bond in amide **3a** rotates freely.

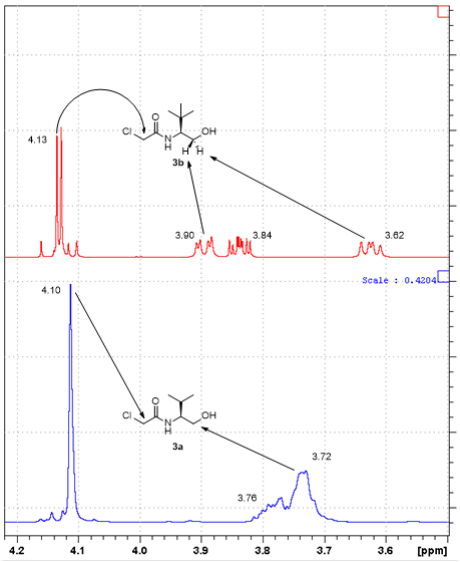

Figure 3.3: A comparison of the ^{1}H-NMR spectra for **3a** (bottom) and **3b** (top) visualising the effect of different steric environments on the molecules' geometric configuration.

3.1.4 Condensation Complications

In the amide condensation of amino alcohols **1a,b**, distinct byproducts **12a,b** were repeatedly formed parallel to amides **3a,b** (fig. 3.4).

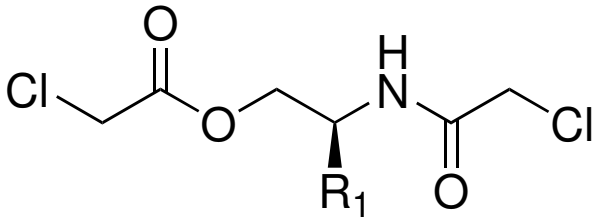

12

Figure 3.4: By-product identified and isolated in condensation of **1**.

These byproducts were isolated by flash column chromatography and identified by NMR-characterisation and HRMS. The 1-amide-2-esters **12a,b** are results of additional hydroxy attack of amino alcohol **1** on acetylchloride **2** in parallel with the amino group (scheme 22).

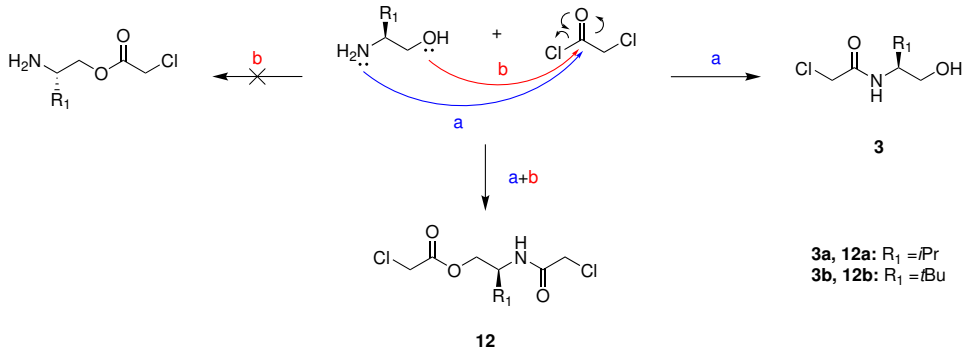

Scheme 22: Reaction mechanism for the formation of amide **3** and the formation of the undesired dimer **12**

Whilst the amide-ester **12** was formed in large quantities, the pure ester formed through pathway **b** was never isolated, indicating that the amino groups are more potent nucleophiles than the alcohols. Despite this, the dimer is formed in large amounts (25-100%). A possible explanation for this is the triethylamine completely or partially deprotonating the hydroxy group, activating it as a nucleophile.

3.1.5 The Oxazoline Obstacle

The first attempt at synthesising the oxazoline **5a** resulted in the, rather disappointingly, complete loss of product (crude NMR had proven the presence of the oxazoline). After purification of by flash column chromatography (4:1 pentane:EtOAc), with subsequent removal of the solvent on the rotary evaporator (40^{o}C, 1 mbar) no product remained. A look into the literature revealed that oxazoline **5a** has a bp. of 40^{o}C, at 1 mbar. Other reported methods purify the oxazoline by distillation, but the mechanic loss that distillation entails would be punishing to the yields in this synthesis due to the scale on which it is performed (50 - 180 mg theoretical mass). It was therefore attempted two different ways of circumventing the volatility of the oxazoline **5a**.

Heavier compounds are less volatile than light ones, and since the both chloromethyl oxazolines **5a,b** were set to undergo halogen exchange to its iodised counterpart, the idea of reacting compound **5a** further directly before isolation therefore fell quite naturally. Two attempts at circumventing this problem were performed (scheme 23).

The volatility of the oxazoline **5a** is not an issue until the eluent, EtOAc, needed to be removed since EtOAc also evaporates at 40^{o}C, 240 mbar. EtOAc is only introduced as en eluent in the flash column purification, and as so, the first attempted workaround simply skipped the purification. Instead, the reaction mixture was filtered through celite, removing most of the unreacted Burgess reagent and precipitated solids, before the THF was somewhat removed. The rotary evaporator was still employed to remove the solvent, but the pressure was never below 300 mbar. The clear oil was then diluted in acetone, and KI was added to initiate the halogen exchange. After one hour, the precipitation of fine-grained particles had ceased, and so the reaction mixture was filtered, acetone removed on the rotary evaporator (P>300 mbar), and the now yellow oil was diluted in dry MeCN and imidazole **6** was added.

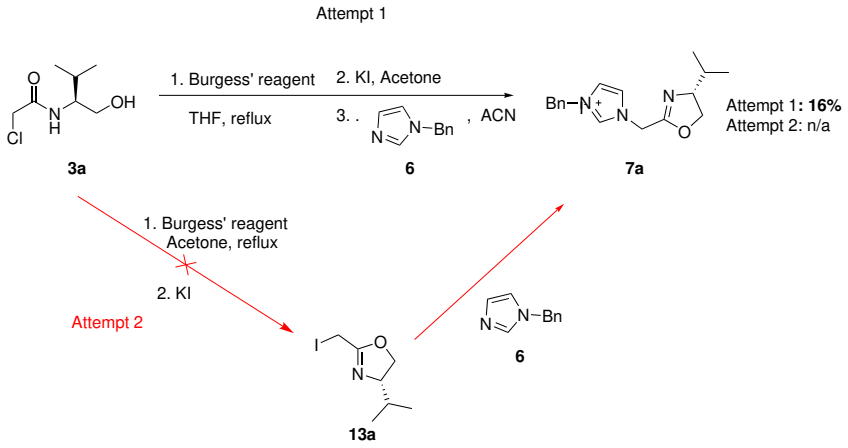

Scheme 23: The attempted workarounds to the volatility of **5a**.

This method did produce the imidazolium **7a**, but ^{1}H-NMR of the crude mixtures showed enormous excess of the imidazole **6** and as so, quantitative control of the reaction becomes an issue when the oxazoline intermediate is not isolated. The final yield of the reaction (16%) was not very informative as the loss of product may have occurred over all, or just one of the reactions performed, and with no intermediate isolation, it is impossible to tell which.

The second attempt tried to address the problems of the first attempt by isolating the iodised oxazoline **13**. Simultaneously it was attempted to avoid the use of THF for the dehydration as well, as it would have to be removed before halogen exchange could be attempted, and residual solvent might affect the solubility of KCl which would interfere with the Finkelstein equilibrium. The dehydration was therefore attempted in acetone as the solvent. This substitution did not achieve full conversion of the amide **3a**, even after 16 hours of reflux. It was therefore decided to move on to the next step despite incomplete conversion. The reaction mixture was filtered through celite with additional acetone and KI was added. After 3.5 hours the mixture had taken on a deep orange colour and the solvent was removed before the formed residue was flashed, eluting with 4:1 Pentane:EtOAc. This did however not result in a pure product, instead, ^{1}H-NMR revealed that most or all of the compound decomposed on the column.

3.1.6 Synthesis of Oxazolines

The intermolecular dehydration of amides **3** using Burgess reagent **4** in dry THF yielded the oxazolines **5** as clear colourless oils in good yields (41-80%) (scheme 24).

The reaction was initiated by dissolving amides **3a,b** and Burgess' reagent **4** in dry THF. The mixtures were then refluxed at 70^{o}Cfor 2-6 hours before the product mixture was concentrated under reduced pressure (>180 mbar), and purified by flash column chromatography eluting with 4:1 pentane:EtOAc. The eluent was removed under reduced pressure (40^{o}C, >180 mbar) and dried further under vaccum at room temperature. Despite this, complete removal of EtOAc was not always achieved, and as such, the yields of the target oxazoline compounds **5a,b** were theoretically calculated by estimating the product composition from the ^{1}H-NMR spectrum and the average molecular weight ($\bar{M}_w$).
The compounds were characterised by HRMS, ^{1}H-NMR , ^{13}C-NMR , COSY, HSQC,

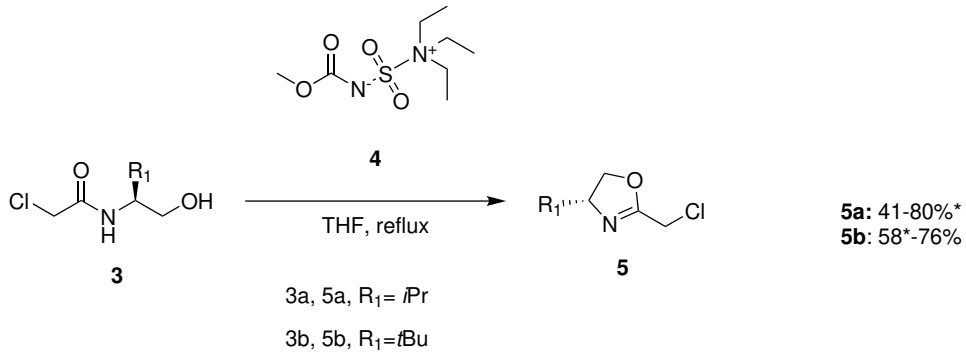

Scheme 24: General reaction scheme for the preparation of Oxazolines **5a-b**. *Calculated yields from ^{1}H-NMR , corrected for EtOAc impurities.

^{1}H,^{13}C-HMBC , and IR. The results of the NMR analysis' are summarised in fig. 3.5 and fig. 3.6. The shifts are readily assigned by their integrals, multiplicity, coupling constants and 2D-spectra.

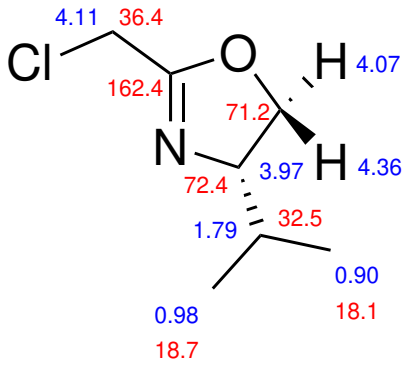

Figure 3.5: Compound **5a** with assigned ^{1}H-NMR and ^{13}C-NMR shifts.

An interesting change occurred in the coupling constant between the vicinal CH_2O protons(H5) and the C*H*N proton (H4) after the ringclosing of the amides **3a,b**. Of the two amides **3a,b**, the *t*Bu-amide **3b** is the only compound that produce two unique ^{1}H-NMR signals for the vicinal H5-protons. These signals couple to the H4-proton in two different ways (J_{trans} = 3 40, J_{cis} = 7 70 Hz). The coupling constants follow the ordinary pattern of $J_{cis} > J_{trans}$. As expected, after ringclosing and the formation of the five-membered oxazoline, both the *i*Pr-oxazoline **5a** and the *t*Bu-oxazoline**5b** observe a splitting of the ^{1}H-NMR signal for the vicinal H5 protons. For the oxazolines **5a,b** the observed coupling constants $J_{cis} = 9\ 72, 10\ 16$ and $J_{trans} = 8\ 31, 8\ 46$ respectively (fig. 3.7).

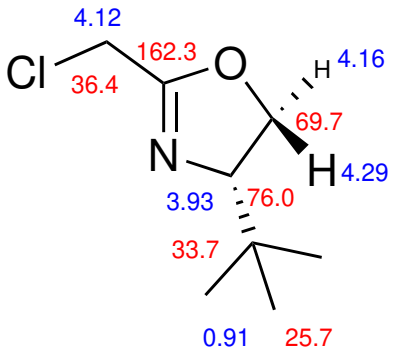

Figure 3.6: Compound **5b** with assigned ^{1}H-NMR and ^{13}C-NMR shifts.

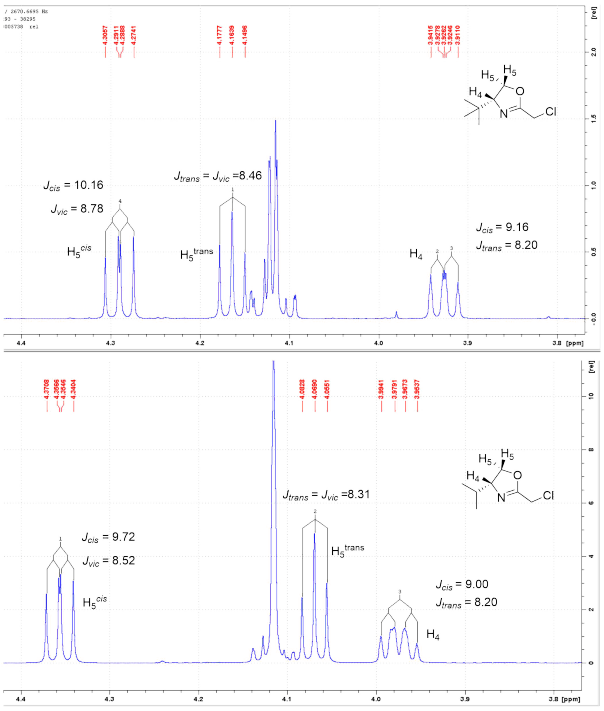

Figure 3.7: The vicinal H5-protons and their coupling constants to the H4 proton for both oxazoline **5a** and **5b**.

The explanation for these similiar values in coupling constants ($J_{cis} \approx J_{trans}$ is elucidated by referring to the Karplus equation, and the Newman projection of the oxazolines (fig. 3.8).

When the five-membered ring is formed, the vicinal CH_2 protons H5 are forced into *cis*,- and *trans*-coplanar positions, eclipsing the H4-proton.
This configuration is formed due to the rigid structure of the five-membered ring. The dihedral angles of the ring are significantly smaller than those found in large rings, such as cyclohexanes. The additional presence of an sp^2 hybridized N,- and C,- atom, and the imine π-bond reduces the flexibility of the ring further, resulting in $J_{cis} \approx J_{trans}$.[108]

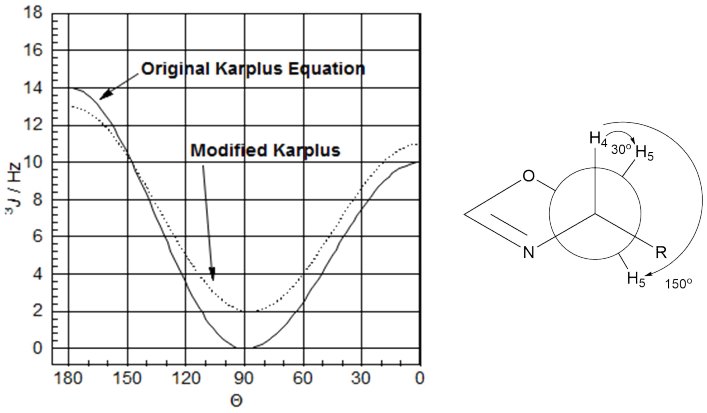

Figure 3.8: A graphical presentation of the original, and modified Karplus equation, along with a sketched Newman projection of the oxazoline **5**.

3.1.7 Imdiazolium Salt Synthesis

Through the Finkelstein halogen exchange with subsequent *N*-alkylation, as shown in scheme 25. The imidazolium salts **7** were prepared in mediocre to good yields (38-77%).

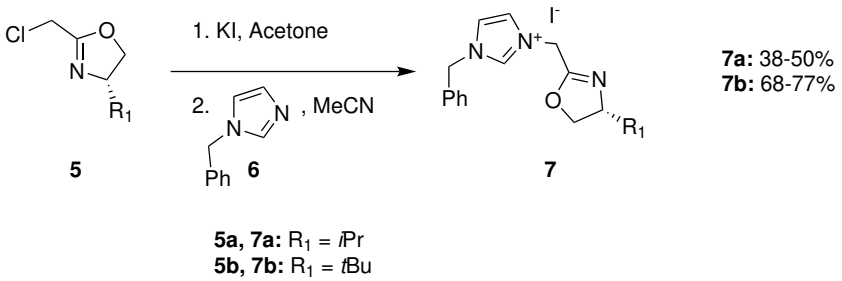

Scheme 25

The first part of the reaction was initiated by dissolving KI in acetone. Upon complete dissolution, one equivalent of oxazoline **5** was added. This caused the precipitation of white solid (KCl) over the course of 1-2 hours. The reaction mixture took on a dim yellow shade over the course of the reaction. After termination, the mixture was filtered through celite in order to remove the precipitated salt.The solvent was then removed under reduced pressure and the residue formed was diluted with dry MeCN before 1-benzylimidazole, **6**, was added. The alkylation was run at room temperature for 2-20 hours before the solvent was removed and the product **7** was purified by flash column chromatography, eluting with 1:5 MeOH:DCM. This yielded the imidazolium salts **7a,b** as yellow,- green-*ish* solids. The compounds **7a,b** were analysed by HRMS, which confirmed that the products were formed, and fully characterised by ^{1}H-NMR , ^{13}C-NMR , COSY, HSQC, ^{1}H,^{13}C-HMBC and IR. The results are summarised in fig. 3.9 and fig. 3.10.

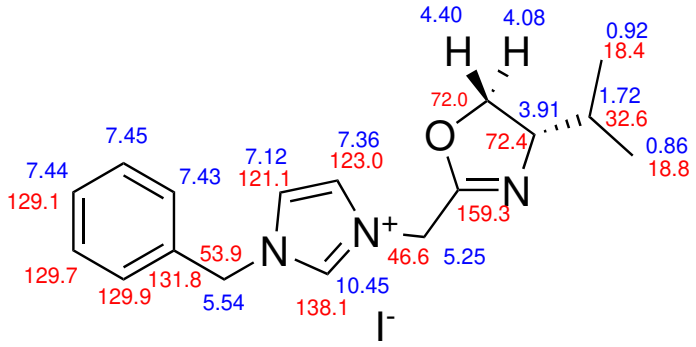

Figure 3.9: Compound **7a** with assigned ^{1}H-NMR and ^{13}C-NMR shifts.

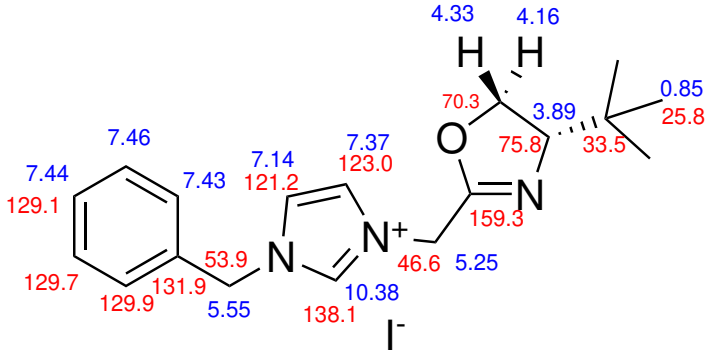

Figure 3.10: Compound **7b** with assigned ^{1}H-NMR and ^{13}C-NMR shifts.

3.2 Synthesis of AuNHC-Complexes

3.2.1 Synthesis of Au(I)NHC-Complexes

Through an initial Ag-coordination and subsequent transmetallation the Au(I)-NHC complexes **8** were prepared in poor to good yields (9-69%) as shown in scheme 26. An instantly apparent trend is the remarkably low yields for *t*Bu-Au(I)NHC-complex **8b** versus the *i*Pr-Au(I)NHC-complex **8a**, which is likely due to the sterically demanding *t*-Bu group on the oxazoline that, as shown in the ^{1}H-NMR spectra of the amides, exerts far more steric effect than the *i*-Pr group.

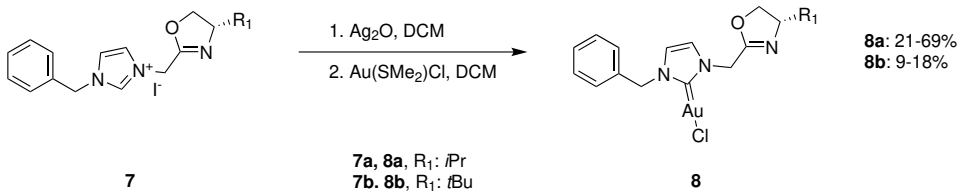

Scheme 26

The initial silver coordination was performed by the well established silver base technique utilizing Ag_2O as both a base and Ag source.[101] The NHC precursor was dissolved in DCM and 0.5 equivalent of base was added to initiate the reaction which proceeded while shielded from light. The deprotonation was confirmed by ^{1}H-NMR and the mixture was filtered through celite and the solvent removed. The resulting white residue

was diluted in DCM before $Au(SMe_2)Cl$ was added. The addition caused the solution to immediately take on a new colour. Interestingly, the colour varied between parallels, even those originating from the same batch of NHC precursors. The two most distinct colours were yellow and purple. The solutions that turned purple did in some instances initially take on a cloudy shade which is likely caused by the precipitation of AgX (X= I, Cl) which indicates the progress of the transmetallation. The solutions that took on a yellow colour and remained clear never yielded any product, which corresponds to the expectation of seeing precipitated silver salts as the silver complex undergoes transmetallation to gold.

The formed products **8a,b** were analysed by HRMS which confirmed that the product had formed. The Au(I)NHC complexes were fully characterised by ^{1}H-NMR , ^{13}C-NMR , COSY, HSQC, ^{1}H,^{13}C-HMBC , ^{1}H,^{15}N-HMBC , and IR. These results are summarized in fig. 3.11 and fig. 3.12.

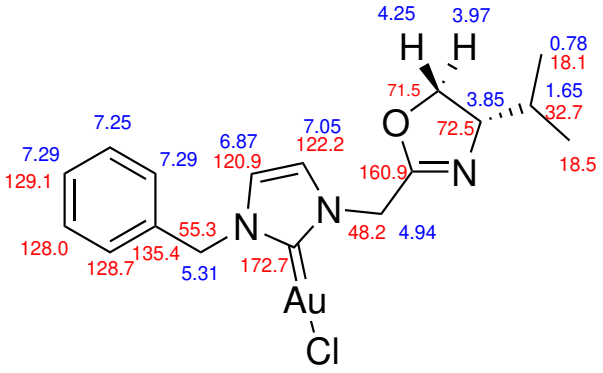

Figure 3.11: Compound **8a** with assigned ^{1}H-NMR and ^{13}C-NMR shifts.

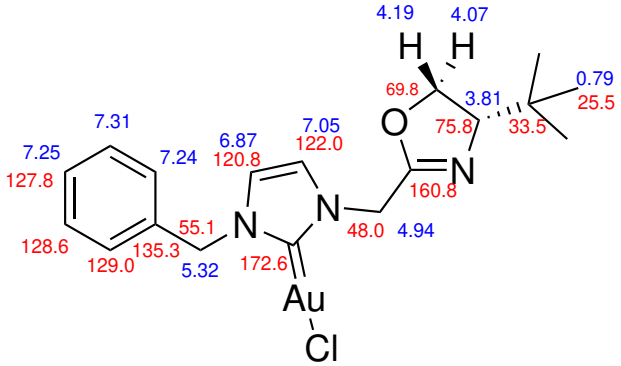

Figure 3.12: Compound **8b** with assigned ^{1}H-NMR and ^{13}C-NMR shifts.

The initial coordination to silver occurred rapidly, and was monitored by ^{1}H-NMR spectroscopy. As described previously, the silver complexes formed in two steps. What is interesting, is that the separation of these steps is visible in the ^{1}H-NMR spectra of the reaction mixture. The free NHC imidazole proton (H2) of **7a** appears at $\delta = 10.50$ ppm. This proton reappeared 1 hour after addition of Ag_2O at $\delta = 8.08$ ppm, with an integral of 0.5. It is unclear what exactly causes this upfield shift, but it seems likely that it was caused by the partial bonding of the H2-proton to the *in situ* formed AgOH (fig. 3.13) which eventually would deprotonate the imidazole salt.

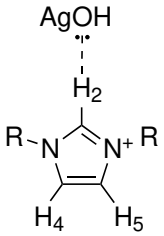

Figure 3.13: Proposed electron interaction which causes the upfield change in the carbenic proton shift.

Figure 3.14 illustrates the characteristic ^{1}H-NMR spectra of the (a) free NHC precursor **7a**, the (b) incomplete Ag-coordinated complex, the (c) complete Ag-NHC-coordinated complex, and the (d) Au(I)NHC-coordinated complex **8a**. The most obvious difference is the upfield shift of the two singlets of the imidazole H4,H5-protons, which experience a shift upwards of 0.25 and 0.19 ppm respectively upon coordinating to the silver atom, and an additional shift upfield by 0.06 ppm upon coordination to gold.
The shift observed upon coordinating to the silver atom is expected to be the largest, as the heterocycle no longer possess a formal charge, and no longer need to donate electron density to stabilise this charge. Upon transmetallation to gold, these protons shift even further upfield, indicating that the Au atom is less acidic than silver, pulling less electron density from the NHC than Ag.

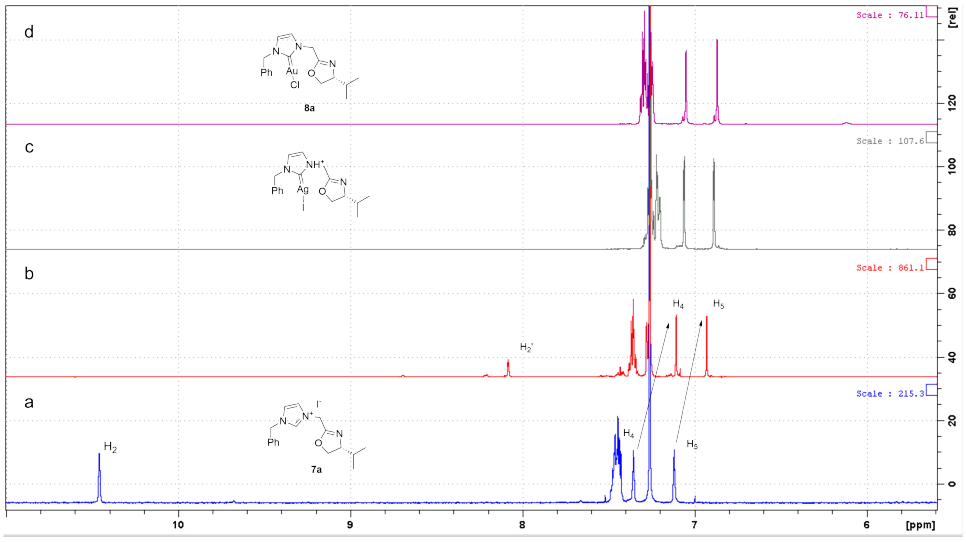

Figure 3.14: ^{1}H-NMR spectra of (a) **7a** and (d) **8a**, with the two intermediate AgNHC complexes (c,d).

The second important NMR change that is observed, is the ^{13}C-NMR of the imidazolium C2 carbon, which for the free NHC precursor **7a** is 138.1, but is vastly shifted downfield to 172.7 ppm upon coordination to gold (fig. 3.15). This observation is in accordance with the theories postulated by Herman *et al.*[109], and shows that the carbenoid carbon has a higher electron density available when coordinated to a metal centre, compared to the salt.

The downfield shift of the C2-carbon signal is the most convincing evidence for the coordination of the NHC ligand **7a** to a gold centre to afford the Au(I)NHC complex **8a**

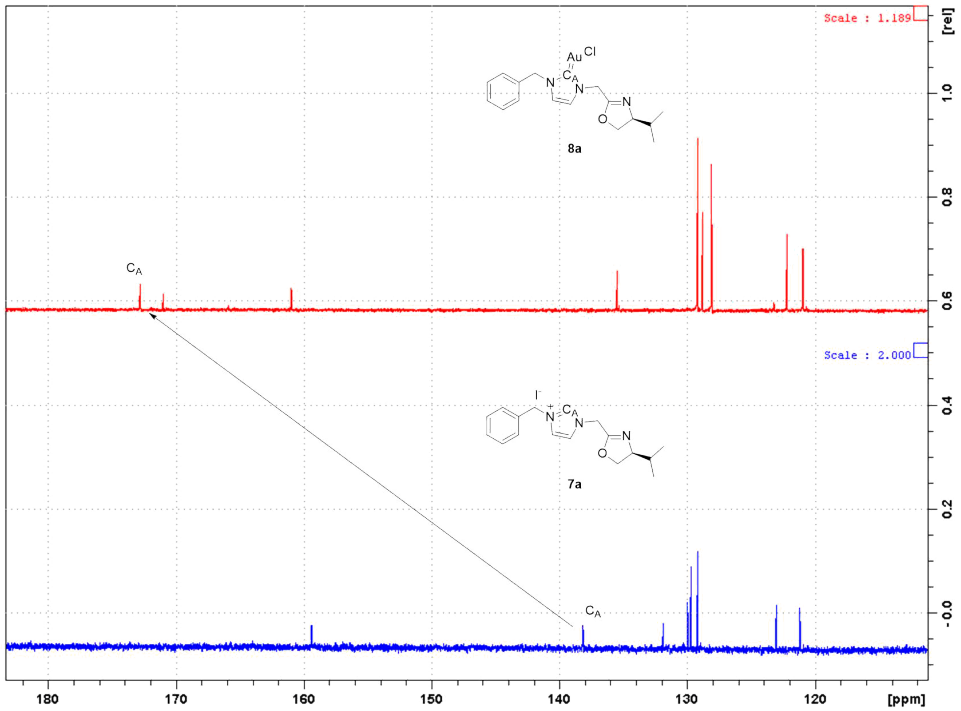

Figure 3.15: Comparison of carbon atoms for the imidazole ligand and Au(I)-complex.

obtained. The C2-carbon signal of the imidazolium salt **7b** was subject to a similar shift, $\delta = 138\ 1ppm \longrightarrow \delta = 172\ 6ppm$ when it was coordinated to a gold atom to afford the Au(I)NHC-complex **8b**.

3.2.2 Synthesis of Au(III)NHC-complexes from Au(I)NHC-complexes

Four different Au(III)-complexes (**10a**, **10b**, **11a**, **11b**) have been synthesised in this project. Originally, the monodentate Au(III)NHC complexes **10a** and **10b** were intended to be intermediates, formed by oxidation of their corresponding Au(I)NHC-complexes through a halogen transfer from dichloroiodobenzene. These Au(III)NHC complexes **10a,b** were intended to be directly reacted further by addition of $AgSbF_6$ which would afford anion exchange ($Cl^- \longrightarrow SbF_6{}^-$), and facilitate the *N*-coordination of the auxiliary oxazoline ligand. However, initial trials of this method proved unsuccessful, and it was therefore attempted to isolate the Au(III)[NHC]Cl_3 compounds **10a,b** before they were reacted further. This step-wise approach proved to be more successful, and allowed for the synthesis of the target compounds **11a,b**. This synthetic route is summarized in scheme 27.

Unfortunately, due to limited time, none of the four Au(III) compounds were fully isolated, and as such not fully characterized by NMR methods or HRMS.

^{1}H-NMR of the Au(III)NHC complexes **10a,b** 30 minutes after addition of $PhICl_2$ usually showed complete conversion of the Au(I)NHC complex **8a,b**, and always full conversion within 1 hour. The conversion could also be estimated by the colour of the reaction mixture, as it went from being bright yellow to an almost colourless solution. The isolation of Au(III)NHC complexes **10** was done by precipitation from DCM by addition of pentane. This method did not remove all impurities from the reaction mixture, but the Au(III)-complexes **10** proved to be too unstable in solution to be eligible for a slow

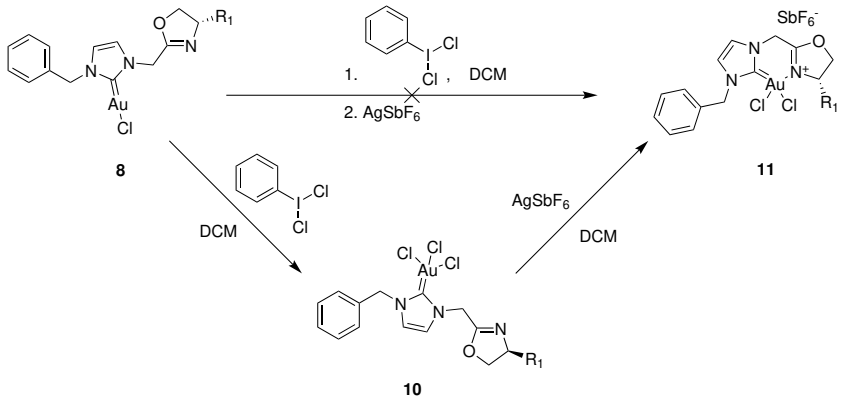

Scheme 27: Schematic presentation of the intended, and the successful synthetic route yielding the bidentate C,N-Au(III)NHC[Oxazoline] complexes **11a,b** via the monodentate Au(III)NHC complexes **10a,b**

recrystallization. Although the Au(III)-complexes **10** were not completely purified, the residue formed was pure enough to survive the counter-ion exchange step of the synthesis. The addition of $AgSbF_6$ was immediately followed by the visible precipitation of a white solid (AgCl (s)) which stopped after 15-30 minutes.

3.2.3 Coordination Effects on Nitrogen

Aware of the time limit on the project and the instability of the complexes which might lead to an unsuccessful isolation, it was decided to run ^{1}H,^{15}N-HMBC experiments of the crude reaction mixtures in order to observe the changes in the nitrogen shifts at different stages of oxidation and geometry. A summary of these results for complexes **8-10-11a** and **8-10-11b** is presented in fig. 3.16 and fig. 3.18. A comparison of the ^{1}H-NMR spectra and 1D ^{15}N-NMR for the complexes **8-10-11a** and **8-10-11b** are also presented in fig. 3.17 and fig. 3.19 respectively.

Assignment of the ^{15}N-shifts (δN) is done by recognising that the correlation between the imidazole protons (H4, H5) and the imidazole nitrogens (N_1, N_2) appear as four distinct correlation peaks, that comprise each corner of a rectangle. In addition to the H4 and H5, the nitrogen nuclei N_1 and N_2 correlate to the benzyllic protons (BnH2) and the methylene oxazoline protons (OxCH2) respectively, the OxCH2 protons also correlate to N_3.

By utilising the correlations described, the δN for the Au(I)NHC-complexes **8a,b** (blue) are easily assigned ($\delta N_{18a,b}$=190.8, 190.8, $\delta N_{28a,b}$=179.7, 179.8, $\delta N_{38a,b}$=235.0, 234.1). The ^{1}H,^{15}N-HMBC of the *t*Bu-Au(I)NHC complex **8b** highlights the benzyllic diastereotope by rendering two peaks for the N_1-BnH2 correlation. This does not occur for the benzyllic protons belonging to *i*Pr-Au(I)NHC **8a**, which might be due to the N_1 signal only correlating to one of the benzyllic protons, or it might simply be due to the resolution of the spectrum.

Upon oxidation of the Au(I)NHC-complexes **8a,b** to their Au(III)NHC[Cl_3] counterparts **10a,b** the ^{1}H,^{15}N-HMBC of both complexes **10a,b** display several new ^{15}N signals in the range associated with the imidazole nitrogens (N_1, N_2). The ^{1}H-NMR of both Au(III)NHC[Cl_3] complexes **10a,b** show an acidic proton (δH=8.49, 8.40 ppm) which indicate the hydrolysis of the auxiliary oxazoline ligands. The range explored by the ^{1}H,^{15}N-HMBC experiment (160 - 350 ppm) is downfield of the area where amines are expected to appear (^{15}N $\approx$ 90), and as such, the nitrogen signals of the free amines do not appear in the produced spectrum.
The imidazole nitrogens of the Au(III)NHC[Cl_3] complexes **10a,b** (red) were elucidated by the peaks formed by the N_1-BnCH2,- and N_2-OxCH2 correlations ($\delta N_{1\,a,b}$=189.1, 188.9, $N_{2\,a,b}$=176.8, 177.0) The oxazoline nitrogen N_3 was easily elucidated by its correlation to the OxCH2 protons ($\delta N_{3\,a,b}$=239.6, 234.1).

The preparation of the Au(III)NHC[Cl_3] complexes **10a,b** by oxidation of the Au(I)NHC-complexes **8a,b** caused a marginal shift of the nitrogen signals. The values of these shifts are expressed by the value $\Delta\delta N^{ox}$, which is defined by eq. (3.1)

$$\Delta\delta N^{ox} = \delta N^{\mathrm{Au(I)}} - \delta N^{\mathrm{Au(III)Cl_3}} \tag{3.1}$$

A positive $\Delta\delta$N value indicates an upfield shift of the nitrogen signal, whilst a negative value represents a downfield shift. This correlation translates further to imply that a positive $\Delta\delta N^{ox}$ value for a nitrogen atom corresponds to a decreased electron density around the nitrogen nuclei, whilst a negative $\Delta\delta$N translates to an increased electron density around the N-nuclei.

The oxidation of the *i*Pr-Au(I)NHC-complex **8a** to the corresponding Au(III)NHC[Cl_3]-complex **10a** caused a marginal upfield shift of the N_1 and N_2 nitrogens ($\Delta\delta N^{ox}_{1a}$ = 1 7 ppm, $\Delta\delta N^{ox}_{2a}$ = 2 9 ppm). This upfield shift was mirrored by a downfield shift of the N_3 oxazoline nitrogen ($\Delta\delta N^{ox}_{3a}$ = $-$4 6 ppm). The observed $\Delta\delta N^{ox}$ values correspond to the expected changes followed by a displacement of the oxazoline ring by the three chloride anions of the Au(III)NHC-complex **10a** that are more spatially demanding than the single chloride anion of the Au(I)NHC-complex **8a**. The displacement moves the oxazoline nitrogen (N_3) away from the acidic gold(III) centre, causing the N_3 to donate less electron density away from its nitrogen nucleus, as is mirrored by the negative $\Delta\delta N^{ox}_3$ value. The decreased electron donation from the displaced oxazoline is countered by an increased electron donation from the imidazolium nitrogens N_1 and N_2, which corresponds to the positive $\Delta\delta N^{ox}_1$ and $\Delta\delta N^{ox}_2$ values.

The same trends as observed for the oxidation of the *i*Pr-Au(I)NHC complex **8a** occur for its *t*Bu-Au(I)NHC counterpart **8b**. The imidazole nitrogens N_1 and N_2 experience an upfield shift, $\Delta\delta N^{ox}_{1b}$ = 1 9 ppm, $\Delta\delta N^{ox}_{2a}$ = 2 8 ppm respectively. While the oxazoline nitrogen N_3 experienced a downfield shift, $\Delta\delta N^{ox}_{3b}$ = $-$3 8 ppm.

The slight geometrical reconfiguration of the Au(I)NHC-complexes **8a,b** upon oxidation to the Au(III)NHC[Cl_3]-complexes **10a,b** also presents itself in the ^{1}H-NMR spectra of the compounds. (fig. 3.17, fig. 3.19).

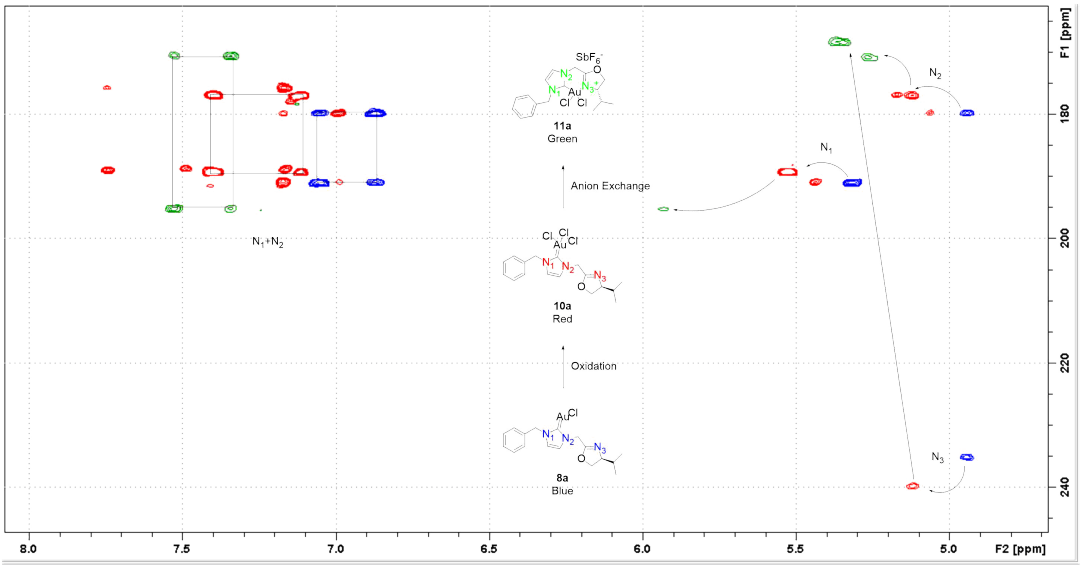

Figure 3.16: Overlapping ^{1}H,^{15}N-HMBC of the Au(I)NHC-complex **8a** (blue), Au(III)NHC-complex **10a** (red), and bidentate C,N-Au(III)NHC[Oxazoline] complex **11a** (green).

Due the non-isolated reaction mixture, the imidazole protons (H4, H5) does not immediately present themselves, but analysis of the ^{1}H,^{15}N-HMBC correlations indicate that they are present at δH4=7.36, H5=7.08 ppm and δ =H4=7.29, H5=7.00 ppm for the Au(III)NHC[Cl_3]-complexes **10a** and **10b** respectively.
The Au(III)NHC[Cl_3] imidazole protons appear at significantly higher shifts than their Au(I)NHC equivalents, which indicates that the imidazole ring donates more electron density to the gold(III) centre compared to the previous gold(I) centre.[109] These shifts are expected as the Au-centre atom obtaines a greater charge ($Au^{+} \longrightarrow Au_3{}^{+}$)-

The benzyllic protons (BnH2) and methylene oxazoline protons (OxCH2) also experience a similar downfield shift, although at a lesser extent than the imidazole protons. The two signals do however undergo a distinct change. The benzyllic protons are diastereotopic, and appear as two signals in the ^{1}H-NMR of the Au(I)NHC-complexes **8a,b**, but reappear as a singlet in the Au(III)NHC[Cl_3]-complexes at **10a,b**, at δH=5.89 and 5.41 ppm respectively.
The diastereotopic methylene oxazoline protons however, appear as a singlet in the Au(I)NHC-complexes **8a,b** at δH=4.94. Upon oxidation to the Au(III)NHC[Cl_3] complexes **10a,b**, the OxCH2 protons reappear as two signals. This change implies that the Au(I)NHC-complexes **8a,b** are spatially arranged in a way that enforce a chiral environment on the benzyllic protons, while the OxCH2 protons are interchangeable. This might occur by the Au(I)-atom attracting the π-system of the benzene so it orientates to place the π system perpendicular to coordination plane of the gold(I) centre.[110]
Upon oxidation to the Au(III)NHC[Cl_3]-complexes **10a,b**, this geometry changes, and rather enforces a chiral environment on the methylene oxazoline protons instead of the BnH2 protons. It can also be observed that the diastereotopic methylene oxazoline protons of the *t*Bu-Au(III)NHC[Cl_3]-complex **10b** are split further apart than the OxCH2 protons of the *i*Pr-Au(III)NHC[Cl_3] complex **10a**, which indicates that the *tert*-butyl oxazoline of the complex **10b** experiences a more rigid environment.
Each of the diasteretopic OxCH2 protons correlate independently with both the N_2,-

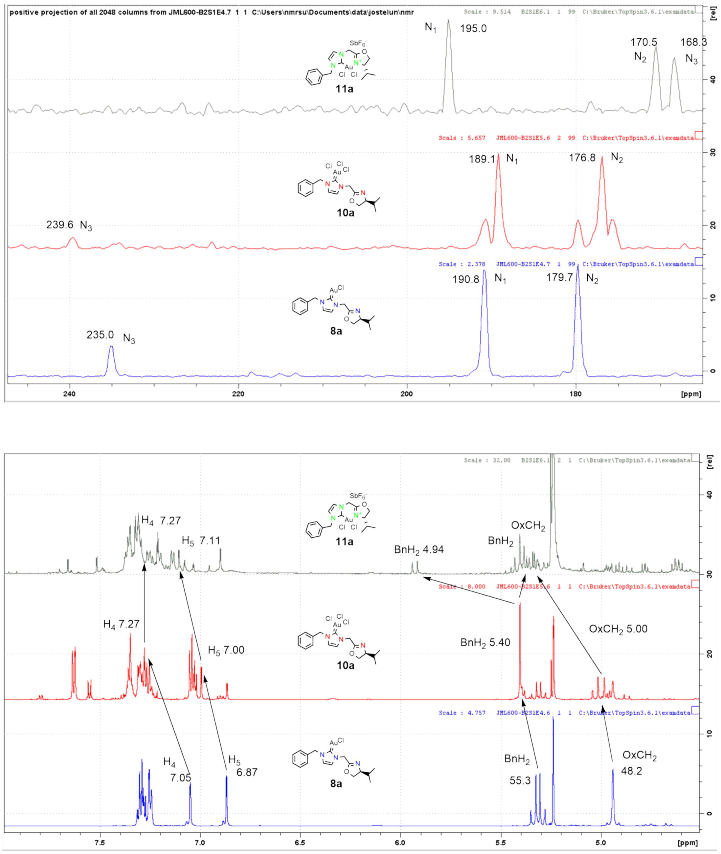

Figure 3.17: Individual 1D ^{15}N,- and ^{1}H-NMR for the complexes **8a, 10a,** and **11a**

and N_3-nitrogen of the Au(III)NHC[Cl_3]-complex **10b**, and the N_2-nitrogen of the corresponding *i*Pr-Au(III)NHC[Cl_3] complex **10a**.

Elucidation of the ^{1}H,^{15}N-HMBC of the bidentate C,N-Au(III)NHC[Oxazoline] complexes **11a,b** afforded from the Au(III)NHC[Cl_3]-complexes **10a,b** by anion exchange proved to be more complicated than the previous ^{1}H,^{15}N-HMBC spectra. This is in large due to the cluttered ^{1}H-NMR spectrum, caused by the impure mixture analysed, complicating the elucidation of the protons contributing to the correlation peaks of the ^{1}H,^{15}N-HMBC spectra.
The ^{1}H,^{15}N-HMBC spectrum of the bidentate C,N-Au(III)NHC[*i*Pr-Oxazoline] **11a** displayed three distinct ^{15}N-signals at δ=195, 170.5, and 168.3 ppm. The distinct imidazole N_1, N_2, H4, H5 correlations in the upper left part of the spectrum implies that $\delta N_3 = 168\ 3$ ppm. It would be expected that the N_3 nitrogen correlates to the methylene oxazoline protons.

The OxCH2 protons have previously shown that their two diastereotopic protons can correlate independently to the N_2 and N_3-nitrogens. Keeping this in mind, an argument can be made that the adjacent correlation peak at δH,η=5.27, 170.7 ppm belongs to the imidazole nitrogen N_2. This leaves the δN=195.0 ppm as the N_1 nitrogen.
The N_1-nitrogen does produce a small correlation peak at δH,η=5.94, 195.0 ppm, which corresponds to a doublet in the ^{1}H-NMR spectrum of the C,N-Au(III)NHC[Oxazoline] complex **11a** (δH=5.94 ppm, J=15.00 (Hz)). The ^{1}H-NMR signal at δH=5.94 is small,

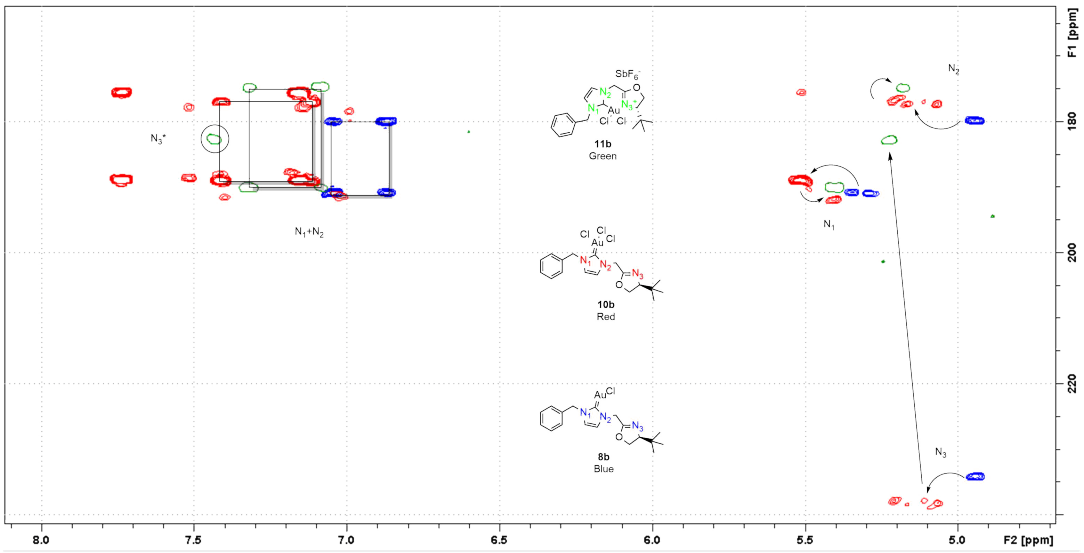

Figure 3.18: Overlapping ^{1}H,^{15}N-HMBC of the Au(I)NHC-complex **8b** (blue), Au(III)NHC-complex **10b** (red), and bidentate C,N-Au(III)NHC[Oxazoline] complex **11b** (green).

but there are no other distinct proton signals that can be assigned to the C,N-Au(III)NHC[oxazoline] complex with certainty, so it can not be immediately dismissed. The signal also displays a slight roofing effect upfield, hinting at a coupling to another signal among the mulitplet at δH=5.5-5.3 ppm. A coupling constant of 15.0 Hz also corresponds well with a vicinal proton, and so the signal might belong to one of the benzyllic protons, which also implies that the benzyllic protons experience the same phenomeon as the methylene oxazoline protons, where the nitrogen signal only correlates to one of the two vicinal protons.

With the anion exchange of the Au(III)NHC[Cl_3]-complex **10a** to the bidentate C,N-Au(III)NHC[Oxazoline] complex **11a**, a need to express the changes in the δN shifts arose. An expression for this change is formulated in eq. (3.2). The values of $\Delta\delta N^{AE}$ express the same spectroscopic and physical implications as the values of $\Delta\delta N^{ox}$.

$$\Delta\delta N^{AE} = \delta N^{\text{Au(III)NHC[Cl}_3} - \delta N^{\text{C, N-Au(III)NHC}} \tag{3.2}$$

The $\Delta\delta N_a{}^{AE}$ for the anion exchange of the *i*Pr-Au(III)NHC[Cl_3]-complex **10a** to yield the bidentate *i*Pr-C,N-Au(III)NHC[Oxazoline]-complex **11a** becomes; $\Delta\delta N_{1a}{}^{AE}$= -5.9, $\Delta\delta N_{2a}{}^{AE}$= 6.3, and $\Delta\delta N_{1a}{}^{AE}$= 71.3 ppm. The huge upfield shift expressed by the $\Delta\delta N_{3a}{}^{AE}$ is the most significant evidence to argue the coordination of the oxazoline nitrogen atom (N_3) to the gold(III) centre. The massive upfield shift corresponds to a decreased shielding of the N_3-nuclei which occurs by the increased electron donation from the N_3-nitrogen to the acidic gold atom. The small positive value of $\Delta\delta N_{2a}{}^{AE}$=6.3 can be explained by the six-membered metallacycle which dislocates more of the electron density from the imidazole N_2-nitrogen. The negative value of $\Delta\delta N_{1a}{}^{AE}$=-5.9 stands apart as the only downfield N_1 shift which might be explained by its position outside the metallacycle.

Similar arguments as the ones used for the elucidation of the bidentate *iso*-propyl C,N-Au(III)NHC[Oxazoline] complex **11a** nitrogens, can also be applied for the elucidation of

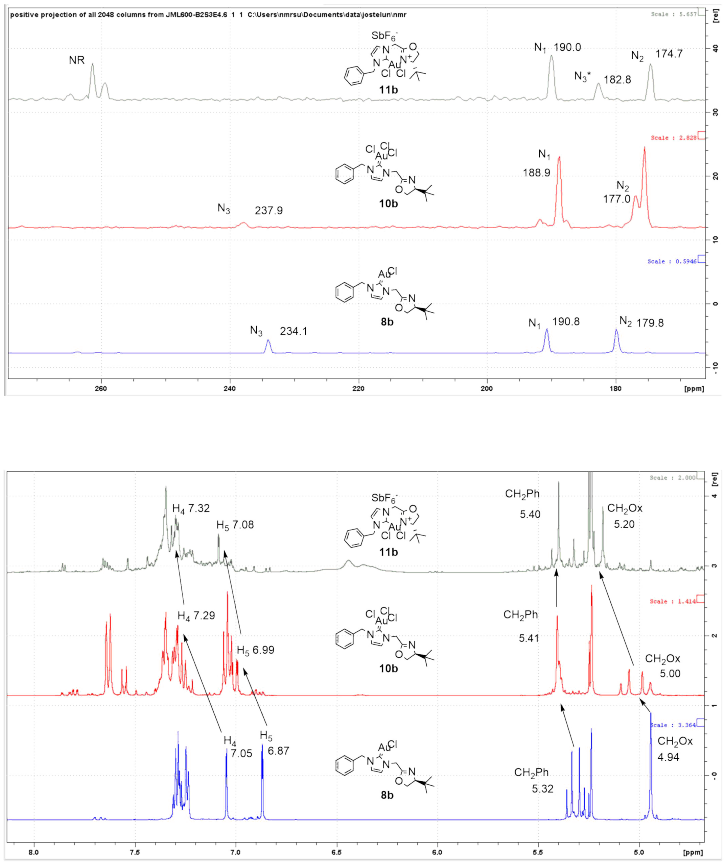

Figure 3.19: Caption

the bidentate C,N-*t*Bu-Au(III)NHC[Oxazoline] complex **11b** nitrogens. The distinct N_1, N_2, H4, and H5 correlations combined with the BnH2 and OxCH2 correlations affords the assigned nitrogens N_1= 190.0 ppm, and N_2= 174.7 ppm. This leaves N_3=182.8 ppm. Unlike the ^{1}H,^{15}N-HMBC for the bidentate C,N-Au(III) complex **11a**, the ^{1}H,^{15}N-HMBC of the C,N-Au(III) complex **11b** contains several nitrogen signals above δN=260 ppm, which correlate to protons in the δH=6.5-6.3 ppm region. Such signals imply the decomposition of the desired product **11b**. Further doubts about the formation of the bidentate C,N-complex **11b** can be made by the N_3 correlation to a proton in the aromatic region, that is not one of the imidazole protons H4, or H5.

While neither of the Au(III)NHC-complexes **10a, 10b, 11a,** or **11b** were isolated nor fully characterised by NMR, the observed $\Delta\delta N^{ox}$ and $\Delta\delta N^{AE}$ values strongly indicate that the Au(III)NHC[Cl_3]-complexes **10a,b** were formed, and the subsequent anion exchange successfully afforded the bidentate C,N-Au(III)NHC[Oxazoline] complex **11a**. ^{1}H,^{15}N-HMBC of the Au(III)NHC[Cl_3]-complexes **10a,b** visualize the instability of the Au(III)NHC[Cl_3] complexes, which are rapidly hydrolysed at the imine bond of the oxazoline. It might also be suggested that the more sterically demanding *t*Bu-oxazoline C,N-Au(III)NHC-complex **10b** is less easily formed due to repulsive steric interactions.

4 Conclusion

In this project, two unique N-Benzyl, N-methylene-(C_4-substitued)-Oxazoline imidazolium NHC precursors **7a** (*i*Pr-C_4) and **7b** (*t*Bu-C_4) have been prepared in three steps. Initial condensation of the chiral amino alcohols **1a,b** with 2-chloroacetyl chloride (**2**) yielded the corresponding chiral amides **3a,b** (52%, 37%). The amides **3a,b** underwent intramolecular dehydration facilitated by Burgess' reagent, to produce the chloromethylene oxazolines **5a,b** (80%, 76%). Halogen exchange and subsequent N-alkylation of oxazolines **5a,b** with 1-benzyl imidazole **6** to yield the imidazolium salts **7a,b** (50%, 77%) with an overall yield of 21% and 22%.

The imidazolium salts **7a,b** were coordinated to a gold(I) atom centre by transmetallation from a silver intermediate, which yielded the novel Au(I)NHC-complexes **8a,b** (69% and 18%). The Au(I)NHC-complexes **8a,b** and all intermediates were fully characterised by ^{1}H-NMR , ^{13}C-NMR , COSY, HSQC, HMBC, HRMS, and IR. The Au(I)NHC-complexes **8a,b** were additionally analysed by ^{1}H,^{15}N-HMBC .
The synthesis of the the imidazolium salts (**7a,b**) have the potential to be improved by a more selective amidation to more efficiently yield the amide intermediates (**3a,b**)

The coordination of the imidazolium salts (**7a,b**) to gold(I) afford large variations in the yield of the Au(I)-complexes **8a** (69%) and **8b** (18%). NHC precursor **7b** has a more sterically demanding *t*Bu ligand than the *i*Pr ligand of **7a**. As observed by ^{1}H-NMR of amides **3a,b**, the *tert*-butyl group in amide **3b** enforces a more demanding steric environment than the *iso*-propyl amide **3a**, which supports the theory that the preparation of the Au(I)NHC-complex **8b** is complicated by the more sterically hindered *t*Bu ligand than the *i*Pr-Au(I)NHC-complex **8a**.

The novel Au(I)NHC-complexes (**8a,b**) were oxidised to their corresponding Au(III)NHC[Cl_3]-complexes (**10a,b**) by halogen transfer from dichloro-iodobenzene and subsequent anion exchange to the bidentate C,N-Au(III)NHC[Oxazoline] complexes **11a,b**.
While neither of the four Au(III)-complexes were isolated nor fully characterised, their crude reaction mixtures were analysed by ^{1}H-NMR and ^{1}H,^{15}N-HMBC .

The changes in $\delta\eta$-shifts ($\Delta\delta N^{ox}$, $\Delta\delta N^{AE}$) for the nitrogens atoms by oxidation and anion exchange coordination strongly indicate the formation of the Au(III)NHC[Cl_3]complexes **10a,b** and the bidentate C,N-Au(III)NHC[Oxazoline] complex **11a**.

5 Experimental

Preparation of moisture sensitive compounds were performed under dry condition and inert atmoshphere. Dry solvents were collected from a MB SPS-800 solvent purification system. All reactions were monitored by ^{1}H-NMR and thin-layer chromatography (TLC) using silica gel 60 F254 (0.25 mm thickness). TLC plates were developed using UV-light (254 nm) phosphomolybdic acid, and heat. Flash chromatography was performed with Merck silica gel (poresize 60 Å, 230-400 mesh, 40-63 mm particlesize). ^{1}H-NMR and ^{13}C-NMR spectra were recorded using either a Bruker Avance DPX 400 MHz or a Bruker Avance III 600 MHz spectrometer. Chemical shifts are reported in ppm (δ) downfield from tetrametylsilane (TMS) as an internal standard. Accurate mass determination was performed on a S̈ynapt G2SQ̈-TOF instrument from Waters. Samples were ionized with an ASAP probe with no chromatography separation performed before mass analysis. IR spectra were recorded with a Nicolet 20SXC FT-IR spectrometer using EZ OMNIC software to analyse the spectra and a Bruker Alpha FT-IR spectrometer using OPUS V7 software to analyze the spectra.

5.1 Synthesis of Amides

5.1.1 General procedure A

Amine **1a-b** was added to a solution of anhydrous DCM and 1-1.2 equiv. triethylamine was added. The solution was cooled to 0^{o}Cusing an ice-bath and 1 equiv. of 2-chloro acetylchloride **2** was added dropwise over 3-5 minutes. The ice bath was then removed and the mixture was stirred at rt. for 3 - 26 hours
The solvent was removed *in vacuo*, which yielded a white residue that was washed with EtOAc, and filtered off. The product was dried and purified by silica flash chromatography (EtOAc) to afford the pure amides **3a-b**.

(S)-2-Chloro-N-(1-hydroxy-3-methylbutan-2-yl)acetamide (3a)

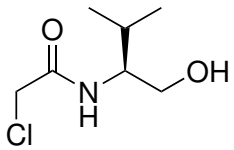

3a

Following general procedure A, **1a** (399.2 mg, 3.86 mmol) was reacted with **2** (438 mg, 309 µl, 3.88 mmol) in DCM (10 ml) in the prescene of NEt_3 (392 mg, 540 µl, 3.87 mmol). This yielded **3a** (361.7 mg, 2.01 mmol, 52%) as a dark oil after purification by flash column chromatography. ^{1}H-NMR (600 MHz, $CDCl_3$, 300K): δ(ppm)= 6.74 (br, 1H; N*H*), 4.10 (s, 2H; ClC*H2*), 3.76 (m, 1H; NHC*H*), 3.73 (d, 2H; C*H2*OH J(Hz)=4.70 Hz), 2.30 (br, 1H; O*H*), 1.96 (m, 1H; C*H*$(CH_3)_2$ J(Hz)=6.80), 0.99 (d, 3H; CH_3, J(Hz)=6.79), 0.96 (d, 3H; CH_3, J(HZ)=6.83); ^{13}C-NMR (151 MHz, $CDCl_3$, 300K): δ(ppm)=166.7 (*C*O), 63.5 (N*C*H*iPR*), 57.5 (*C*H_2OH, 42.8 (*C*H_2Cl), 28.9 (*C*H$(CH_3)_2$, 19.5 (*C*H_3), 18.6 (*C*H_3)
HRMS: 180.79 m/z = M+H

(S)-2-Chloro-N-(1-hydroxy-3,3-dimethylbutan-2-yl)acetamide (3b)

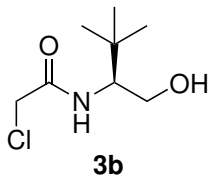

3b

Following general procedure A, **1b** (583.4 mg, 4.98 mmol) was reacted with **2** (567 mg, 400 µl, 5.02 mmol) in DCM (10 ml) in the prescene of NEt_3 (508 mg, 700 µl, 5.02 mmol). This yielded **3b** (357.1 mg, 1.844 mmol, 37%) as a yellow solid after purification by flash column chromatography. ^{1}H-NMR (600 MHz, $CDCl_3$, 300K): δ (ppm) = 6.76 (br, 1H; NH), 4.13 (s, 2H, CH_2Cl), 3.90 (dd, 1H; CH_2OH, J(Hz)=3.56, 11.5), 3.84 (m, 1H; NHCHtBU, J(Hz)=3.56, 7.58), 3.62 (dd, 1H; CH_2OH, J(Hz)=11.5, 7.58), 2.08 (br, 1H; OH) 0.99 (s, 9H; CH_3). ^{13}C-NMR 151 MHz, $CDCl_3$, 300K), 167.0, 63.0, 60.2, 42.9, 33.6, 26.9. HRMS: 194.095 m/z = M+H

5.2 Synthesis of Oxazolines

5.2.1 General procedure B

Amide **3a-b** was dissolved in anhydrous THF. 1 equiv. of **4** was added and the mixture was refluxed for 2-4 hours at 70^{o}C. THF was removed under reduced pressure and the resulting dark oil was purified by flash column cromatography, eluting with 4:1 Pentane:EtOAc.

5.2.2 (R)-2-(Chloromethyl)-4-isopropyl-4,5-dihydrooxazole (5a)

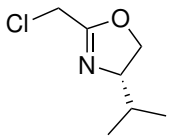

5a

Following general procedure B. **3a** (121.3 mg, 675 µmol) was reacted with **4** (161.3 mg, 675 µmol) in anhydrous THF (5 ml). This yielded the product as a colourless oil after purification, 108.4 mg (80%). ^{1}H-NMR (600 MHz, $CDCl_3$, 300K): δ (ppm) = 4.36 (t, 1H; CH_2O, J(Hz)=8.42, 9.69), 4.11 (s, 2H; CH_2Cl), 4.07 (t, 1H; CH_2O), J(Hz)=8.32), 3.97 (k, 1H; NCH, J(Hz)= 9.47, 8.18), 1.79 (o, 1H; CH(CH_3)$_2$, J(Hz)=6.74), 0.98 (d, 3H; CH_3, J(Hz)=6.76), 0.90 (d, 3H; CH_3, J(Hz)=6.76). ^{13}C-NMR (151 MHz, $CDCl_3$, 300K): δ (ppm) = 162.4, 72.5, 71.2, 36.5, 32.5, 18.7, 18.1. HRMS: 162.069 m/z = M+H

5.2.3 (R)-4-(*tert*-Butyl)-2-(chloromethyl)-4,5-dihydrooxazole (5b)

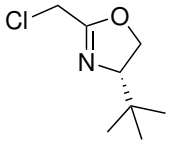

5b

Following general procedure B. **3b** (117.1 mg, 605 µmol) was reacted with **4** (152.8 mg, 641 µmol) in anhydrous THF (10 ml). This yielded the product as a colourless oil after purification 80.6 mg (76%). ^{1}H-NMR (600 MHz, $CDCl_3$, 300K): δ (ppm) = 4.29 (t, 1H; CH_2O, J(Hz)=10.17, 8.79), 4.16 (t, 1H; CH_2O, J(Hz)=8.43), 4.12 (d, 2H; CH_2Cl), 3.93 (t, 1H; NCH, J(Hz)=10.11, 8.19), 0.91 (s, 9H; CH_3). ^{13}C-NMR (151 MHz, $CDCl_3$, 300K): δ (ppm) = 162.3, 76.0, 69.7, 36.4, 33.7, 25.7. HRMS: 176.085 m/z = M+H.

5.3 Synthesis of Iodized Oxazolines

(R)-2-(Iodomethyl)-4-isopropyl-4,5-dihydrooxazole (13a)

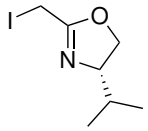

13a

3a (182.7 mg, 1.02 mmol) was dissolved in acetone (10 ml) and **4** (268.7 mg, 1.13 mmol) was added. The reaction was refluxed at 50^{o}Cfor 4.5 hours before the heat was turned off, and KI 180.2 mg, 1.09 mmol) was added, and the reaction was run overnight. The precipitated KCl was filtered off, and the product flashed, eluting with EtOAc. ^{1}H-NMR showed a highly contaminated product, and so it was flashed one more time (EtOAc). After this second run it appeared as if the product had completely decomposed.

5.4 Synthesis of Imidazolium Salts

5.4.1 General procedure C

The oxazoline **3a-b**, was dissolved in acetone and 1 equiv. of KI was added. The reaction was let stir at rt for 1-3 hours before the precipitated solid was filtered off and the solvent removed. The new iodized oxazoline (**9a-b**) was dissolved in anhydrous MeCN and 1 equiv. of 1-benzyl-1H-imidazole (**6**) was added. The reaction was run at rt (2-20 hours). The solvent was removed, and the product was purified by silica column chromatography, eluting with 1:5 MeOH:DCM.

5.4.2 (R)-1-Benzyl-3-((4-isopropyl-4,5-dihydrooxazol-2-yl)methyl)-1H-imidazol-3-ium iodide (7a)

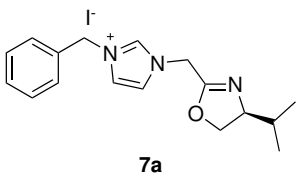

7a

Following general procedure C, **5a** (26.3 mg, 163 µmol) was reacted with KI 28.4 mg, 171 µmol) in acetone (2 ml. The formed product was reacted further with **6** (28.4 mg, 180 µmol) in MeCN (10 ml). This yielded the product as a dim yellow solid after purification, (33.5 mg, 50%). ^{1}H-NMR (600 MHz, $CDCl_3$, 300K): δ (ppm) = 10.45 (s, 1H;

NC*H*N), 7.47-7.43 (m, 5H; Ar – *H*), 7.36 (s, 1H; Imid C*H*), 7.12 (s, 1H; Imid C*H*), 5.54 (s, 2H; ArCH_2), 5.25 (k, 2H; OxCH_2), 4.40 (t, 1H; OCH_2, J(Hz)=9.55), 4.08 (t, 1H; OCH_2, J(Hz)=8.42), 3.91 (k, 1H; OxC*H*, J(Hz)=8.42), 1.72 (o, 1H; C*H*(CH_3)$_2$, J(Hz)=6.75), 0.92 (d, 3H; CH_3, J(Hz)=6.75), 0.86 (d, 3H; CH_3, J(Hz)=6.75). ^{13}C-NMR (151 MHz, $CDCl_3$, 300K): δ (ppm) = 159.3, 138.1, 131.9, 129.9, 129.7, 129.2, 123.0, 121.1, 72.4, 72.0, 53.9, 46.6, 32.6, 18.8, 18.4. HRMS: 284.177 m/z = M+

5.4.3 (R)-1-Benzyl-3-((4-(tert-butyl)-4,5-dihydrooxazol-2-yl)methyl)-1H-imidazol-3-ium iodide (7b)

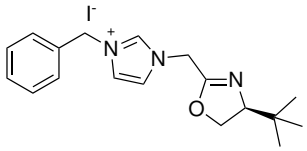

7b

Following general procedure C, **5b** (14.3 mg, 81 µmol) was reacted with KI (15.2 mg, 92 µmol) in acetone (2 ml). The formed product was reacted further with **6** (13.3 mg), 84 µmol) in MeCN (10 ml). This yielded the product as a dim yellow solid after purification, (26.6 mg, 77%). ^{1}H-NMR (600 MHz, $CDCl_3$, 300K): δ (ppm) = 10.38 (s, 1H; NC*H*N), 7.46-7.43 (m, 5H; Ar*H*), 7.37 (s, 1H; Imid C*H*), 7.14 (s, 1H; Imid C*H*), 5.55 (s, 2H; ArCH_2), 5.25 (k, 2H; OxCH_2), 4.33 (t, 1H; OCH_2, J(Hz)=9.49), 4.16 (t, 1H; OCH_2, J(Hz)=8.61), 3.89 (t, 1H; OxC*H*, J(Hz)=9.35), 0.85 (s, 9H; CH_3). ^{13}C-NMR (151 MHz, $CDCl_3$, 300K) δ (ppm)= 159.3, 138.1, 131.9, 129.9, 129.7, 129.1, 123.0, 121.2, 75.8, 70.3, 53.9, 46.6, 33.5, 25.8. HRMS: 288.192 m/z = M+

5.5 Synthesis of Au(I)-NHC complexes

5.5.1 General Procedure D

The imidazole salt **7** was dissolved in dry DCM, 0.5-1.5 equiv. of Ag_2O was added and the mixture was stirred at rt for 1-2 hours. After deprotonation, the mixture was filtered through celite, and the solvent was removed. The formed residue was dissolved dry DCM and 1 equiv. of Au(SMe_2)Cl was added. The mixture was stirred at rt for 1-4.5 hours before the mixture was filtered through celite and purified by flash column chromatography eluting with EtOAc.

5.5.2 (1-Benzyl-3-(((S)-4-isopropyl-4,5-dihydrooxazol-2-yl)methyl)-2,3-dihydro-1H-imidazol-2-yl)gold(I) chloride (8a)

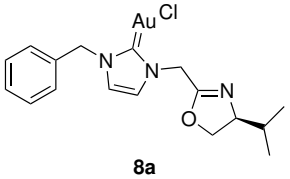

8a

Following general procedure D, imidazole **7a** (8.7 mg, 21 µmol) was reacted with Ag_2O (3.8 mg, 16 µmol) in DCM (2 ml). The formed product was further reacted with $Au(SMe_2)Cl$ (6.4 mg, 22 µmol) in DCM (2 ml). This caused the solution to take on a cloudy shade which slowly turned into a solid purple. The reaction yielded **8a** as a weakly yellow solid after purification, (7.5 mg, 69%). ^{1}H-NMR (600 MHz, CD_2Cl_2, 300K): δ (ppm) = 7.3017.24 (m, 5H; Ar-H), 7.05 (s, 1H; Imid-C*H*), 6.87 (s, 1H; Imid-C*H*), 5.32 (q, 2H; ArCH_2), 4.94 (s, 2H; OxCH_2), 4.25 (t, 1H; OCH_2, J(Hz)=9.12), 3.97 (t, 1H; OCH_2, J(Hz)=7.64), 3.85 (k, 1H; OxC*H*, J(Hz)=8.01), 1.65 (o, 1H; C*H*$(CH_3)_2$, J(Hz)=6.68), 0.85 (d, 3H; CH_3, J(Hz)=6.75), 0.78 (d, 3H; CH_3, J(Hz)=6.76). ^{13}C-NMR (151 MHz, CD_2Cl_2, 300 K): δ (ppm) = 172.7, 160.9, 135.4, 129.2, 128.8, 128.1, 122.2, 120.9, 72.5, 71.5, 55.3, 48.2, 32.7, 18.5. ^{15}N-NMR (61 MHz, CD_2Cl_2, 300K): δ (ppm) = 235.0 (Imin-N), 190.8 (Bn-N), 179.7 (Oxazoline-N). HRMS: 521.162 m/z = M+ MeCN - Cl

5.5.3 (1-Benzyl-3-(((S)-4-(tert-butyl)-4,5-dihydrooxazol-2-yl)methyl)-2,3-dihydro-1H-imidazol-2-yl)gold(I) chloride (8b)

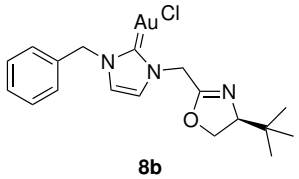

8b

Following general procedure D, imidazole **7b** (49.8 mg, 117 µmol) was reacted with Ag_2O (13.6 mg, 59 µmol) in DCM (2 ml). The formed product was further reacted with $Au(SMe_2)Cl$ (37.3 mg, 127 µmol) in DCM (1 ml). This caused the solution to instantly take on a cloudy yellow shade. The reaction yielded **8b** as a weakly yellow solid after purification (11.4 mg, 18%). ^{1}H-NMR (600 MHz, CD_2Cl_2, 300K): δ (ppm) = 7.31- 7.24 (m, 5H; Ar-H), 7.05 (s, 1H; Imid-C*H*), 6.87 (s, 1H; Imid-C*H*), 5.32 (q, 2H; ArCH_2), 4.94 (s, 2H; OxCH_2), 4.19 (t, 1H; OCH_2), J(Hz) = 10.02, 8.90), 4.07 (t, 1H; OCH_2, J(Hz)=8.39), 3.81 (t, 1H; OxC*H*, J(Hz)=9.90, 8.21), 0.79 (s, 9H; C*H*$(CH_3)_2$). ^{13}C-NMR (151 MHz, CD_2Cl_2, 300 K): δ (ppm) = 172.6, 160.8, 135.3, 129.0, 128.6, 127.8, 122.0, 120.8, 75.8, 69.8, 55.1, 48.0, 33.5, 25.5. ^{15}N-NMR (61 MHz, CD_2Cl_2, 300K): δ (ppm) = 234.1 (Imin-N), 190.8 (Bn-N), 179.8 (Oxazoline-N). HRMS: 535.178 m/z = M+ MeCN - Cl

5.6 Synthesis of Au(III)NHC[Cl_3] complexes

5.6.1 General Procedure E

The Au(I) complex **8** was dissolved in deuterated DCM and 1 equiv. of **9** was added. The mixture was stirred at rt for 30 min before the product was precipitated from solution by addition of pentane. The formed residue was washed with pentane, before the residue was directly diluted in deuterated DCM and 1 equiv. of $AgSbF_6$ was added. The mixture was stirred at rt for 15 minutes before it was filtered through celite and dried *in vacuo*. The product was then recrystallised from DCM/pentane.

5.6.2 (S)-(1-Benzyl-3-((4-isopropyl-4,5-dihydrooxazol-2-yl)methyl)-1,3-dihydro-2H-imidazol-2-ylidene)gold(III) chloride (10a)

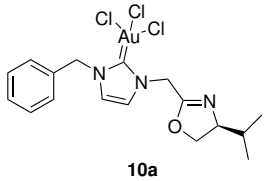

10a

Following general procedure E, **8a** (8.0 mg, 16 µmol) was dissolved in DCM (0.5 ml) and **9** (4.4 mg, 16 µmol) The formed product was directly reacted further after recrystalization. ^{15}N-NMR (61 MHz, CD_2Cl_2, 300K): δ (ppm) = 239.6 (Imin-N), 189.1 (Bn-N), 176.8 (Oxazoline-N).

5.6.3 (S)-(1-Benzyl-3-((4-(tert-butyl)-4,5-dihydrooxazol-2-yl)methyl)-1,3-dihydro-2H-imidazol-2-ylidene)gold(III) chloride (10b)

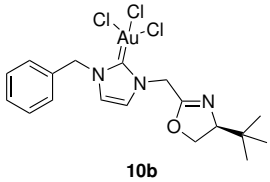

10b

Following general procedure E, **8b** (10.2 mg, 19 µmol) was dissolved in DCM (0.5 ml) and **9** (5.7 mg, 21 µmol) The formed product was directly reacted further after recrystalization. ^{15}N-NMR (61 MHz, CD_2Cl_2, 300K): δ (ppm) = 237.9 (Imin-N), 188.9 (Bn-N), 177.0 (Oxazoline-N).

5.7 Synthesis of Bidentate C,N-Au(III)NHC[Oxazoline] complexes

5.7.1 (S)-(1-Benzyl-3-((4-isopropyl-4,5-dihydrooxazol-2-yl)methyl)-1,3-dihydro-2H-imidazol-2-ylidene) bidentate C,N-gold(III) dichloride-antimony hexafluoride (11a)

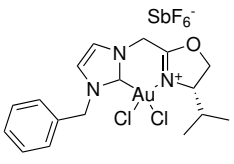

11a

After precipitation from DCM, **10a** (2.0 mg, 3 µmol) was dissolved in DCM (0.5 ml) and $AgSbF_6$ (0.8 mg, 5.2 µmol). The formed product was unsuccessfully recrystallised from pentane and DCM. ^{15}N-NMR (61 MHz, CD_2Cl_2, 300K): δ (ppm) = 195.0 (Bn-N), 170.5 (Oxazoline-N), 168.3 (Imin-N).

5.7.2 (S)-(1-Benzyl-3-((4-(tert-butyl)-4,5-dihydrooxazol-2-yl)methyl)-1,3-dihydro-2H-imidazol-2-ylidene) bidentate C,N-gold(III) dichloride-antimony hexafluoride (11b)

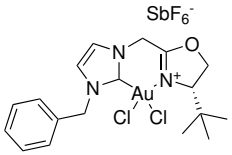

11b

After precipitation from DCM, **10b** was dissolved in DCM (0.5 ml) and $AgSbF_6$ (6.6 mg, 19 µmol). The formed product was unsuccessfully recrystallised from pentane and DCM.

References

[1] Georgiana Hedesan Stephen Skinner, Rafal T. Prinke and Jocely Godwin. *Splendor Solis*. Watkins, 2019.

[2] American Mueseum of Natural History. Golden ages.

[3] Royal Society of Chemistry. Alchemy, gold.

[4] American Mueseum of Natural History. Sweat of the sun.

[5] American Mueseum of Natural History. Crossroads of gold.

[6] Royal Society of Chemistry. Alchemy.

[7] American Mueseum of Natural History. Gold properties.

[8] Harold H. Harris. Is it real gold? *Journal of Chemical Education*, 76(2):198, 1999.

[9] J. Marsden and I. House. *The Chemistry of Gold Extraction*. Society for Mining, Metallurgy, and Exploration, 2006.

[10] Andreas Rubo, Raf Kellens, Jay Reddy, Norbert Steier, and Wolfgang Hasenpusch. *Alkali Metal Cyanides*. American Cancer Society, 2006.

[11] H Schmidbaur. Gold-chemie: ein eldorado. *Naturwissenschaftliche Rundschau*, 48(12):443–451, 1995.

[12] Lüder-Ulrich Meyer and Armin [de Meijere]. Gold catalysed rearrangements of strained small ring hydrocarbons. *Tetrahedron Letters*, 17(6):497 – 500, 1976.

[13] Masatake Haruta, Tetsuhiko Kobayashi, Hiroshi Sano, and Nobumasa Yamada. Novel gold catalysts for the oxidation of carbon monoxide at a temperature far below 0 °c. *Chemistry Letters*, 16(2):405–408, 1987.

[14] G.J. Hutchings. Vapor phase hydrochlorination of acetylene: Correlation of catalytic activity of supported metal chloride catalysts. *Journal of Catalysis*, 96(1):292 – 295, 1985.

[15] A. Stephen K. Hashmi and Graham J. Hutchings. Gold catalysis. *Angewandte Chemie International Edition*, 45(47):7896–7936, 2006.

[16] C. Rhodes, G.J. Hutchings, and A.M. Ward. Water-gas shift reaction: finding the mechanistic boundary. *Catalysis Today*, 23(1):43 – 58, 1995. Recent Advances in C1 Chemistry.

[17] Donka Andreeva, Vasko Idakiev, Tatjana Tabakova, Atanas Andreev, and Rudolf Giovanoli. Low-temperature water-gas shift reaction on au/α-fe2o3 catalyst. *Applied Catalysis A: General*, 134(2):275 – 283, 1996.

[18] Don Cameron, Richard Holliday, and David Thompson. Gold's future role in fuel cell systems. *Journal of Power Sources*, 118(1):298 – 303, 2003. Scientific Advances in Fuel Cell Systems.

[19] N Lopez, T.V.W Janssens, B.S Clausen, Y Xu, M Mavrikakis, T Bligaard, and J.K Nørskov. On the origin of the catalytic activity of gold nanoparticles for low-temperature co oxidation. *Journal of Catalysis*, 223(1):232 – 235, 2004.

[20] J.K. Nørskov, T. Bligaard, A. Logadottir, S. Bahn, L.B. Hansen, M. Bollinger, H. Bengaard, B. Hammer, Z. Sljivancanin, M. Mavrikakis, Y. Xu, S. Dahl, and C.J.H. Jacobsen. Universality in heterogeneous catalysis. *Journal of Catalysis*, 209(2):275 – 278, 2002.

[21] Rudy Coquet, Kara L. Howard, and David J. Willock. Theory and simulation in heterogeneous gold catalysis. *Chem. Soc. Rev.*, 37:2046–2076, 2008.

[22] H.H. Kung, M.C. Kung, and C.K. Costello. Supported au catalysts for low temperature co oxidation. *Journal of Catalysis*, 216(1):425 – 432, 2003. 40th Anniversary Commemorative Issue.

[23] Geoffrey C. Bond and David T. Thompson. Gold-catalysed oxidation of carbon monoxide. *Gold Bulletin*, 33:41–50, 2000.

[24] Takashi Takei, Tomoki Akita, Isao Nakamura, Tadahiro Fujitani, Mitsutaka Okumura, Kazuyuki Okazaki, Jiahui Huang, Tamao Ishida, and Masatake Haruta. Chapter one - heterogeneous catalysis by gold. volume 55 of *Advances in Catalysis*, pages 1 – 126. Academic Press, 2012.

[25] Masatake Haruta. Spiers memorial lecture role of perimeter interfaces in catalysis by gold nanoparticles. *Faraday Discuss.*, 152:11–32, 2011.

[26] Graham J. Hutchings. Heterogeneous gold catalysis. *ACS Central Science*, 4(9):1095–1101, 2018.

[27] Yi-Ming Wang, Aaron D. Lackner, and F. Dean Toste. Development of catalysts and ligands for enantioselective gold catalysis. *Accounts of Chemical Research*, 47(3):889–901, 2014.

[28] Hashmi K. Stephen, A. Homogeneous catalysis by gold. *Gold Bull*, 37:51–65, 2004.

[29] Weiwei Zi and F. Dean Toste. Recent advances in enantioselective gold catalysis. *Chem. Soc. Rev.*, 45:4567–4589, 2016.

[30] Yoshihiko Ito, Masaya Sawamura, and Tamio Hayashi. Catalytic asymmetric aldol reaction: reaction of aldehydes with isocyanoacetate catalyzed by a chiral ferrocenylphosphine-gold (i) complex. *Journal of the American Chemical Society*, 108(20):6405–6406, 1986.

[31] J. Henrique Teles, Stefan Brode, and Mathieu Chabanas. Cationic Gold(I) Complexes: Highly Efficient Catalysts for the Addition of Alcohols to Alkynes. *Angewandte Chemie International Edition*, 37(10):1415–1418, 6 1998.

[32] Sohail Anjum Shahzad, Muhammad Aamir Sajid, Zulfiqar Ali Khan, and Daniel Canseco-Gonzalez. Gold catalysis in organic transformations: A review. *Synthetic Communications*, 47(8):735–755, 2017.

[33] Phil Ho Lee, Heechul Kim, Kooyeon Lee, Misook Kim, Kwanghyun Noh, Hyunseok Kim, and Dong Seomoon. The indium-mediated selective introduction of allenyl and propargyl groups at the c4-position of 2-azetidinones and the aucl3-catalyzed cyclization of 4-allenyl-2-azetidinones. *Angewandte Chemie International Edition*, 44(12):1840–1843, 2005.

[34] Naoki Asao, Kumiko Takahashi, Sunyoung Lee, Taisuke Kasahara, and Yoshinori Yamamoto. Aucl3-catalyzed benzannulation: Synthesis of naphthyl ketone derivatives from o-alkynylbenzaldehydes with alkynes. *Journal of the American Chemical Society*, 124(43):12650–12651, 2002. PMID: 12392398.

[35] Rashmi Roy, Ashok Kumar Palanivel, Asadulla Mallick, and Yashwant D. Vankar. Aucl3- and aucl3-phenylacetylene-catalyzed glycosylations by using glycosyl trichloroacetimidates. *European Journal of Organic Chemistry*, 2015(18):4000–4005, 2015.

[36] A. Stephen K. Hashmi, Lothar Schwarz, Ji-Hyun Choi, and Tanja M. Frost. A new gold-catalyzed c-c bond formation. *Angewandte Chemie International Edition*, 39(13):2285–2288.

[37] Francis Medcalf Dean. Naturally occurring oxygen ring compounds. 1963.

[38] WQ Fan. In comprehensive heterocyclic chemistry ii; katritzky, ar; rees, cw; scriven, efv, eds. *Pergamon Press: New York, NY, USA*, 4:1–126, 1996.

[39] Tuanli Yao, Xiaoxia Zhang, and Richard C. Larock. Aucl3-catalyzed synthesis of highly substituted furans from 2-(1-alkynyl)-2-alken-1-ones. *Journal of the American Chemical Society*, 126(36):11164–11165, 2004. PMID: 15355093.

[40] A. Stephen K. Hashmi, Tanja M. Frost, and Jan W. Bats. Gold catalysis: On the phenol synthesis. *Organic Letters*, 3(23):3769–3771, 2001. PMID: 11700134.

[41] Hassan Rabaâ, Bernd Engels, Thomas Hupp, and A. Stephen K. Hashmi. Theoretical study of the reaction of alkynes with furan catalyzed by aucl3 and aucl. *International Journal of Quantum Chemistry*, 107(2):359–365, 2007.

[42] Ruming Yuan and Zhenyang Lin. Mechanistic insight into the gold-catalyzed carboxylative cyclization of propargylamines. *ACS Catalysis*, 5(5):2866–2872, 2015.

[43] Benito Alcaide, Pedro Almendros, José M. Alonso, Eduardo Busto, Israel Fernández, M. Pilar Ruiz, and Gulinigaer Xiaokaiti. Versatile synthesis of polyfunctionalized carbazoles from (3-iodoindol-2-yl)butynols via a gold-catalyzed intramolecular iodine-transfer reaction. *ACS Catalysis*, 5(6):3417–3421, 2015.

[44] Cang-Hai Shen, Long Li, Wei Zhang, Shuang Liu, Chao Shu, Yun-Er Xie, Yong-Fei Yu, and Long-Wu Ye. Gold-catalyzed tandem cycloisomerization/functionalization of in situ generated α-oxo gold carbenes in water. *The Journal of organic chemistry*, 79(19):9313–9318, 2014.

[45] Stefan RK Minkler, Nicholas A Isley, Daniel J Lippincott, Norbert Krause, and Bruce H Lipshutz. Leveraging the micellar effect: gold-catalyzed dehydrative cyclizations in water at room temperature. *Organic letters*, 16(3):724–726, 2014.

[46] Bin Pan, Xiaodong Lu, Chunxiang Wang, Yancheng Hu, Fan Wu, and Boshun Wan. Gold (i)-catalyzed intra-and intermolecular alkenylations of β-yne-pyrroles: Facile formation of fused cycloheptapyrroles and functionalized pyrroles. *Organic letters*, 16(8):2244–2247, 2014.

[47] Hirofumi Ueda, Minami Yamaguchi, Hiroshi Kameya, Kenji Sugimoto, and Hidetoshi Tokuyama. Autotandem catalysis: synthesis of pyrroles by gold-catalyzed cascade reaction. *Organic letters*, 16(18):4948–4951, 2014.

[48] Christian A. Sperger, Jørn E. Tungen, and Anne Fiksdahl. Gold(i)-catalyzed reactions of propargyl esters with vinyl derivatives. *European Journal of Organic Chemistry*, 2011(20-21):3719–3722, 2011.

[49] Naseem Iqbal, Christian A. Sperger, and Anne Fiksdahl. Gold(i)-catalysed alkene cycloaddition reactions of propargyl acetals. *European Journal of Organic Chemistry*, 2013(5):907–914, 2013.

[50] Naseem Iqbal and Anne Fiksdahl. Gold(i)-catalyzed benz[c]azepin-4-ol synthesis by intermolecular [5 + 2] cycloaddition. *The Journal of Organic Chemistry*, 78(16):7885–7895, 2013. PMID: 23808661.

[51] Sigvart Evjen and Anne Fiksdahl. Gold(i)-catalysed [3+3] cycloaddition of propargyl acetals and nitrones. *Tetrahedron*, 72(23):3270 – 3276, 2016.

[52] Helgi Freyr Jónsson, Sigvart Evjen, and Anne Fiksdahl. Gold(i)-catalyzed [2 + 2 + 2] cyclotrimerization of 1,3-diarylpropargyl acetals. *Organic Letters*, 19(9):2202–2205, 2017.

[53] Huey-San Melanie Siah, Maya Kaur, Naseem Iqbal, and Anne Fiksdahl. Gold(i)-catalysed tandem cyclisation of propargyl acetals and vinyl esters. *European Journal of Organic Chemistry*, 2014(8):1727–1740, 2014.

[54] Huey-San Melanie Siah, Morten Christian Hogsnes, Naseem Iqbal, and Anne Fiksdahl. Gold(i)-catalysed tandem cyclization of propargyl acetals and alkynes. *Tetrahedron*, 72(8):1058 – 1068, 2016.

[55] Longwu Ye, Yanzhao Wang, Donald H. Aue, and Liming Zhang. Experimental and computational evidence for gold vinylidenes: Generation from terminal alkynes via a bifurcation pathway and facile c–h insertions. *Journal of the American Chemical Society*, 134(1):31–34, 2012. PMID: 22176593.

[56] A. Stephen K. Hashmi, Ingo Braun, Matthias Rudolph, and Frank Rominger. The role of gold acetylides as a selectivity trigger and the importance of gem-diaurated species in the gold-catalyzed hydroarylating-aromatization of arene-diynes. *Organometallics*, 31(2):644–661, 2012.

[57] Ximei Zhao, Matthias Rudolph, and A. Stephen K. Hashmi. Dual gold catalysis – an update. *Chem. Commun.*, 55:12127–12135, 2019.

[58] A. Stephen K. Hashmi. Dual gold catalysis. *Accounts of Chemical Research*, 47(3):864–876, 2014. PMID: 24533563.

[59] Steffen Mader, Lise Molinari, Matthias Rudolph, Frank Rominger, and A. Stephen K. Hashmi. Dual gold-catalyzed head-to-tail coupling of iodoalkynes. *Chemistry - A European Journal*, 21(10):3910–3913, 2015.

[60] Huey-San Melanie Siah and Anne Fiksdahl. Dual-gold(i)-generated trifluoromethylation of terminal alkynes with togni's reagent. *Journal of Fluorine Chemistry*, 197:24 – 33, 2017.

[61] Huey-San Melanie Siah and Anne Fiksdahl. Preparation and catalytic activity of novel σ,π-dual gold(i) acetylide complexes. *European Journal of Organic Chemistry*, 2020(3):367–377, 2020.

[62] Roopender Kumar and Cristina Nevado. Cyclometalated gold(iii) complexes: Synthesis, reactivity, and physicochemical properties. *Angewandte Chemie International Edition*, 56(8):1994–2015, 2017.

[63] Yongchun Yang, Yanan Shen, Xiaoli Wang, Yao Zhang, Dawei Wang, and Xiaodong Shi. Triazole acetyl gold (iii) catalyzed meyer–schuster rearrangement of propargyl alcohols. *Tetrahedron Letters*, 57(21):2280–2282, 2016.

[64] A. Stephen K. Hashmi, Jan P. Weyrauch, Matthias Rudolph, and Elzen Kurpejović. Gold catalysis: The benefits of n and n,o ligands. *Angewandte Chemie International Edition*, 43(47):6545–6547, 2004.

[65] Nathan D. Shapiro and F. Dean Toste. Synthesis of azepines by a gold-catalyzed intermolecular [4 + 3]-annulation. *Journal of the American Chemical Society*, 130(29):9244–9245, 2008. PMID: 18576648.

[66] Yifan Li, Jonathan P. Brand, and Jérôme Waser. Gold-catalyzed regioselective synthesis of 2- and 3-alkynyl furans. *Angewandte Chemie International Edition*, 52(26):6743–6747, 2013.

[67] Marcel Brill and Steven P Nolan. Chiral carbophilic gold lewis acid complexes in enantioselective catalysis. In *Chiral Lewis Acids*, pages 51–90. Springer, 2015.

[68] Manfred T. Reetz, Hongchao Guo, Jun-An Ma, Richard Goddard, and Richard J. Mynott. Helical triskelion monophosphites as ligands in asymmetric catalysis. *Journal of the American Chemical Society*, 131(11):4136–4142, 2009. PMID: 19249837.

[69] Ana Z. González and F. Dean Toste. Gold(i)-catalyzed enantioselective [4 + 2]-cycloaddition of allene-dienes. *Organic Letters*, 12(1):200–203, 2010. PMID: 19961192.

[70] Guozhu Zhang and Liming Zhang. Au-containing all-carbon 1, 3-dipoles: generation and [3+ 2] cycloaddition reactions. *Journal of the American Chemical Society*, 130(38):12598–12599, 2008.

[71] W. Michalak, M. Kośnik. Chiral n-heterocyclic carbene gold complexes: Synthesis and applications in catalysis. *Catalysts*, 9:890, 2019.

[72] Avelino Corma, Irene Domínguez, Antonio Doménech, Vicente Fornés, Carlos J. Gómez-García, Tania Ródenas, and María J. Sabater. Enantioselective epoxidation of olefins with molecular oxygen catalyzed by gold(iii): A dual pathway for oxygen transfer. *Journal of Catalysis*, 265(2):238 – 244, 2009.

[73] Ann Christin Reiersølmoen, Elise Østrem, and Anne Fiksdahl. Gold(III)-Catalysed cis-to-trans Cyclopropyl Isomerization. *European Journal of Organic Chemistry*, 2018(25):3317–3325, 7 2018.

[74] Horibe-T. Jacobsen C. et al. Wu, C. Stable gold(iii) catalysts by oxidative addition of a carbon–carbon bond. *Nature*, 517:449–454, 2015.

[75] Richter-C. Schedler M. et al. Hopkinson, M. An overview of n-heterocyclic carbenes. *Nature*, 510:485–496, 2014.

[76] Laure Benhamou, Edith Chardon, Guy Lavigne, Stéphane Bellemin-Laponnaz, and Vincent César. Synthetic routes to n-heterocyclic carbene precursors. *Chemical Reviews*, 111(4):2705–2733, 2011.

[77] Didier Bourissou, Olivier Guerret, François P. Gabbaï, and Guy Bertrand. Stable carbenes. *Chemical Reviews*, 100(1):39–92, 2000.

[78] Dennis A. Anslyn, Eric V. Dougherty. *Modern Physical Organic Chemistry*. University Science Books, 2006.

[79] Anthony J. Arduengo, Richard L. Harlow, and Michael Kline. A stable crystalline carbene. *Journal of the American Chemical Society*, 113(1):361–363, 1991.

[80] David J Nelson and Steven P Nolan. Quantifying and understanding the electronic properties of n-heterocyclic carbenes. *Chemical Society Reviews*, 42(16):6723–6753, 2013.

[81] Anthony J Arduengo III, Jens R Goerlich, and William J Marshall. A stable diaminocarbene. *Journal of the American Chemical Society*, 117(44):11027–11028, 1995.

[82] Volker PW Böhm and Wolfgang A Herrmann. The "wanzlick equilibrium". *Angewandte Chemie International Edition*, 39(22):4036–4038, 2000.

[83] KA Lutomski and AI Meyers. Asymmetric synthesis, vol. 3, morrison, jd ed, 1983.

[84] Henri Brunner, Uwe Obermann, and Peter Wimmer. Asymmetric catalysis. 44. enantioselective monophenylation of diols with cupric acetate/pyridinyloxazoline catalysts. *Organometallics*, 8(3):821–826, 1989.

[85] Carsten Bolm, Konrad Weickhardt, Margareta Zehnder, and Dorothea Glasmacher. Syntheses and crystal structures of 4,5–dihydro-2-(2-hydroxyphenyl)oxazole-containing metal complexes. *Helvetica Chimica Acta*, 74(4):717–726, 1991.

[86] Andreas Pfaltz. Chiral semicorrins and related nitrogen heterocycles as ligands in asymmetric catalysis. *Accounts of Chemical Research*, 26(6):339–345, 1993.

[87] Craig. Snyder Scott. Solomons, Graham. Fryhle. *Organic Chemistry*. John Wiley & Sons, 2014.

[88] Rudolf Andreasch. Zur kenntniss des allylharnstoffs. *Monatshefte für Chemie und verwandte Teile anderer Wissenschaften*, 5(1):33–46, 1884.

[89] Thomas G. Gant and A.I. Meyers. The chemistry of 2-oxazolines (1985–present). *Tetrahedron*, 50(8):2297 – 2360, 1994.

[90] EDWARD M. FRY. Oxazolines. *The Journal of Organic Chemistry*, 14(5):887–894, 1949.

[91] E Bergmann and AF Brand. Synthesis of 2-oxazoline compounds. *Chem. Ber.*, 56:1280, 1923.

[92] Peter Wipf and Chris P. Miller. An investigation of the mitsunobu reaction in the preparation of peptide oxazolines, thiazolines, and aziridines. *Tetrahedron Letters*, 33(42):6267 – 6270, 1992. The International Journal for the Rapid Publication of Preliminary.

[93] Edward M Burgess, Harold R Penton Jr, and Edward Alan Taylor. Synthetic applications of n-carboalkoxysulfamate esters. *Journal of the American Chemical Society*, 92(17):5224–5226, 1970.

[94] David A Claremon and Brian T Phillips. An efficient chemoselective synthesis of nitriles from primary amides. *Tetrahedron letters*, 29(18):2155–2158, 1988.

[95] Sachin Khapli, Satyajit Dey, and Dipakranjan Mal. Burgess reagent in organic synthesis. *Journal of the Indian Institute of Science*, 81(4):461, 2013.

[96] Peter Wipf and Gregory B. Hayes. Synthesis of oxazines and thiazines by cyclodehydration of hydroxy amides and thioamides. *Tetrahedron*, 54(25):6987 – 6998, 1998.

[97] J.B. Bremner and S. Samosorn. 13.08 - 1,3-oxazepines and 1,3-thiazepines. In Alan R. Katritzky, Christopher A. Ramsden, Eric F.V. Scriven, and Richard J.K. Taylor, editors, *Comprehensive Heterocyclic Chemistry III*, pages 245 – 254. Elsevier, Oxford, 2008.

[98] Peter Wipf and Srikanth Venkatraman. An improved protocol for azole synthesis with peg-supported burgess reagent. *Tetrahedron Letters*, 37(27):4659 – 4662, 1996.

[99] R. David Pace and Yagya Regmi. The finkelstein reaction: Quantitative reaction kinetics of an sn2 reaction using nonaqueous conductivity. *Journal of Chemical Education*, 83(9):1344, 2006.

[100] Steven P. Nolan. The development and catalytic uses of n-heterocyclic carbene gold complexes. *Accounts of Chemical Research*, 44(2):91–100, 2011. PMID: 21028871.

[101] Joseph C. Y. Lin, Roy T. W. Huang, Chen S. Lee, Amitabha Bhattacharyya, Wen S. Hwang, and Ivan J. B. Lin. Coinage metal-n-heterocyclic carbene complexes. *Chemical Reviews*, 109(8):3561–3598, 2009. PMID: 19361198.

[102] Adrián Gómez-Suárez, Rubén S. Ramón, Olivier Songis, Alexandra M. Z. Slawin, Catherine S. J. Cazin, and Steven P. Nolan. Influence of a very bulky n-heterocyclic carbene in gold-mediated catalysis. *Organometallics*, 30(20):5463–5470, 2011.

[103] Renso Visbal, Antonio Laguna, and M. Concepción Gimeno. Simple and efficient synthesis of [mci(nhc)] (m = au, ag) complexes. *Chem. Commun.*, 49:5642–5644, 2013.

[104] Sylvain Gaillard, Alexandra M. Z. Slawin, Allen T. Bonura, Edwin D. Stevens, and Steven P. Nolan. Synthetic and structural studies of [aucl3(nhc)] complexes. *Organometallics*, 29(2):394–402, 2010.

[105] Eleanor A. Merritt and Berit Olofsson. Diaryliodonium salts: A journey from obscurity to fame. *Angewandte Chemie International Edition*, 48(48):9052–9070, 2009.

[106] Luiz F. Silva, Jr. and Berit Olofsson. Hypervalent iodine reagents in the total synthesis of natural products. *Nat. Prod. Rep.*, 28:1722–1754, 2011.

[107] Steve Nanchen and Andreas Pfaltz. Synthesis and application of chiral n-heterocyclic carbene–oxazoline ligands: Iridium-catalyzed enantioselective hydrogenation. *Chemistry – A European Journal*, 12(17):4550–4558, 2006.

[108] Jozef Kowalewski. Calculations of nuclear spin—spin coupling constants. *Progress in Nuclear Magnetic Resonance Spectroscopy*, 11(1):1 – 78, 1977.

[109] Wolfgang A. Herrmann, Oliver Runte, and Georg Artus. Synthesis and structure of an ionic beryllium-"carbene" complex. *Journal of Organometallic Chemistry*, 501(1):C1 – C4, 1995.

[110] Manik Kumer Ghosh, Mats Tilset, Ajay Venugopal, Richard H. Heyn, and Ole Swang. Ping-pong at gold: Proton jump between coordinated phenyl and η1-benzene ligands, a computational study. *The Journal of Physical Chemistry A*, 114(31):8135–8141, 2010. PMID: 20684587.

Trondheim, June 15, 2020

A Spectra of Amides 3a, 3b

^{1}H-NMR of Amide 3a

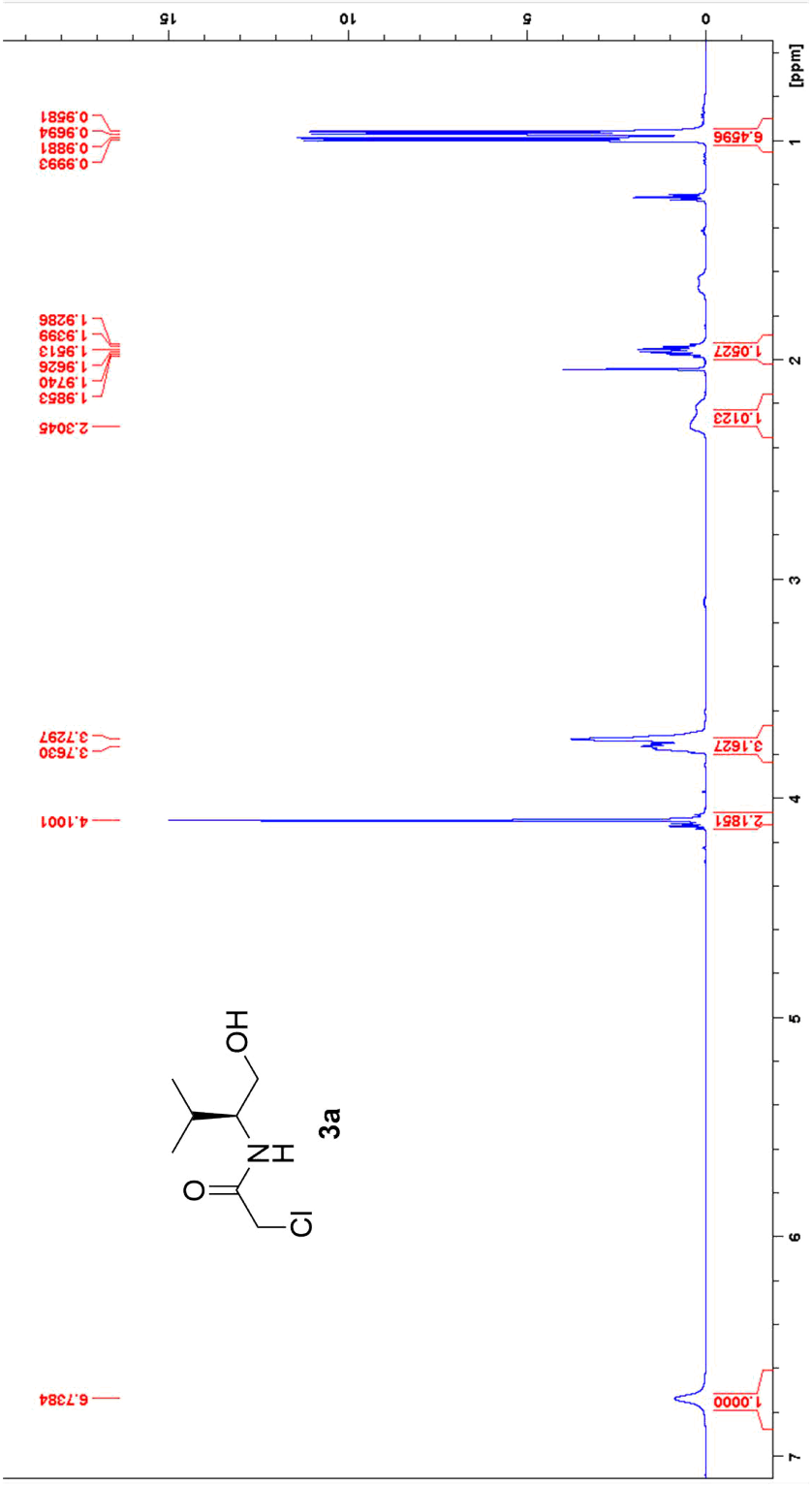

^{13}C-NMR of Amide 3a

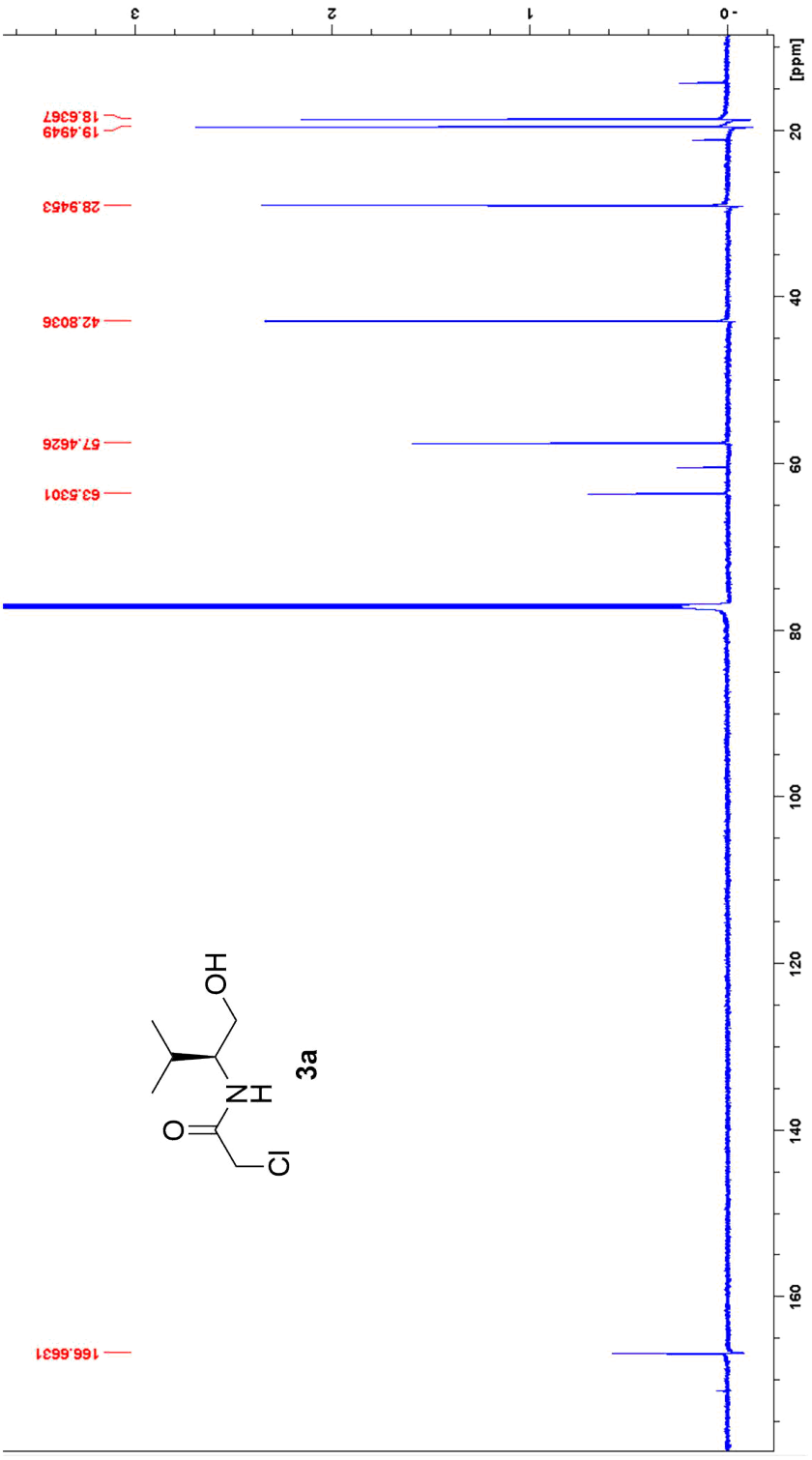

COSY of Amide 3a

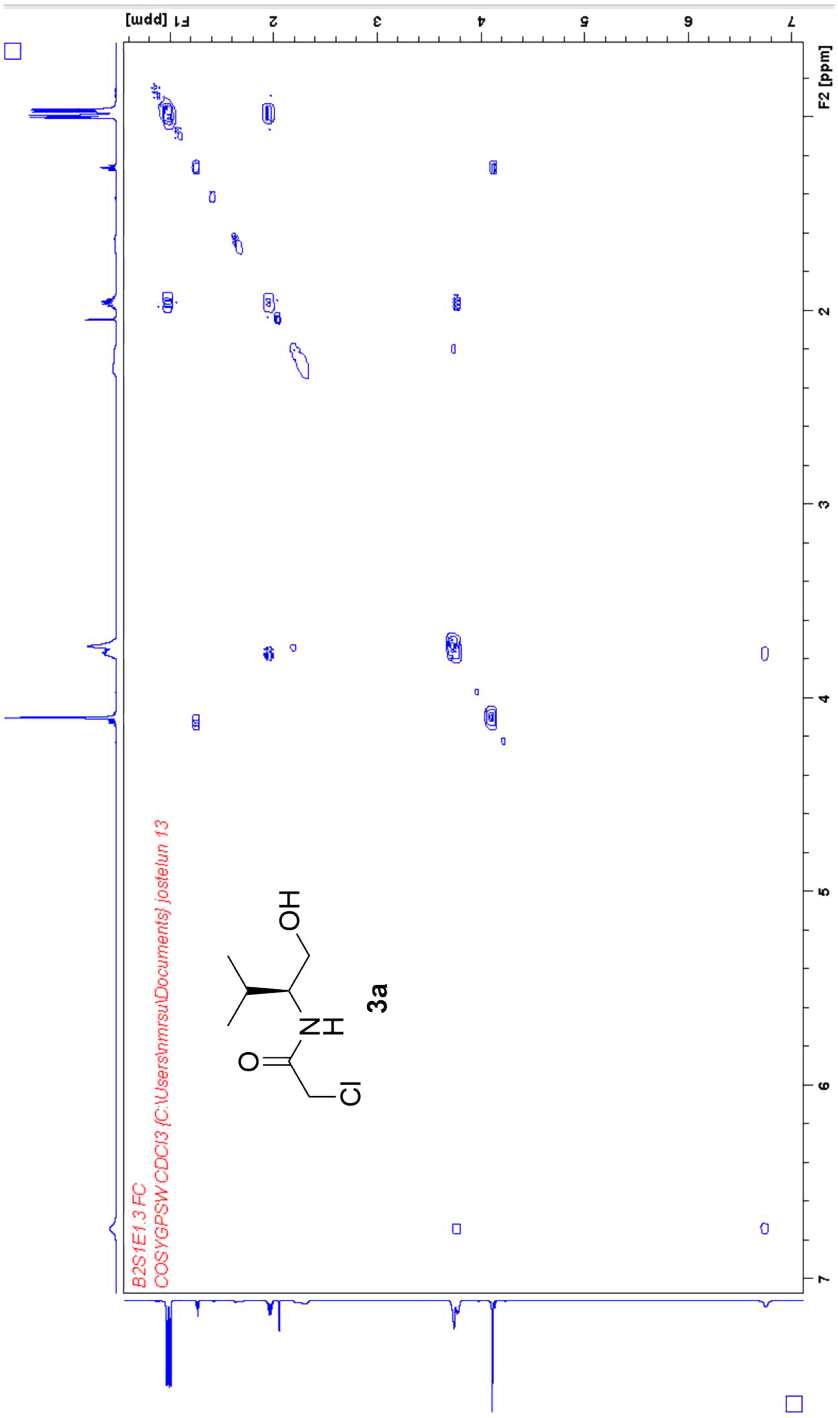

HSQC of Amide 3a

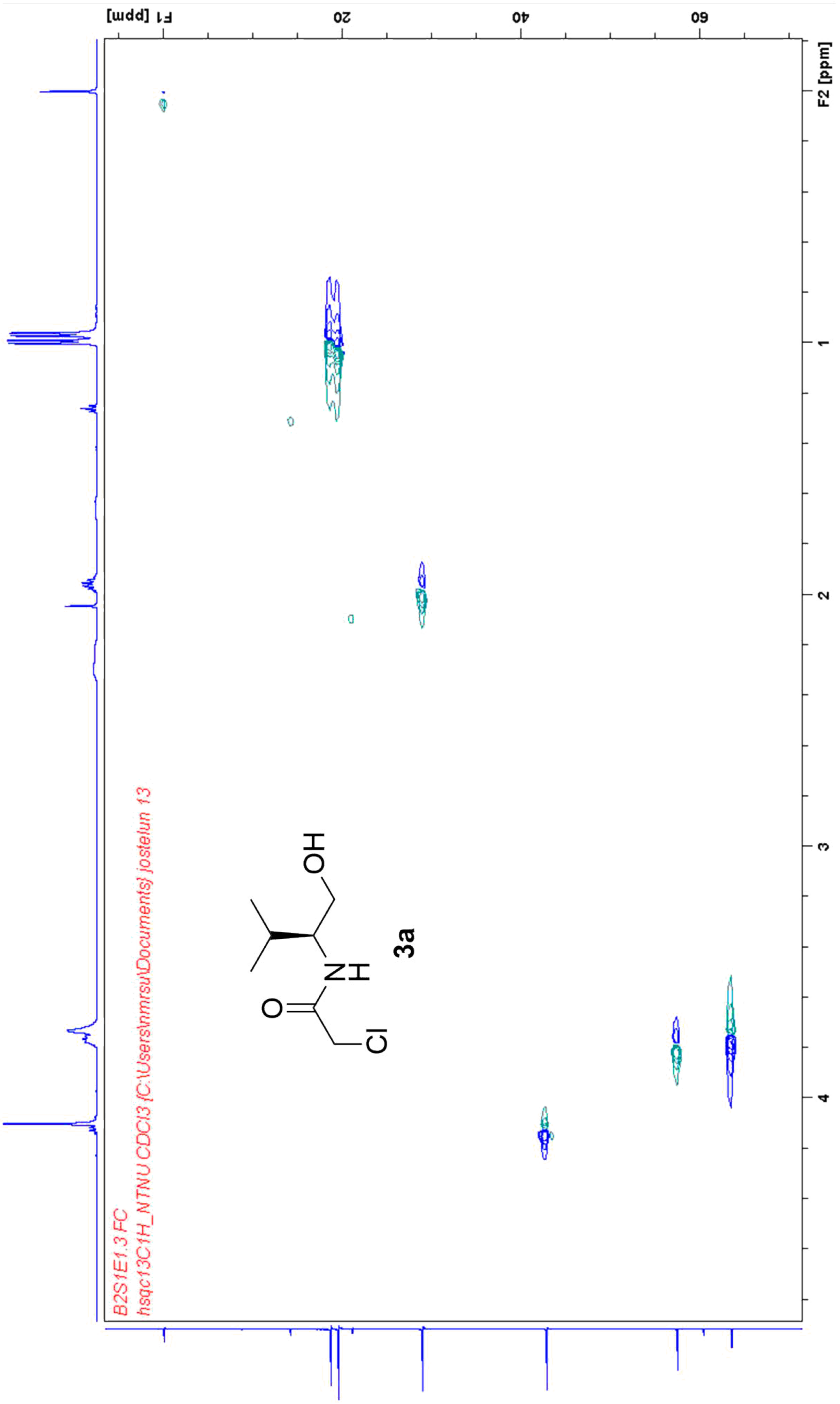

HMBC of Amide 3a

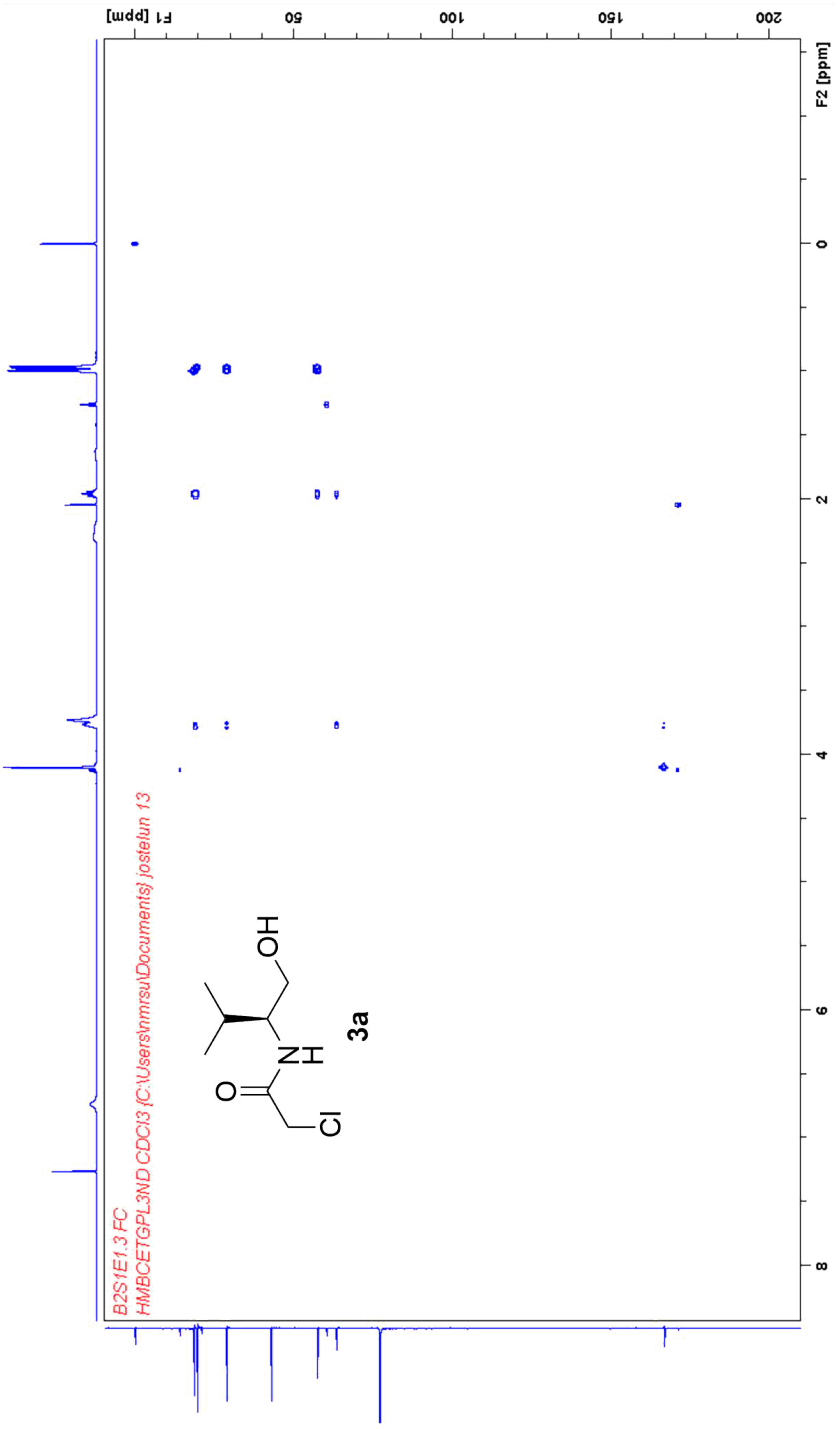

HRMS of Amide 3a

Elemental Composition Report **Page 1**

Single Mass Analysis
Tolerance = 2.0 PPM / DBE: min = -5.0, max = 50.0
Element prediction: Off
Number of isotope peaks used for i-FIT = 3

Monoisotopic Mass, Even Electron Ions
253 formula(e) evaluated with 1 results within limits (all results (up to 1000) for each mass)
Elements Used:
C: 0-100 H: 0-100 N: 0-2 O: 0-10 Na: 0-1 Cl: 0-1
2020 169 117 (1.109) AM2 (Ar,35000.0,0.00,0.00); Cm (112:117)
1: TOF MS ES+

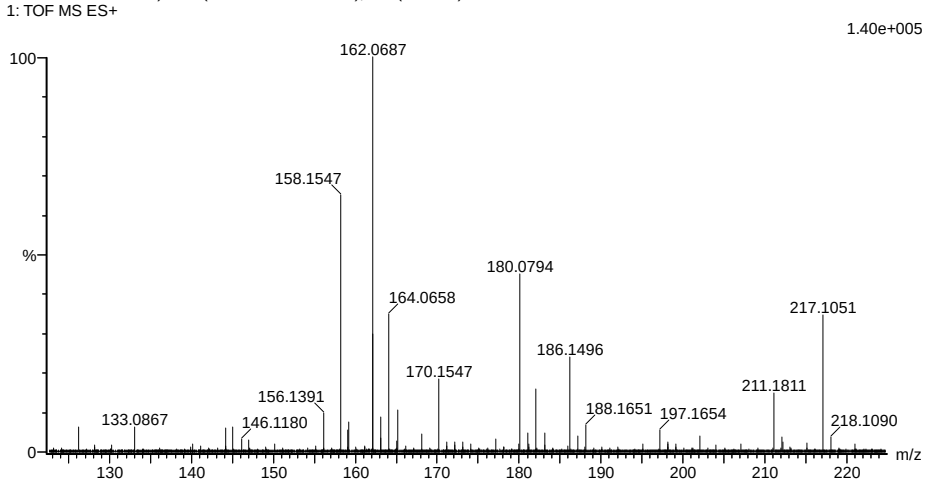

Minimum:				-5.0				
Maximum:		5.0	2.0	50.0				
Mass	Calc. Mass	mDa	PPM	DBE	i-FIT	Norm	Conf(%)	Formula
180.0794	180.0791	0.3	1.7	0.5	1477.2	n/a	n/a	C7 H15 N O2 Cl

IR of Amide 3a

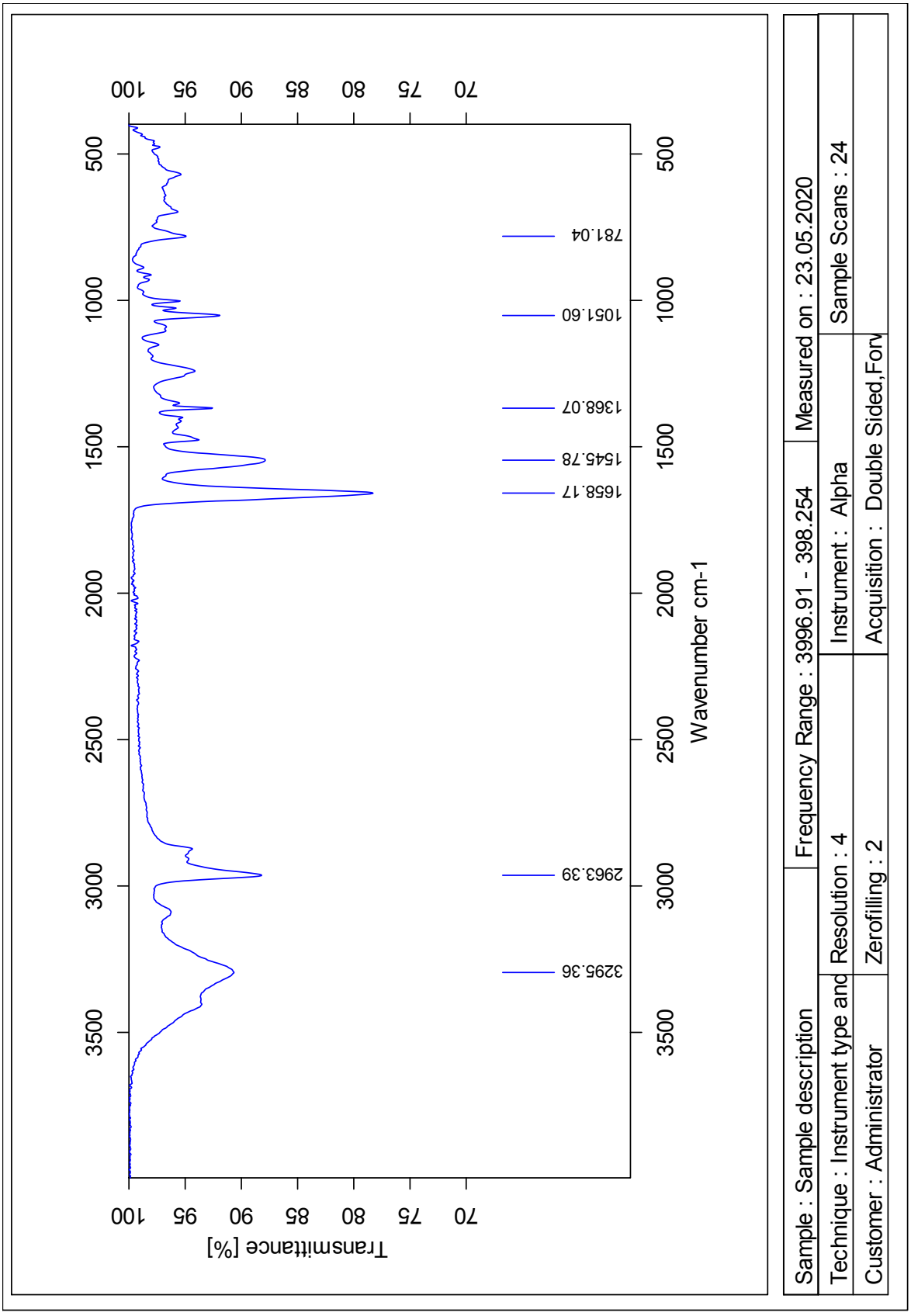

^{1}H-NMR of Amide 3b

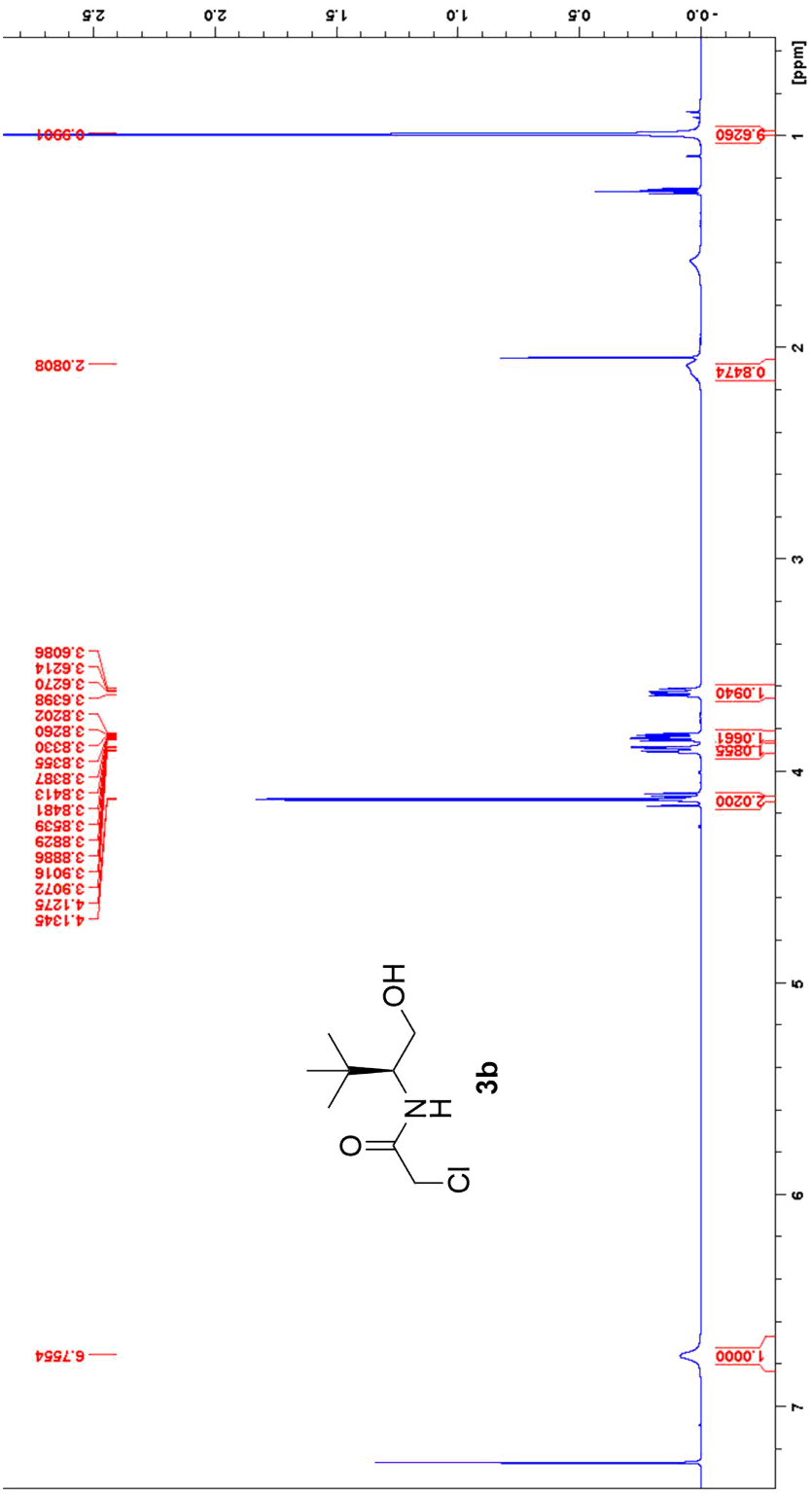

^{13}C-NMR of Amide 3b

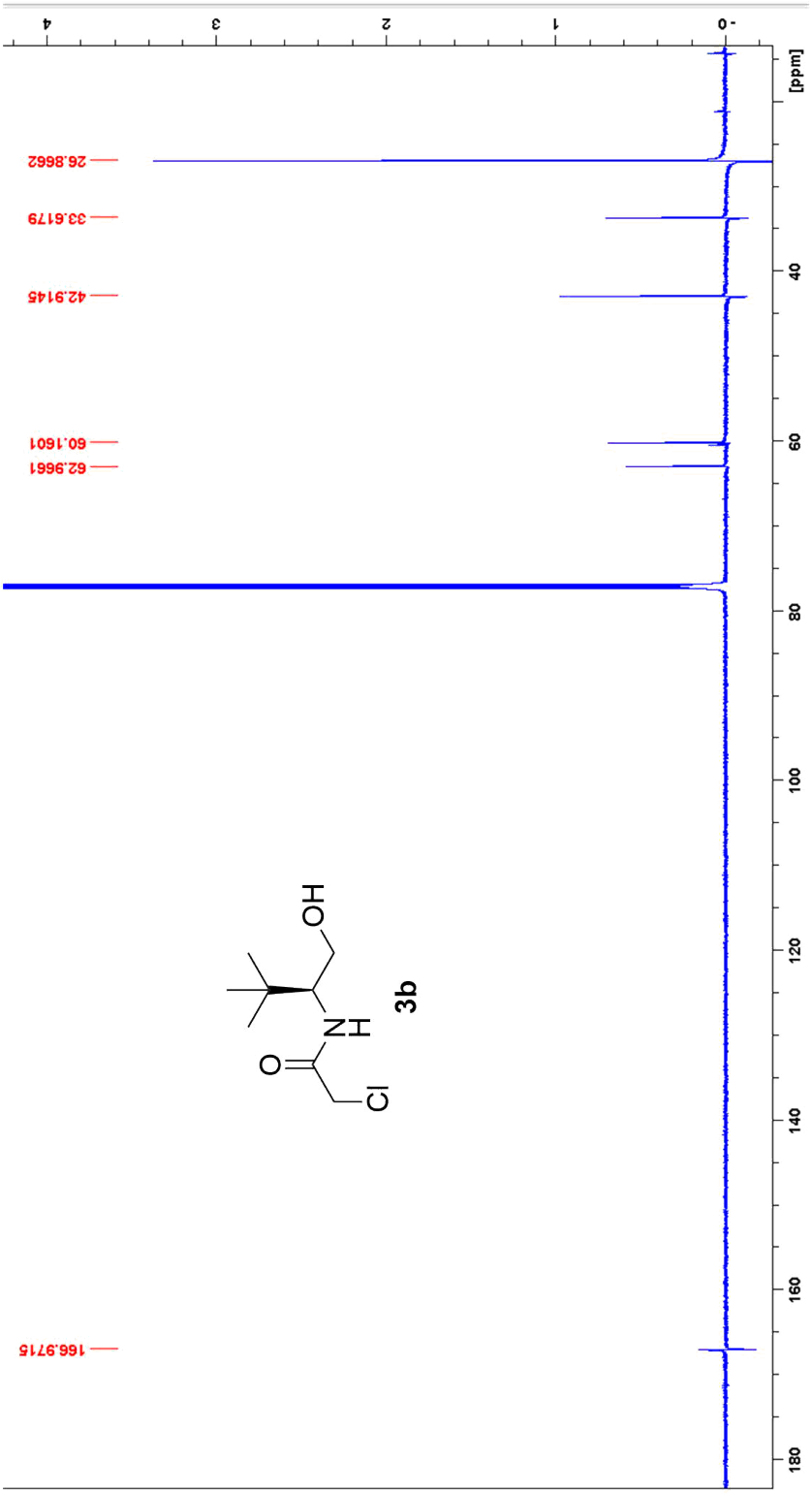

COSY of Amide 3b

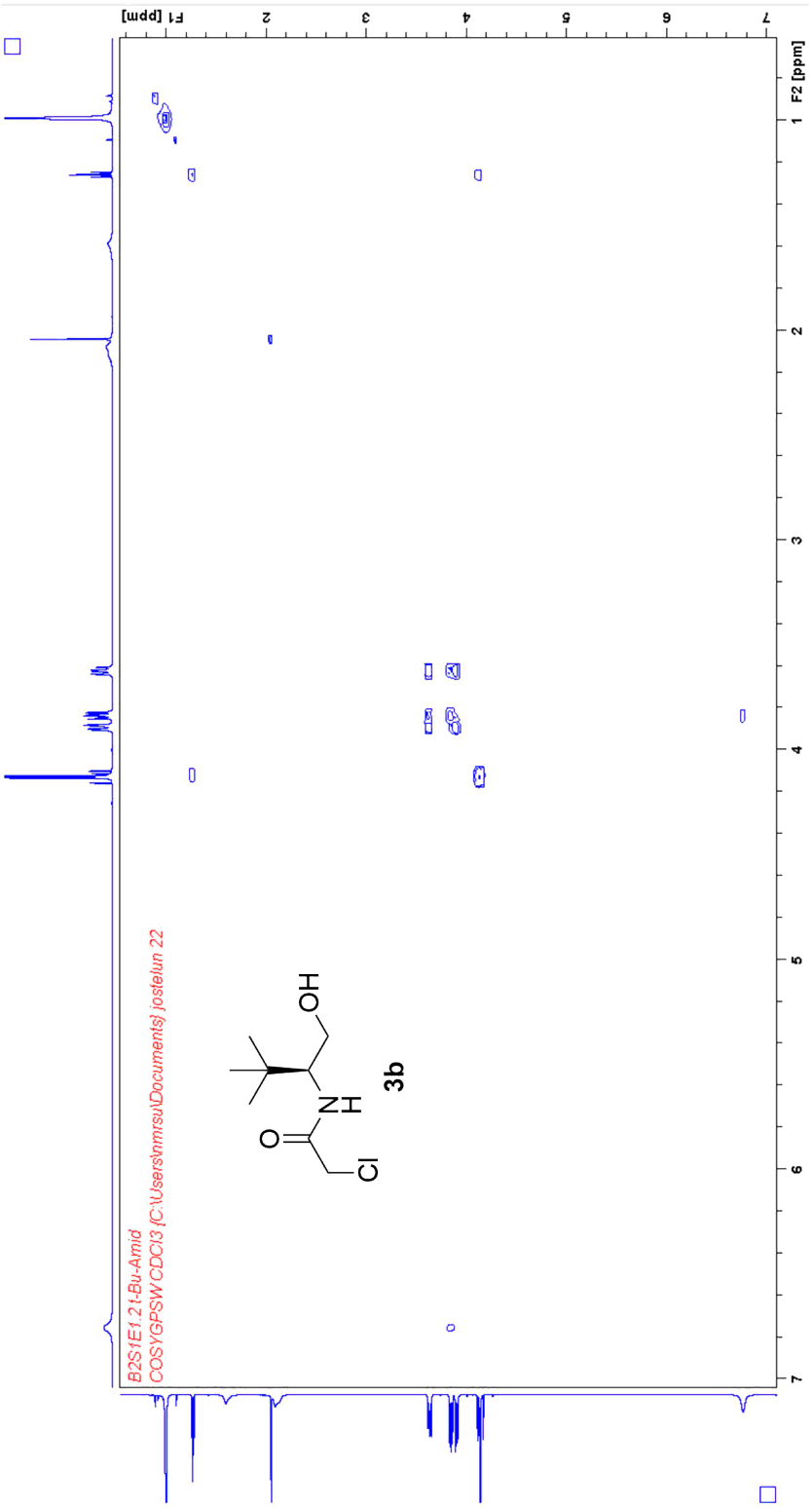

HSQC of Amide 3b

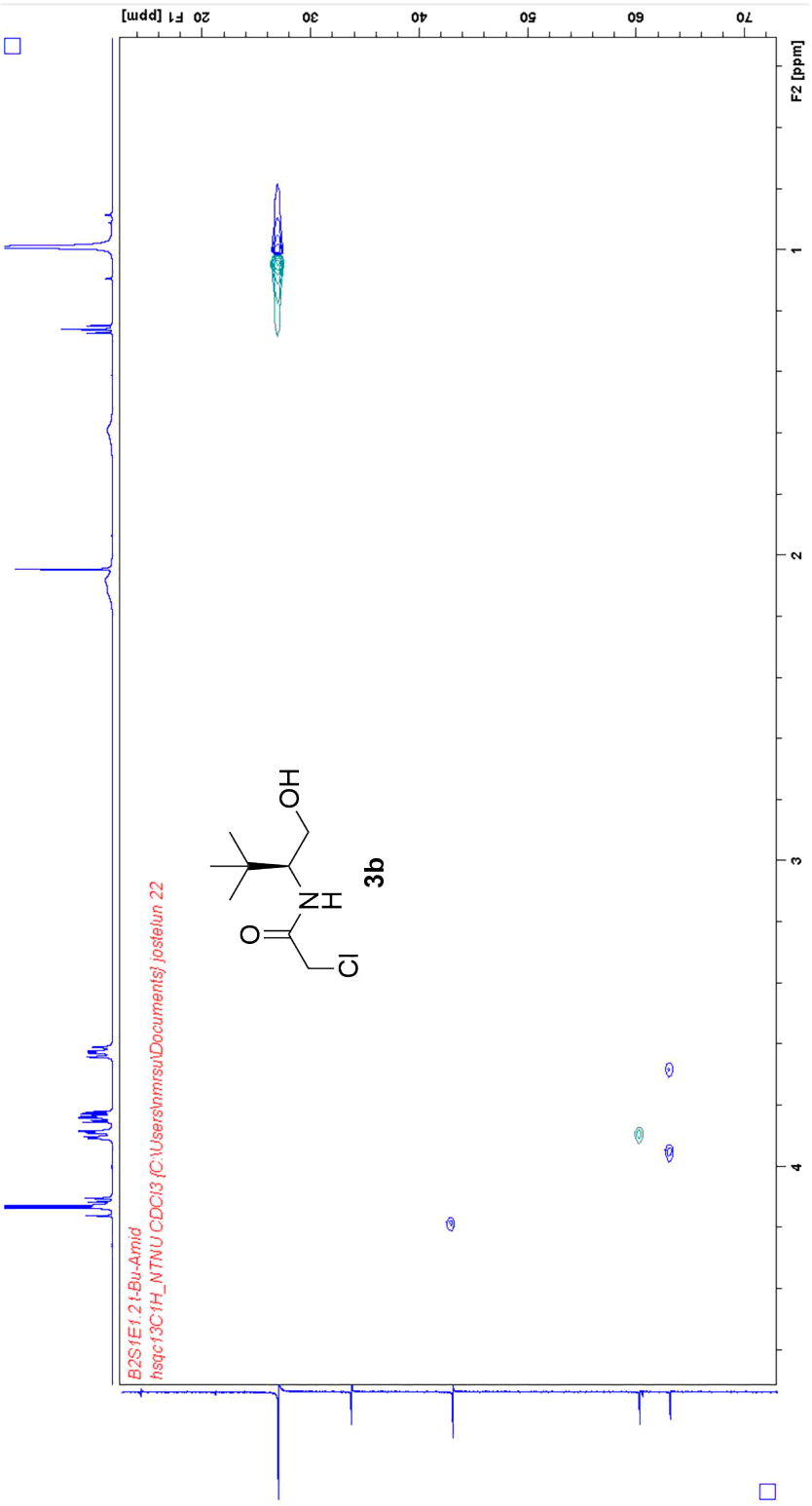

HMBC of Amide 3b

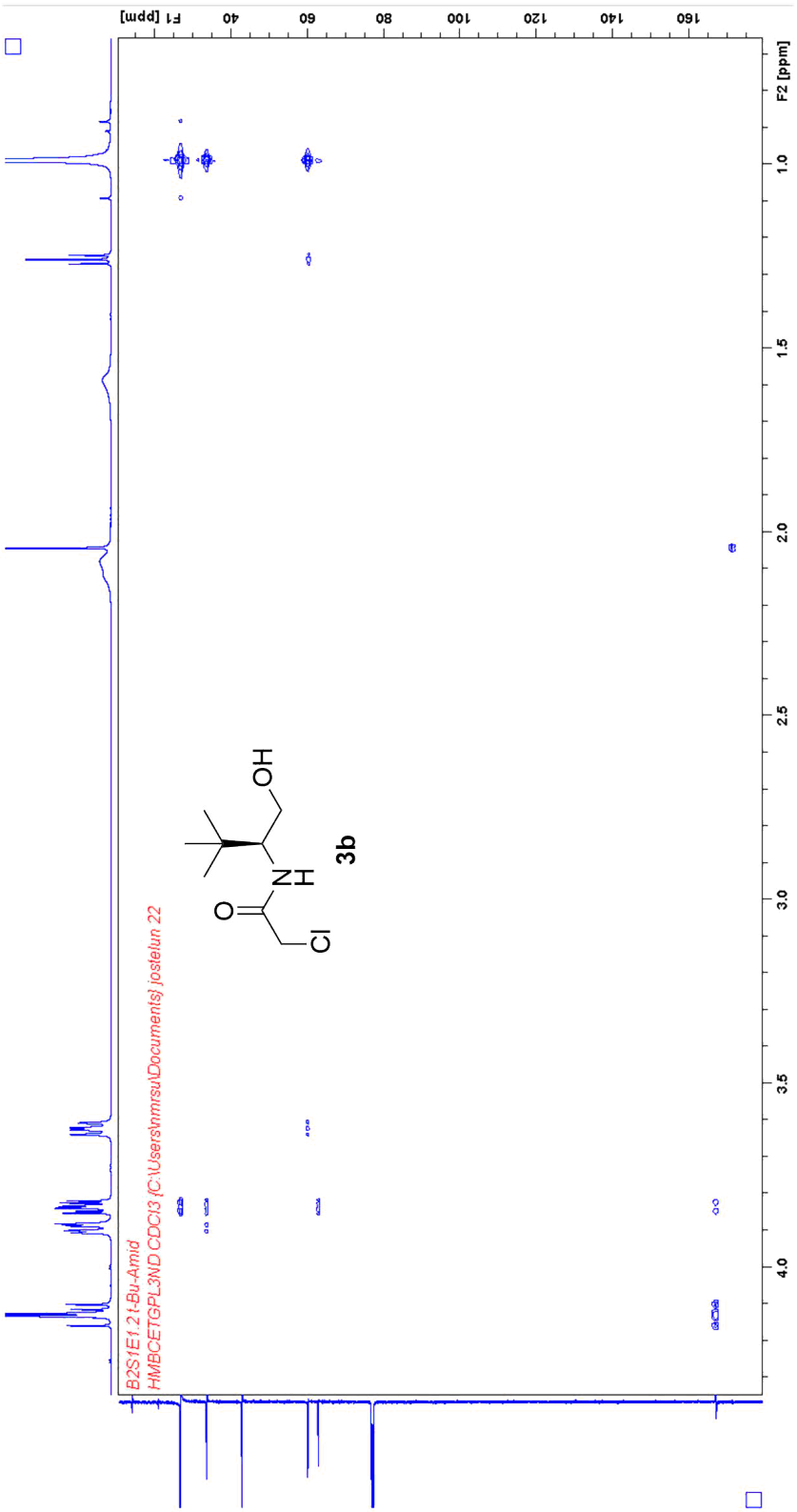

HRMS of Amide 3b

Elemental Composition Report **Page 1**

Single Mass Analysis
Tolerance = 2.0 PPM / DBE: min = -5.0, max = 50.0
Element prediction: Off
Number of isotope peaks used for i-FIT = 3

Monoisotopic Mass, Even Electron Ions
289 formula(e) evaluated with 1 results within limits (all results (up to 1000) for each mass)
Elements Used:
C: 0-100 H: 0-100 N: 0-2 O: 0-10 Na: 0-1 Cl: 0-1
2020 170 58 (0.553) AM2 (Ar,35000.0,0.00,0.00); Cm (46:58)
1: TOF MS ES+

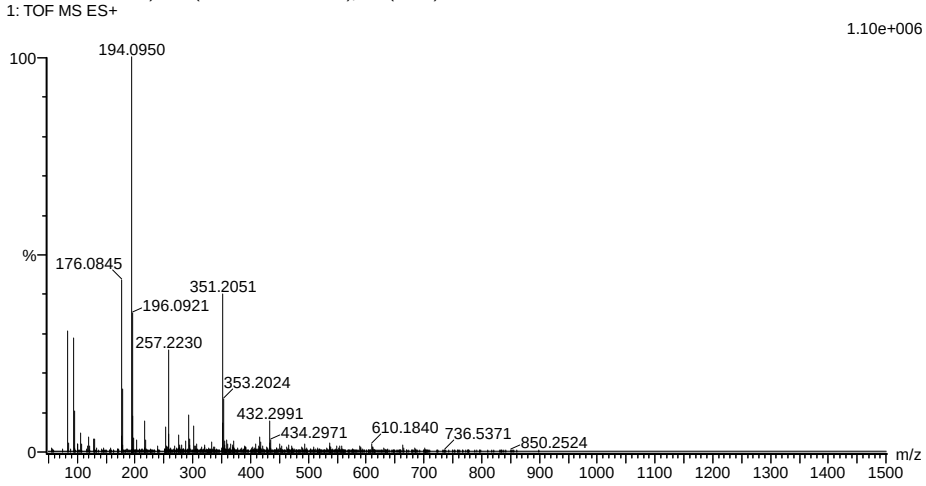

Minimum:				-5.0				
Maximum:		5.0	2.0	50.0				
Mass	Calc. Mass	mDa	PPM	DBE	i-FIT	Norm	Conf(%)	Formula
194.0950	194.0948	0.2	1.0	0.5	1740.8	n/a	n/a	C8 H17 N O2 Cl

IR of Amide 3b

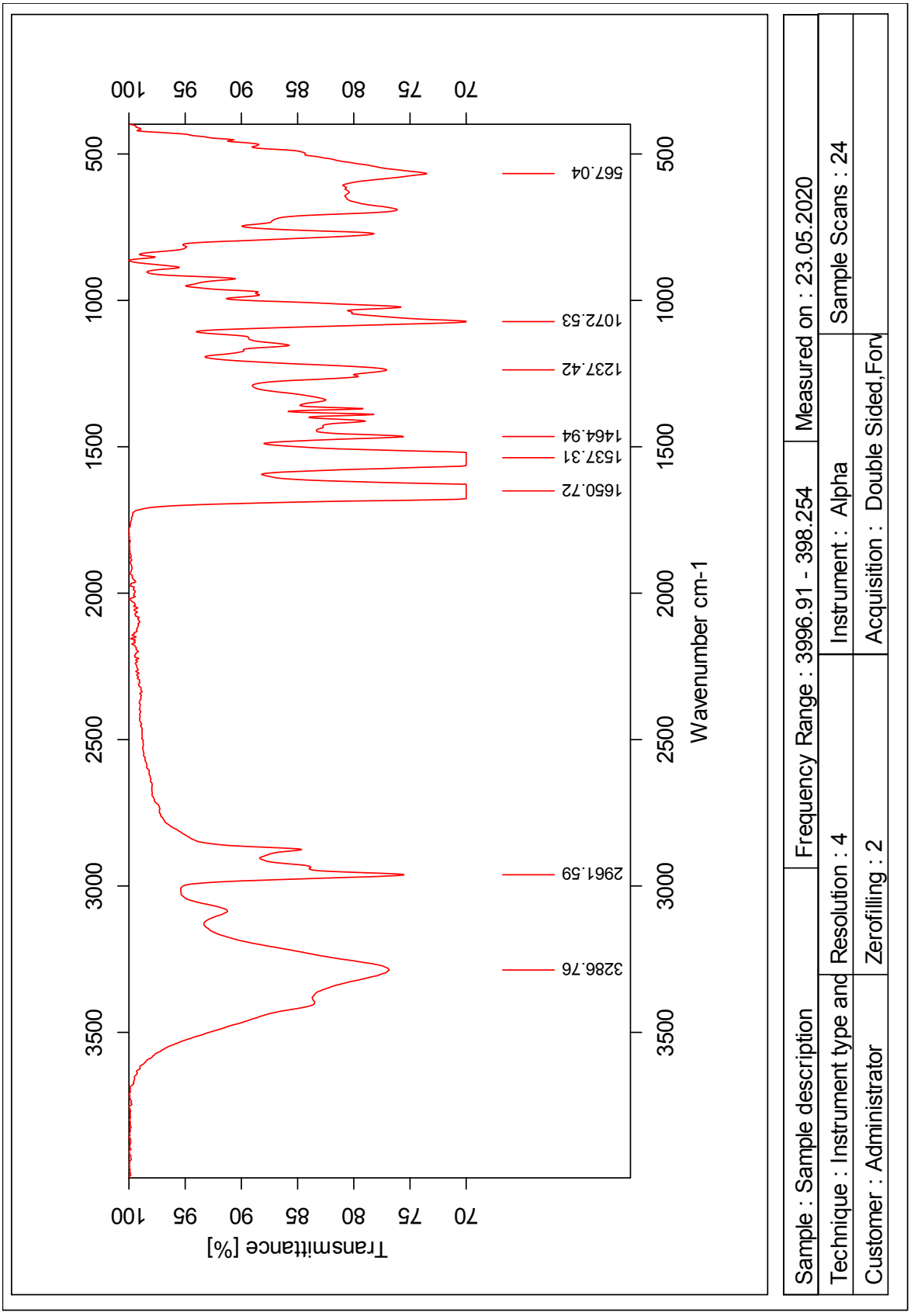

B Spectra of Oxazolines 5a, 5b

^{1}H-NMR of Oxazoline 5a

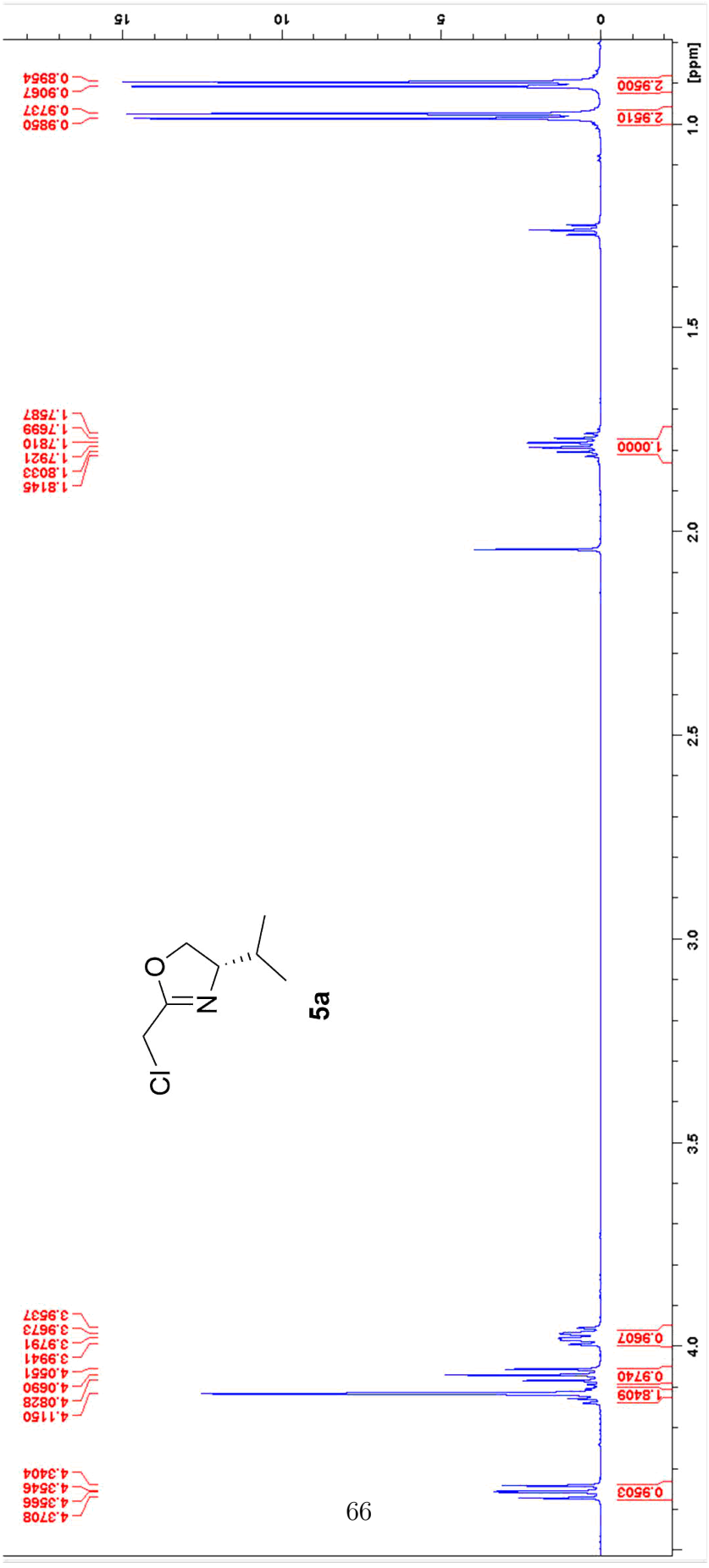

^{13}C-NMR of Oxazoline 5a

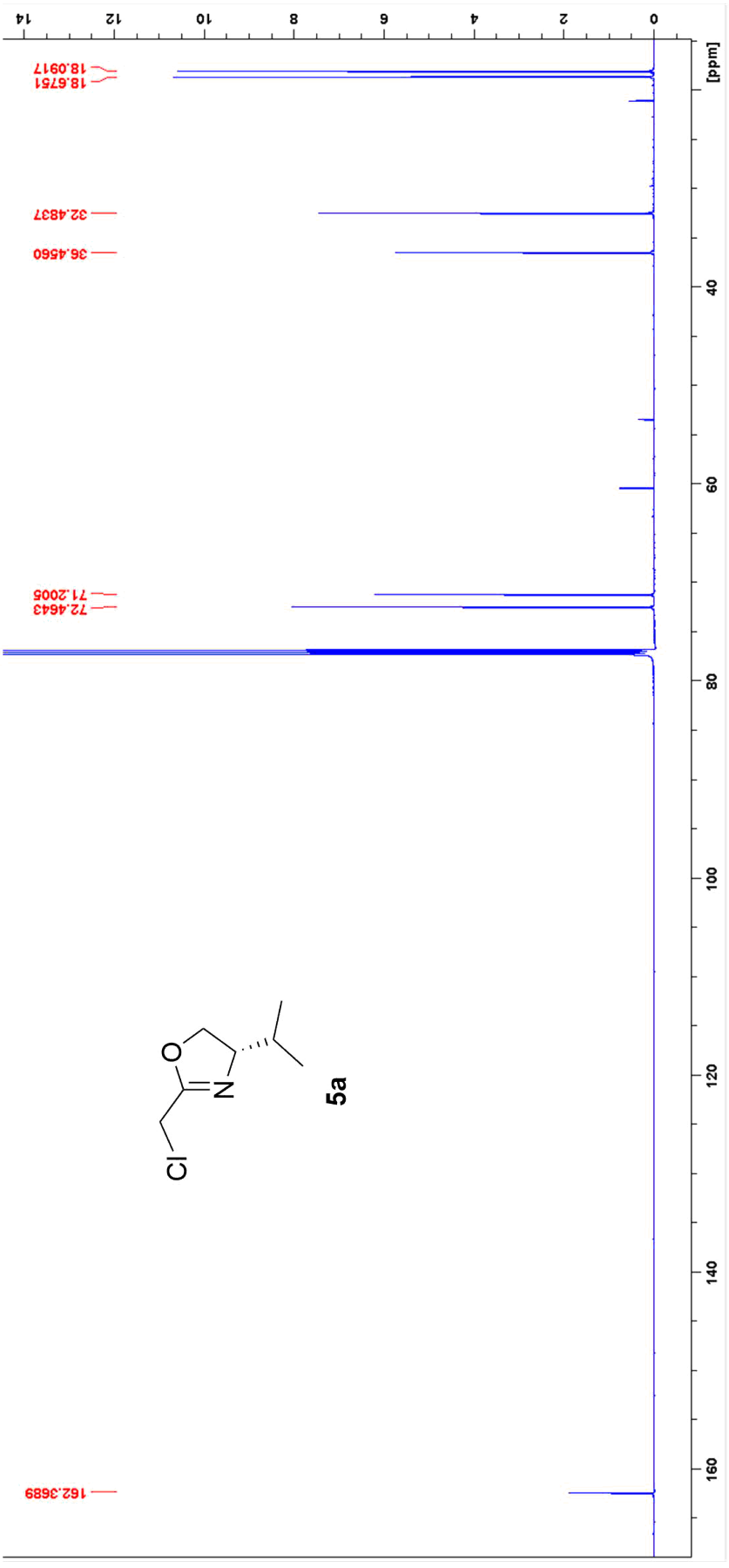

COSY of Oxazoline 5a

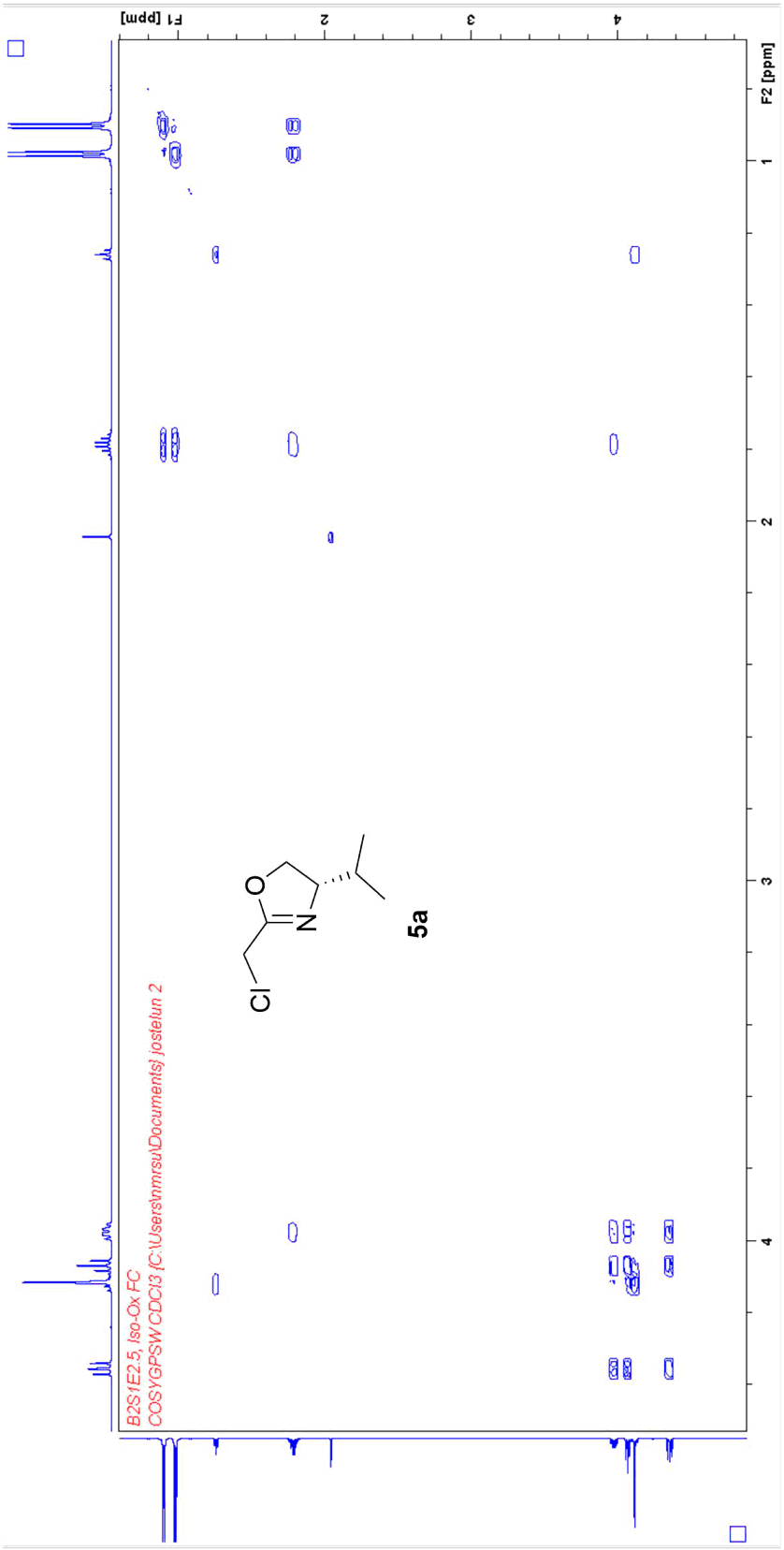

HSQC of Oxazoline 5a

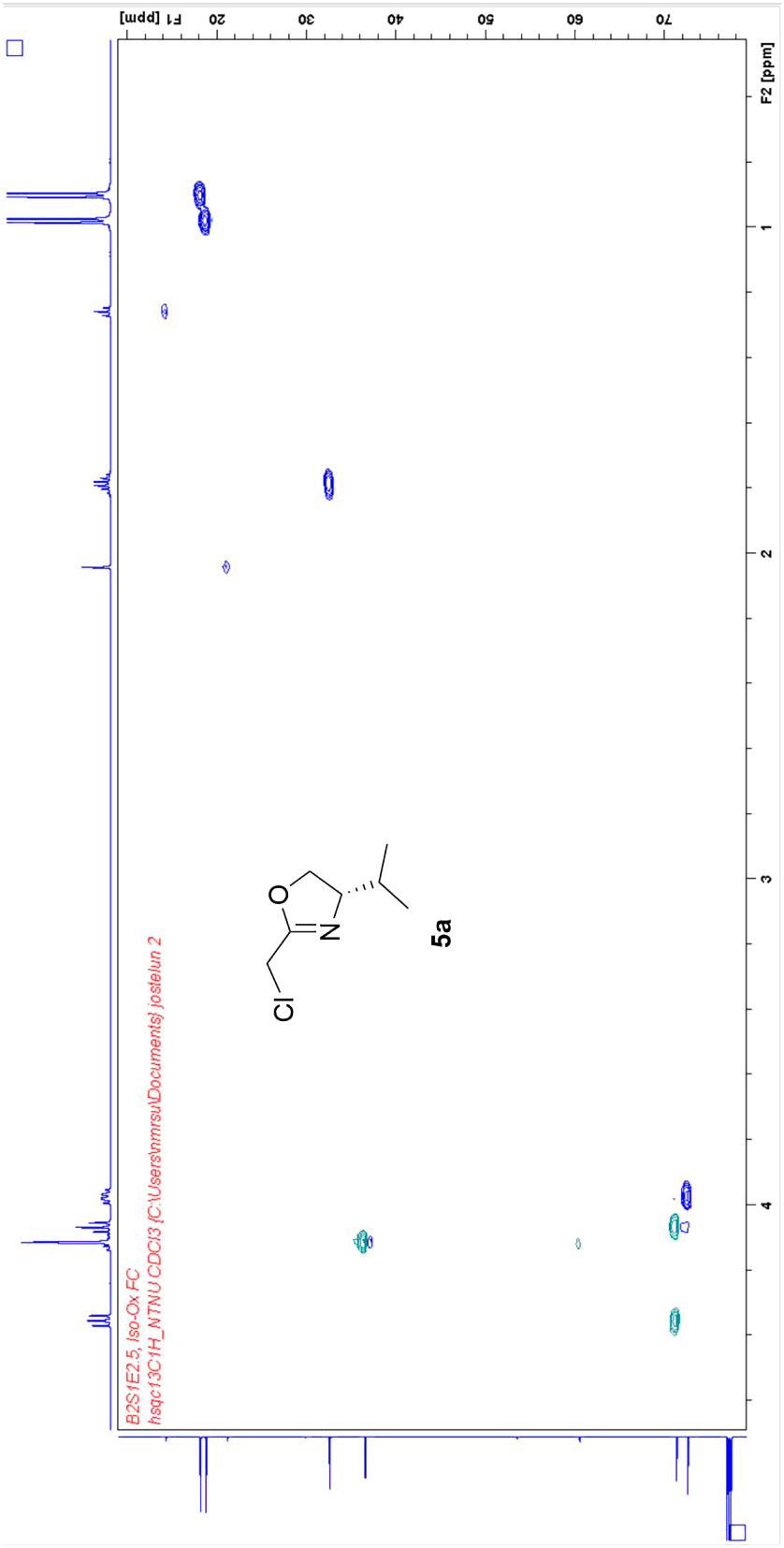

HMBC of Oxazoline 5a

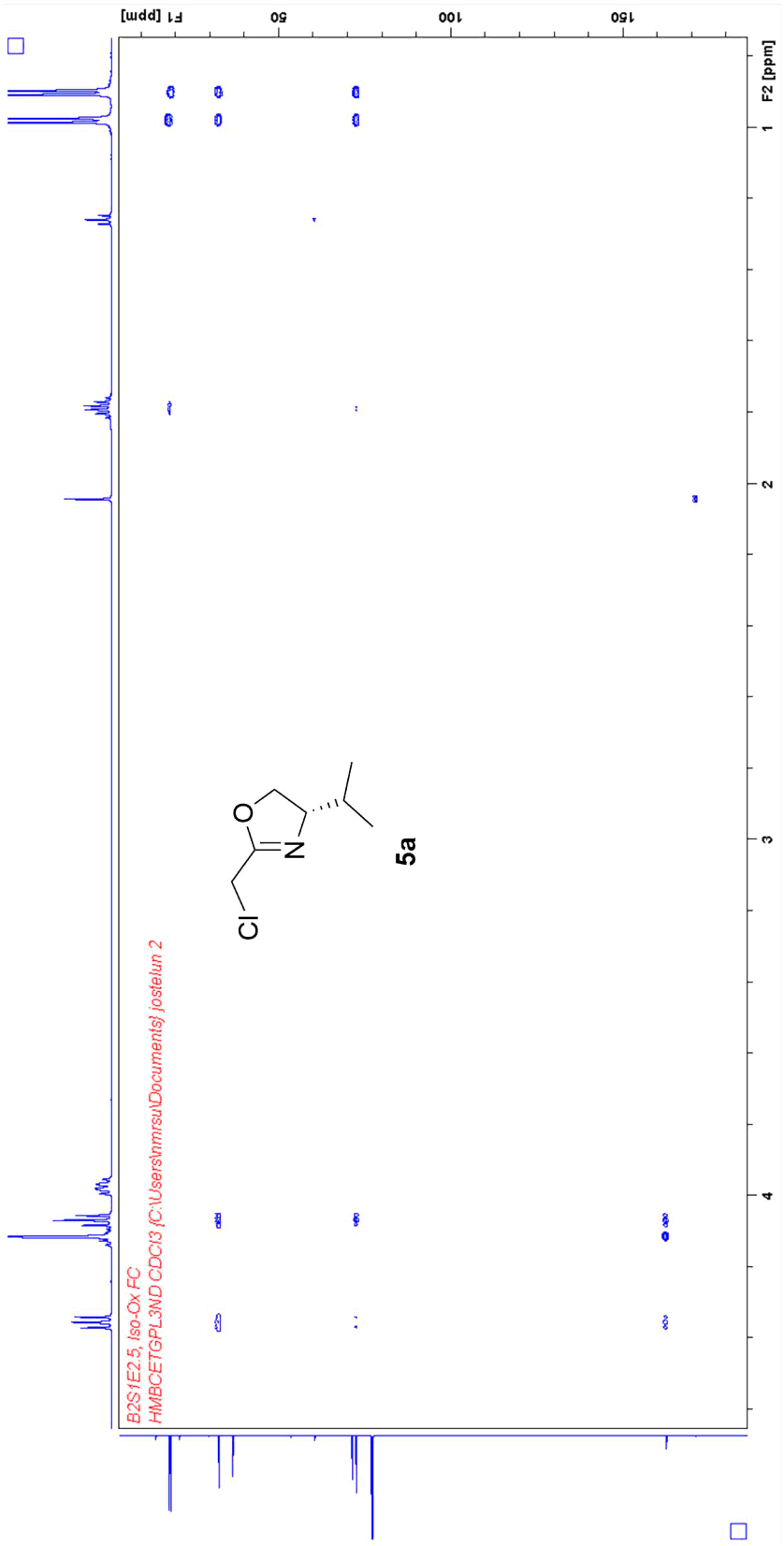

HRMS of Oxazoline 5a

Elemental Composition Report **Page 1**

Single Mass Analysis
Tolerance = 5.0 PPM / DBE: min = -5.0, max = 50.0
Element prediction: Off
Number of isotope peaks used for i-FIT = 3

Monoisotopic Mass, Even Electron Ions
177 formula(e) evaluated with 1 results within limits (all results (up to 1000) for each mass)
Elements Used:
C: 0-100 H: 0-100 N: 0-3 O: 0-5 Cl: 0-3
JA SVG 20200507_138 31 (0.585) AM2 (Ar,35000.0,0.00,0.00); Cm (29:31)
1: TOF MS ES+

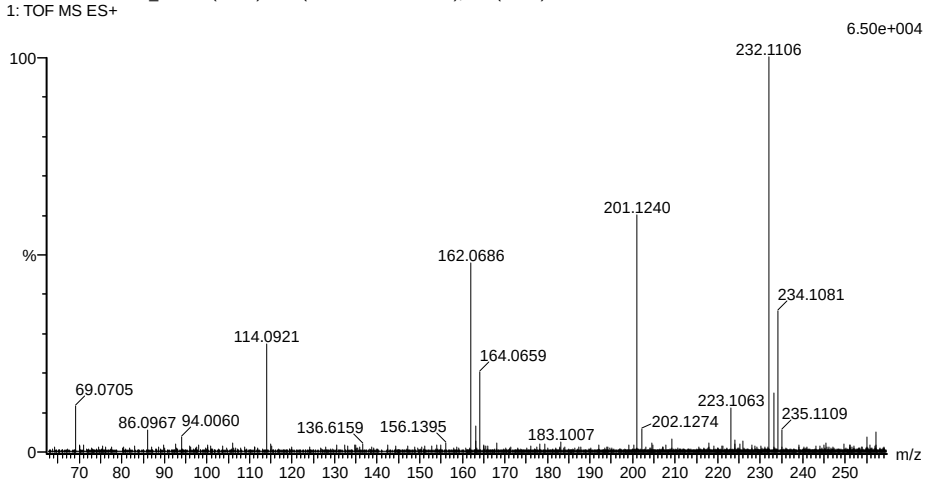

Minimum:				-5.0				
Maximum:		5.0	5.0	50.0				
Mass	Calc. Mass	mDa	PPM	DBE	i-FIT	Norm	Conf(%)	Formula
162.0686	162.0686	0.0	0.0	1.5	1082.6	n/a	n/a	C7 H13 N O Cl

IR of Oxazoline 5a

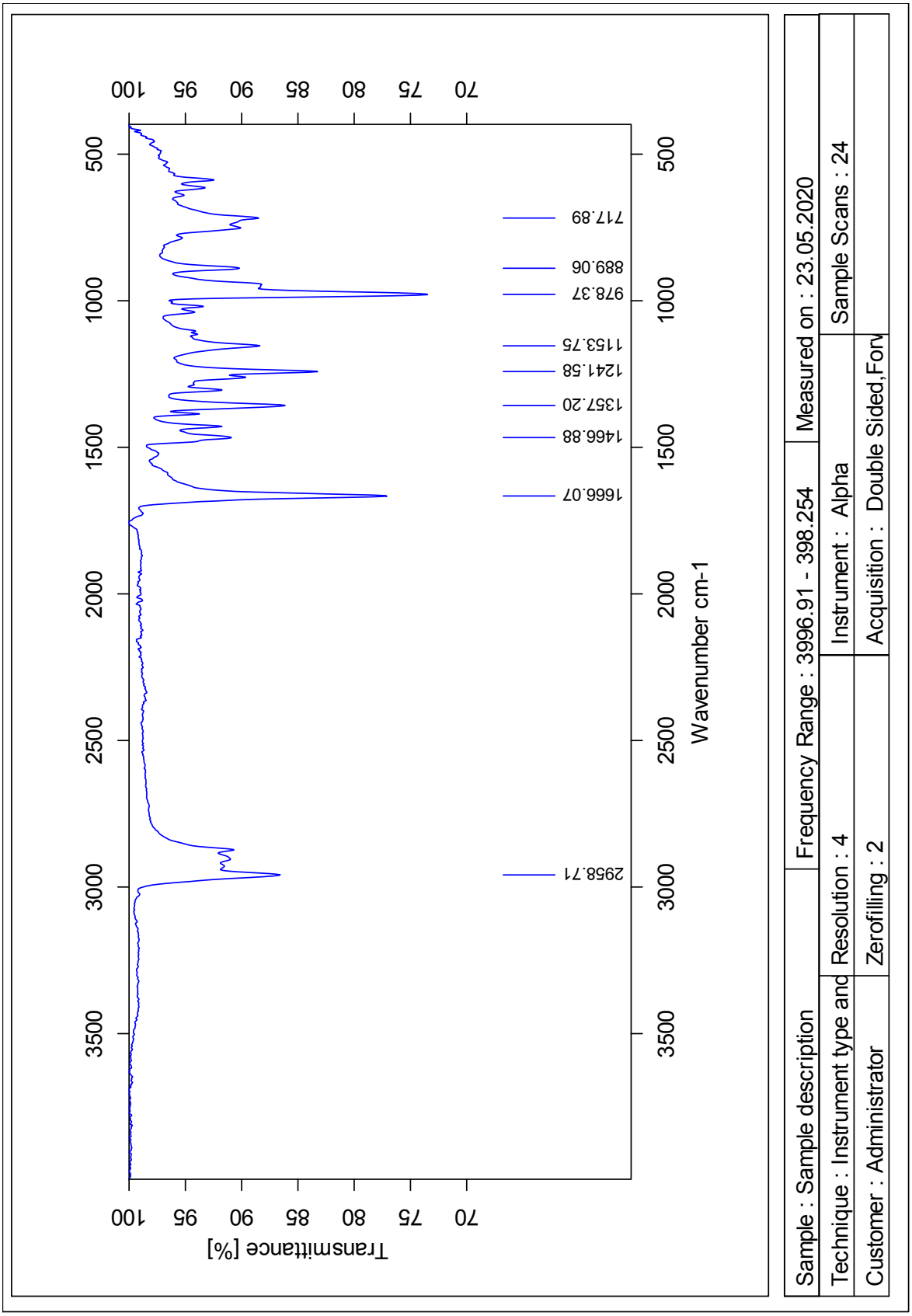

^{1}H-NMR of oxazooline 5b

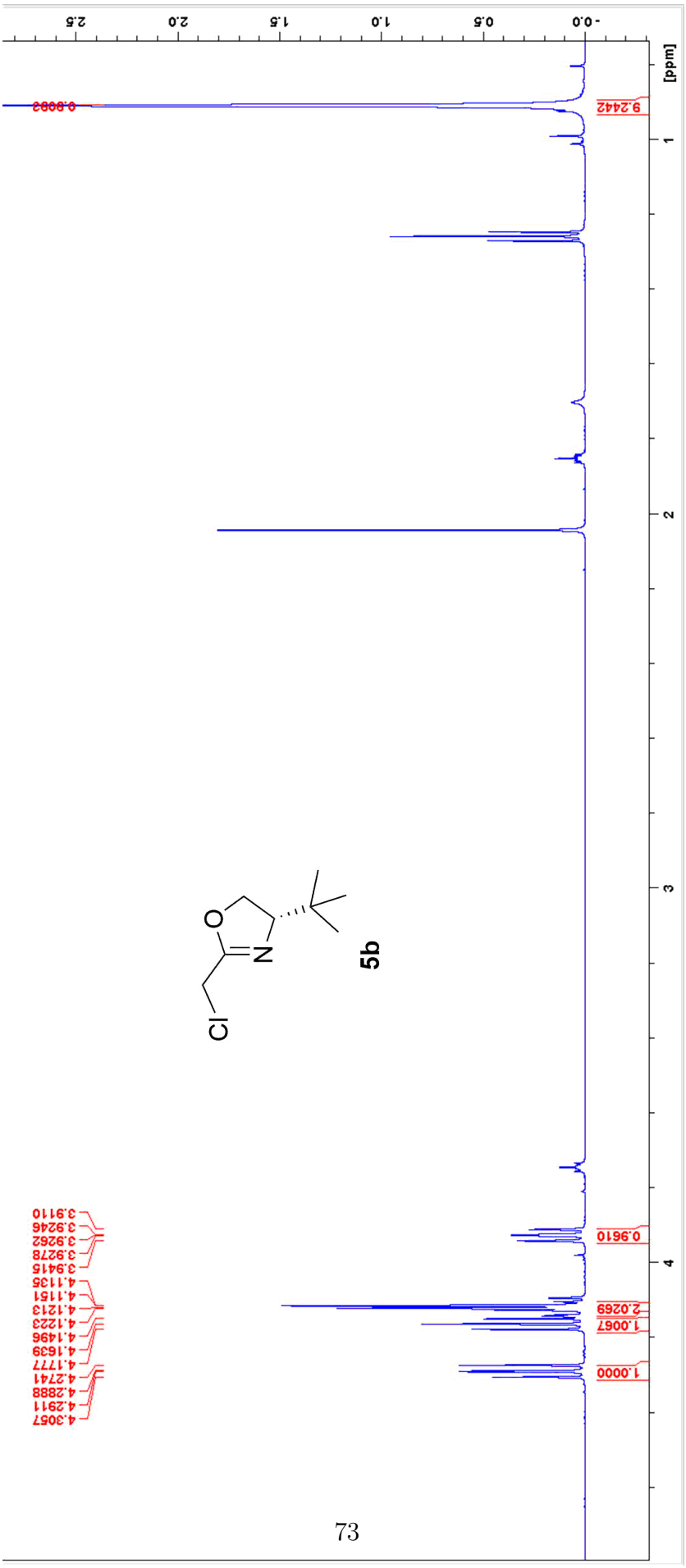

^{13}C-NMR of oxazoline 5b

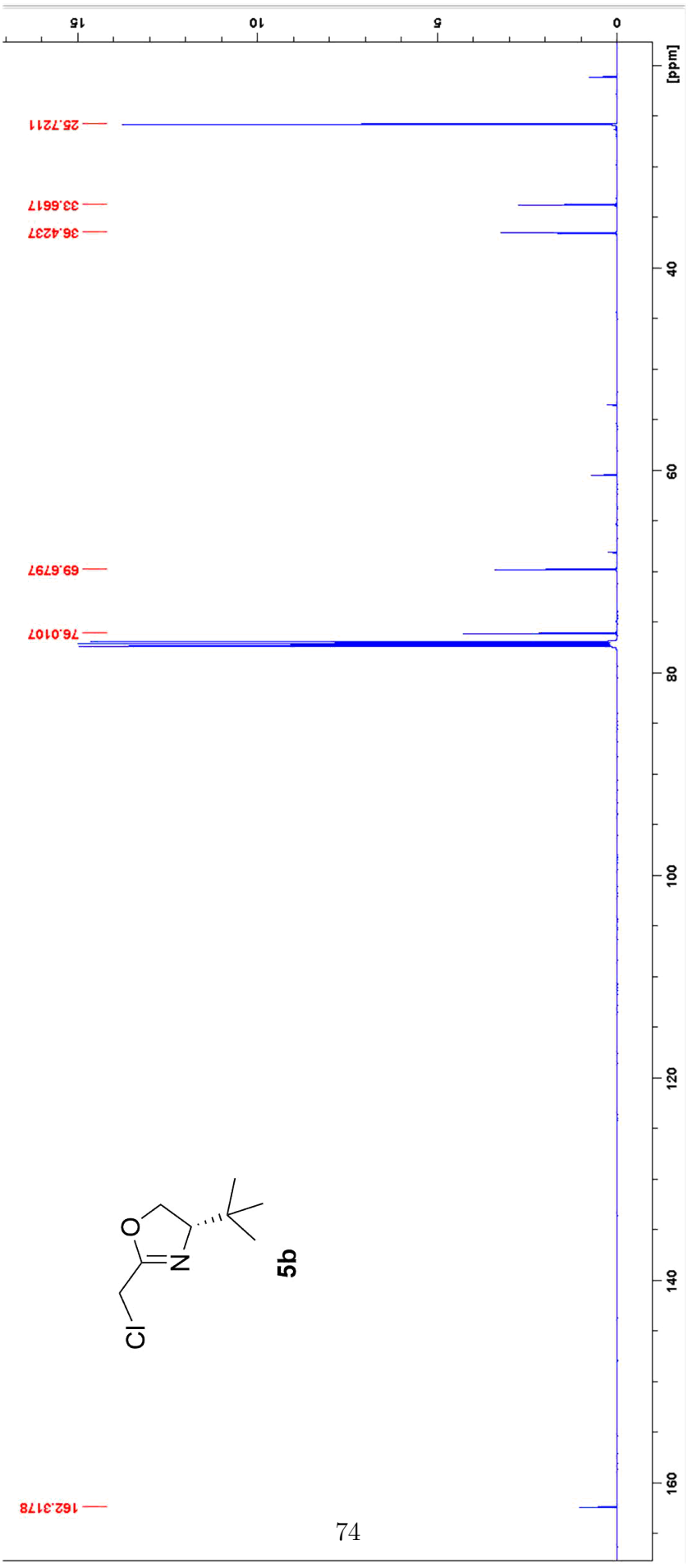

COSY of oxazoline 5b

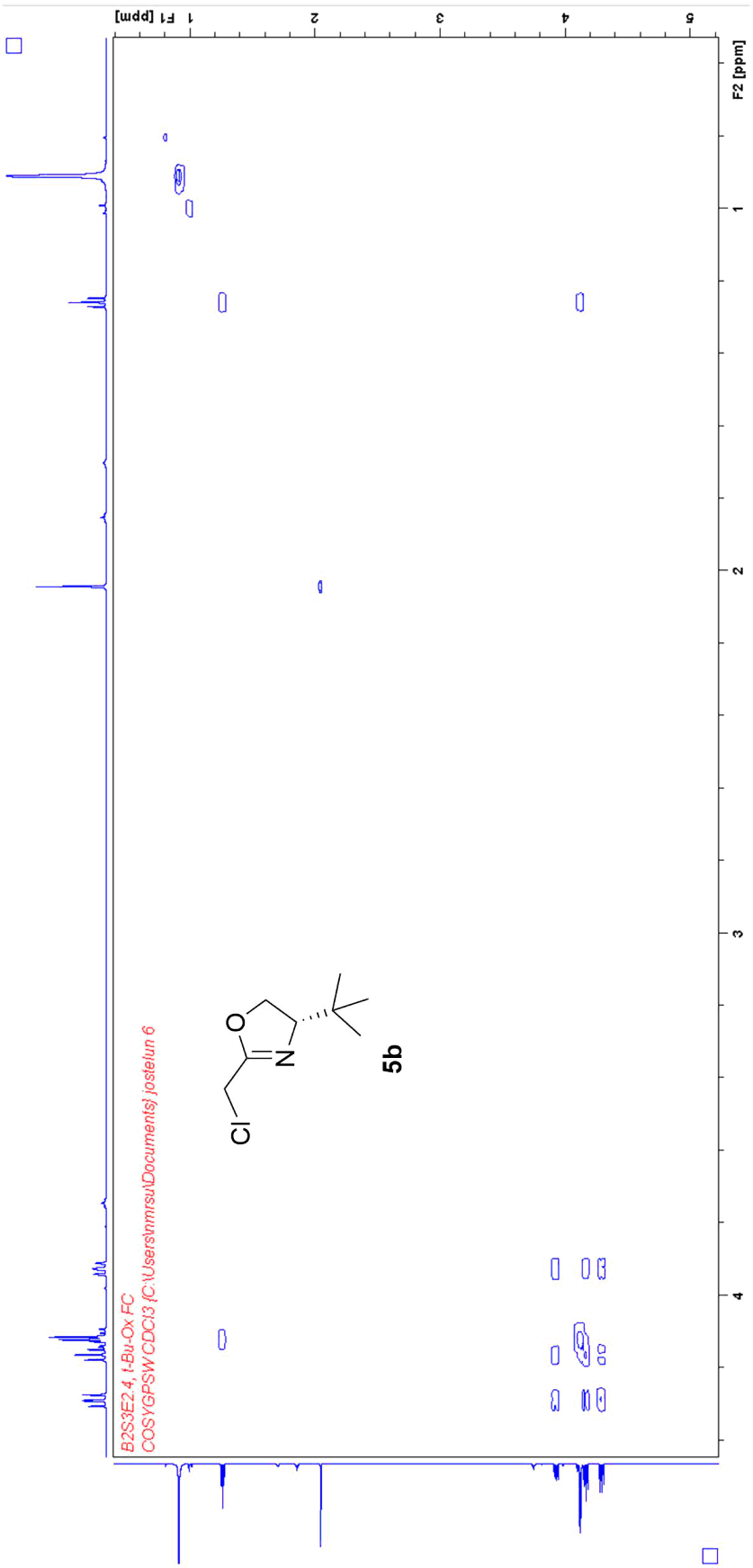

HSQC of oxazoline 5b

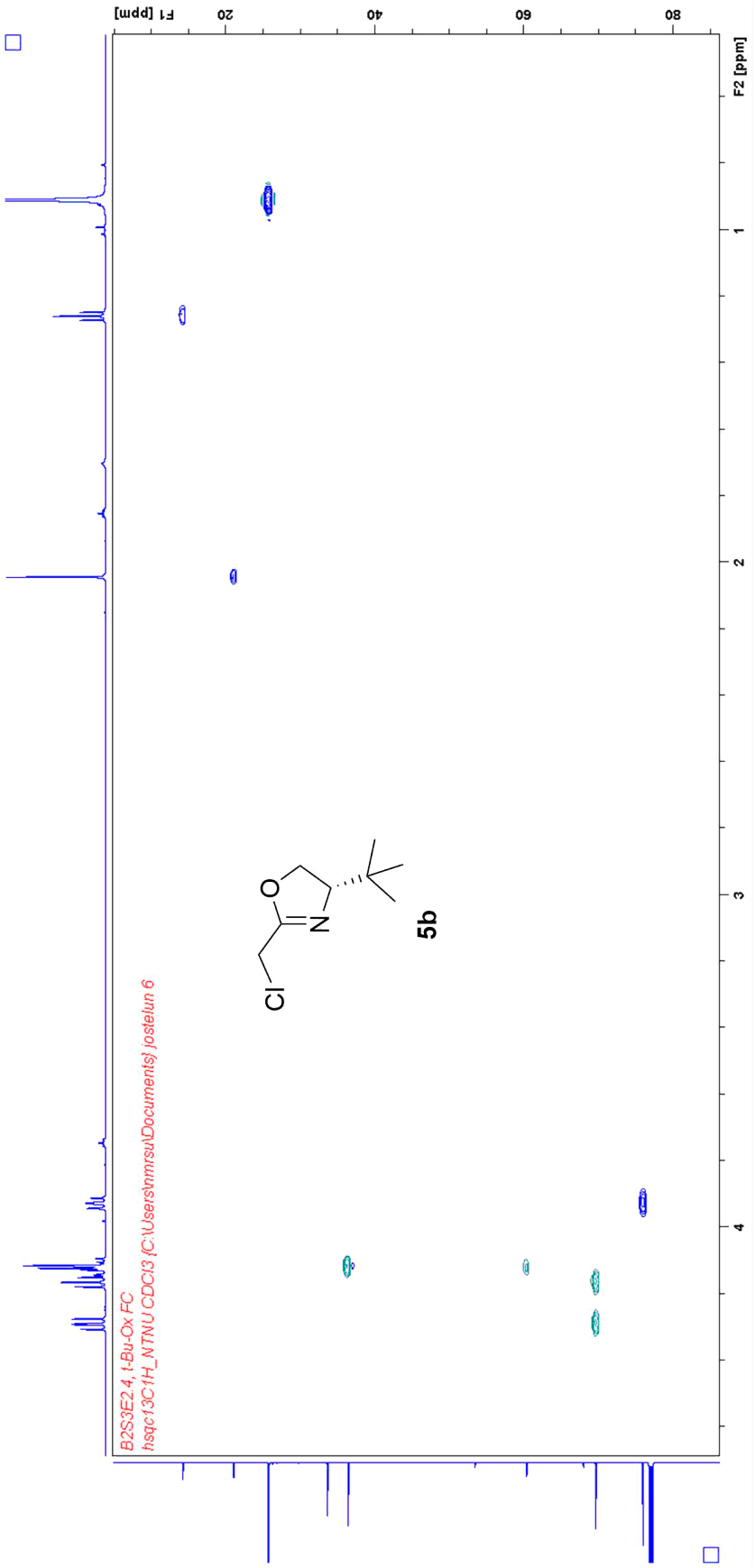

HMBC of oxazoline 5b

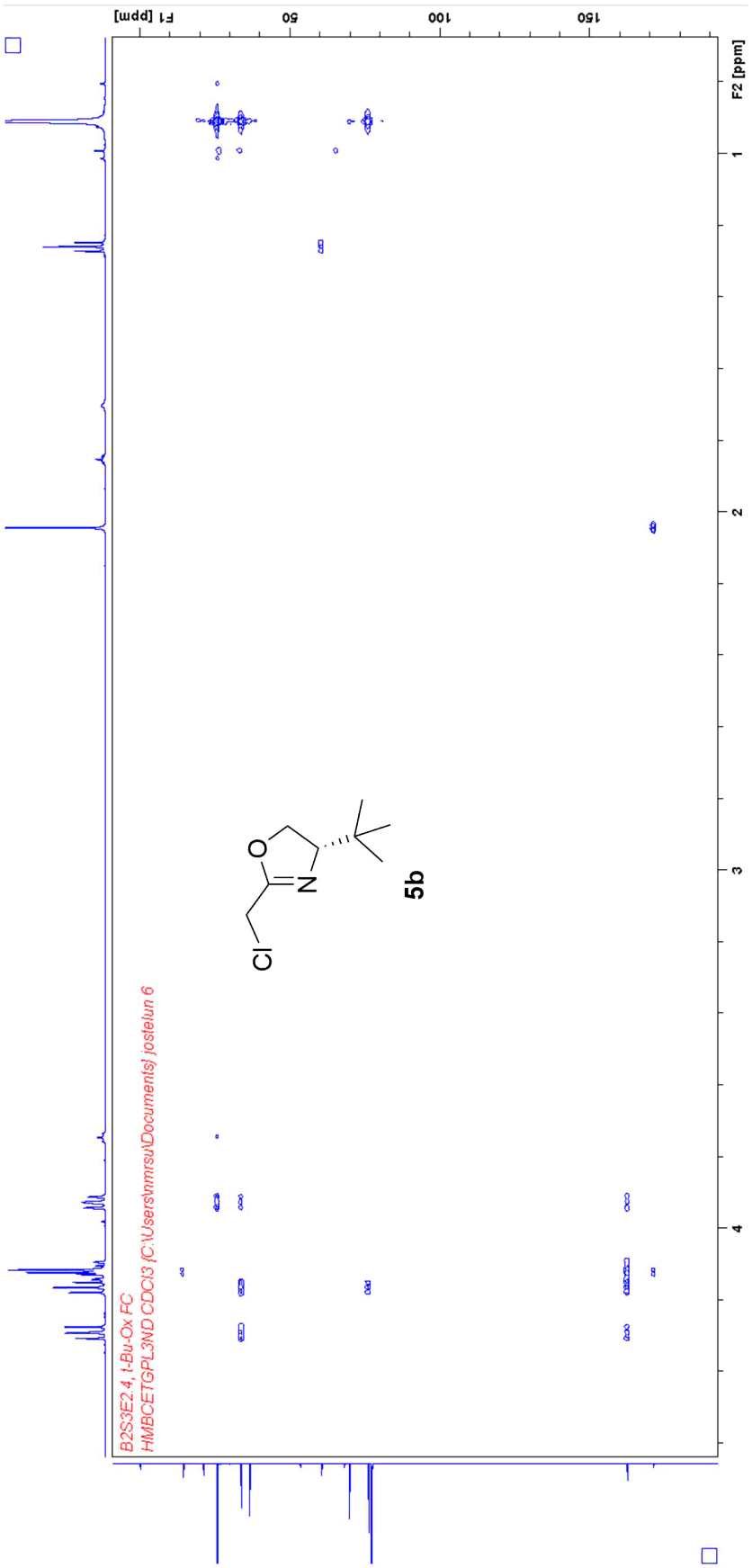

HRMS of Oxazoline 5b

Elemental Composition Report **Page 1**

Single Mass Analysis
Tolerance = 5.0 PPM / DBE: min = -5.0, max = 50.0
Element prediction: Off
Number of isotope peaks used for i-FIT = 3

Monoisotopic Mass, Even Electron Ions
201 formula(e) evaluated with 1 results within limits (all results (up to 1000) for each mass)
Elements Used:
C: 0-100 H: 0-100 N: 0-3 O: 0-5 Cl: 0-3
2020 125 30 (0.341) AM2 (Ar,35000.0,0.00,0.00); Cm (28:30)
1: TOF MS ES+

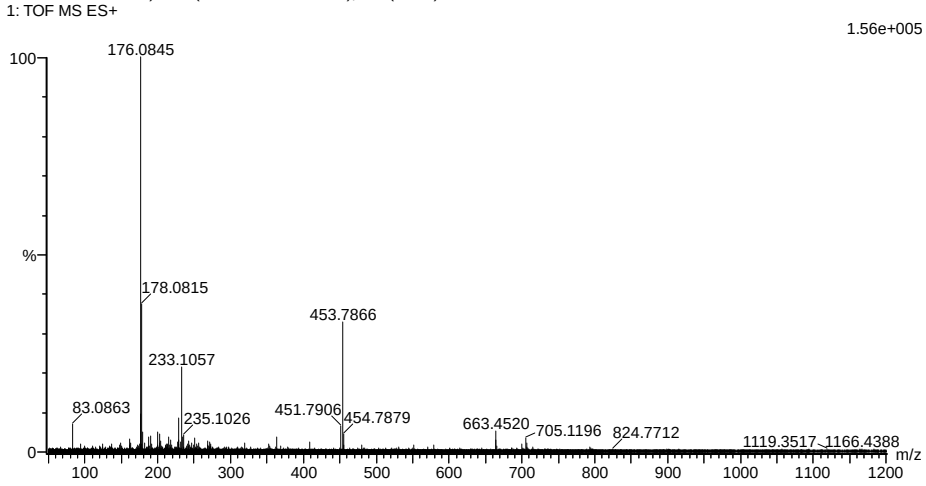

Minimum:				-5.0				
Maximum:		5.0	5.0	50.0				
Mass	Calc. Mass	mDa	PPM	DBE	i-FIT	Norm	Conf(%)	Formula
176.0845	176.0842	0.3	1.7	1.5	1495.2	n/a	n/a	C8 H15 N O Cl

IR of Oxazoline 5b

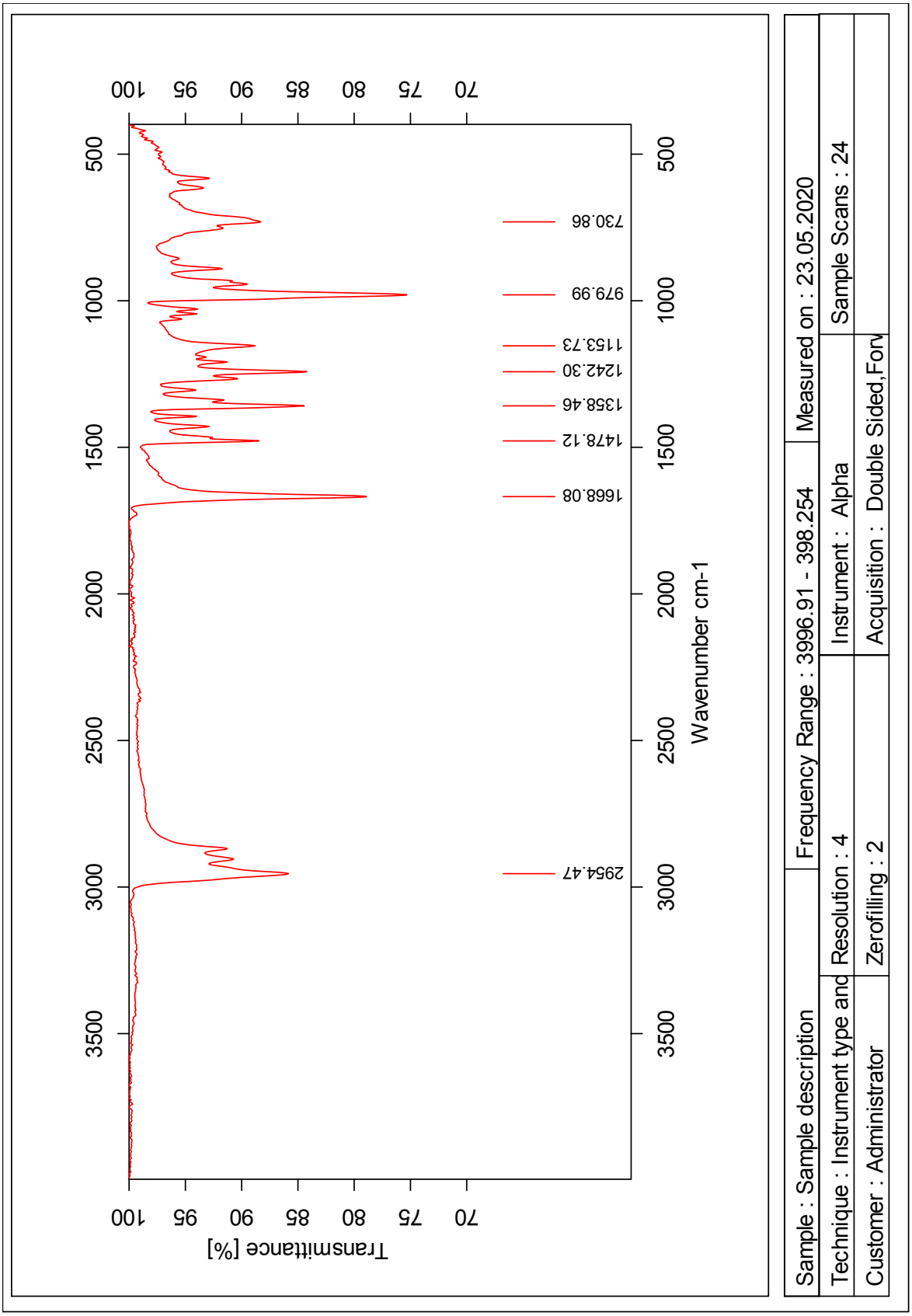

C Spectra of Imidazollium salts 7a, 7b

^{1}H-NMR of Imidazolioum salt 7a

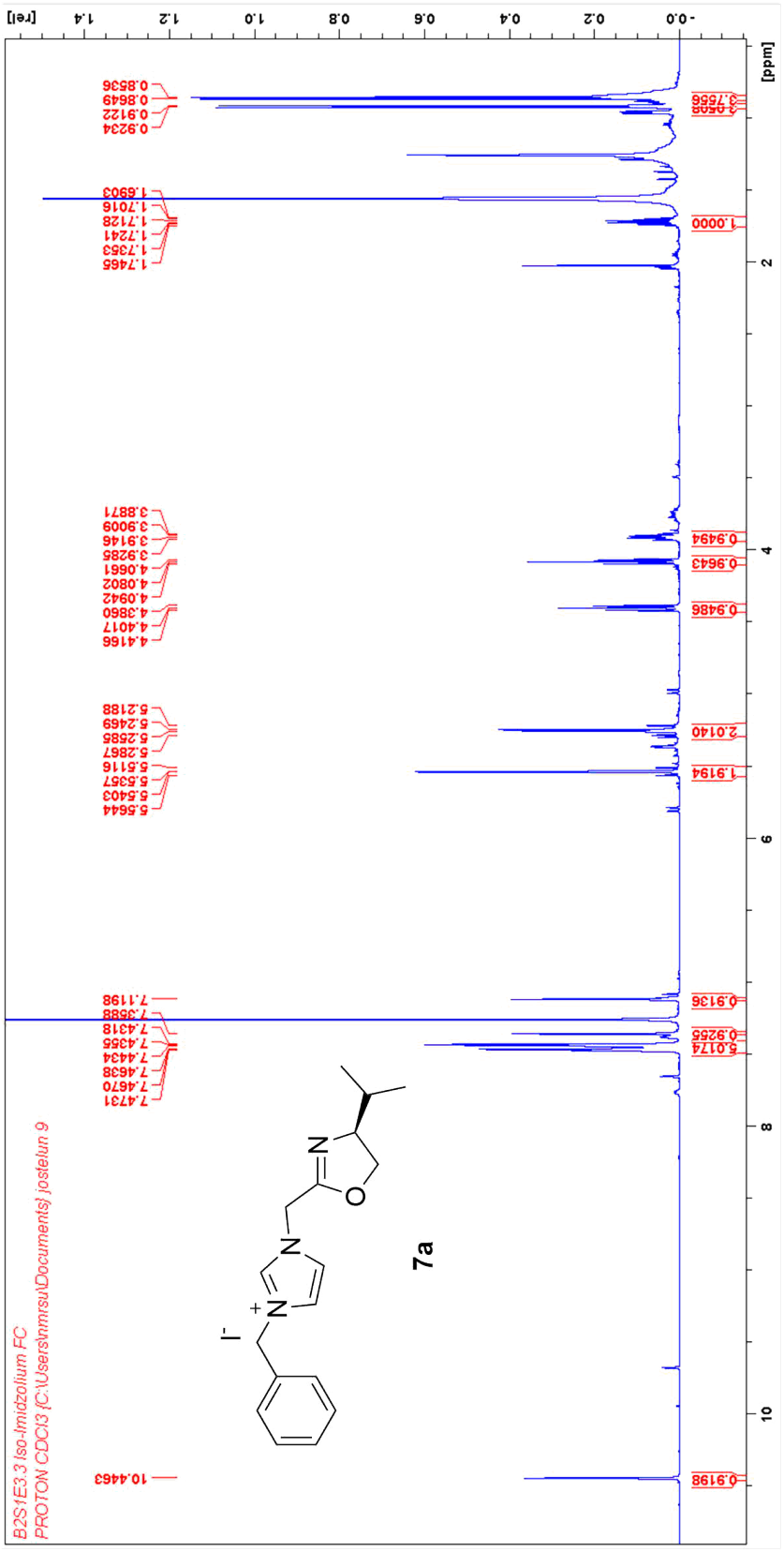

^{13}C-NMR of Imidazolioum salt 7a

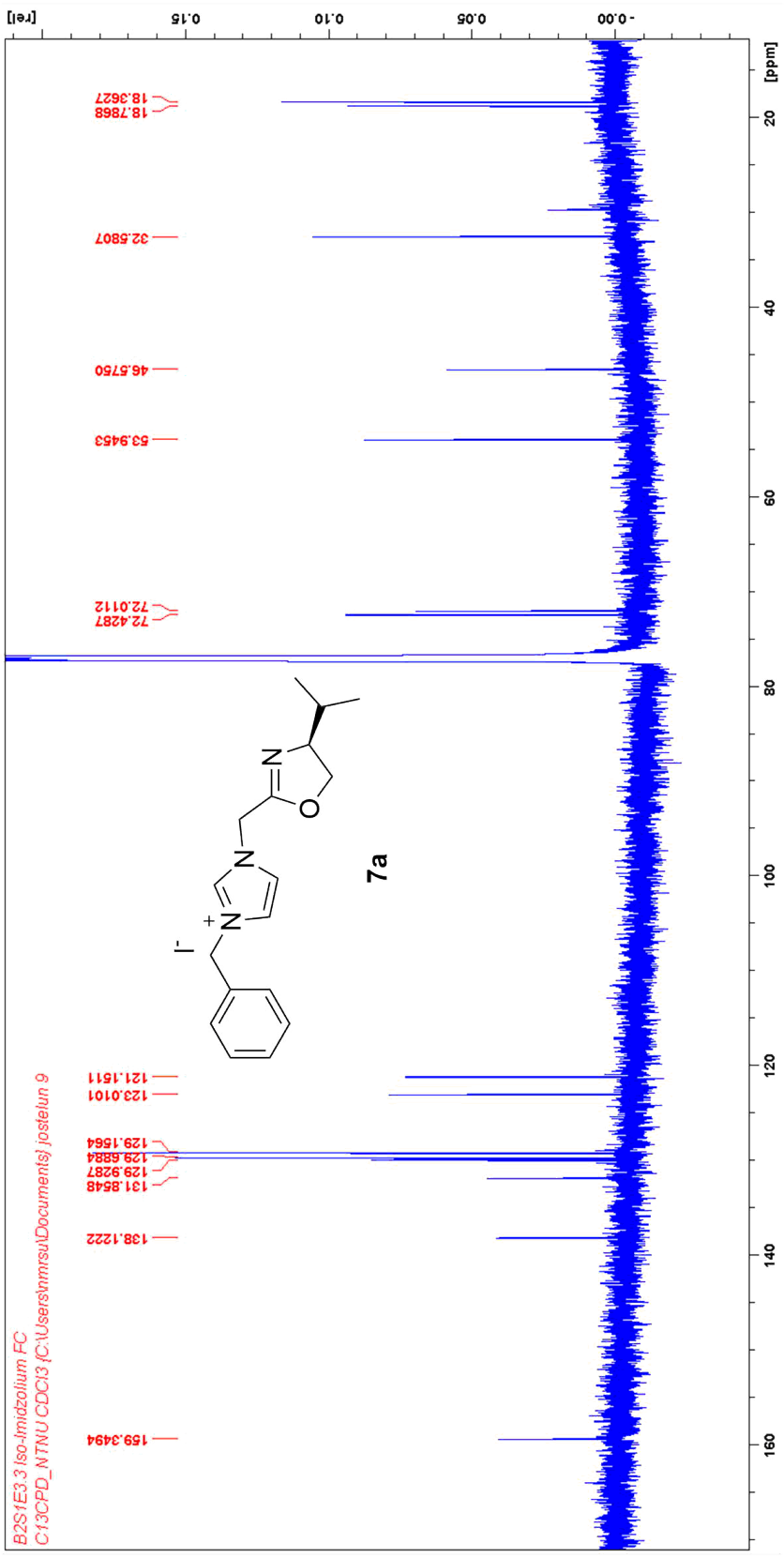

COSY of Imidazolioum salt 7a

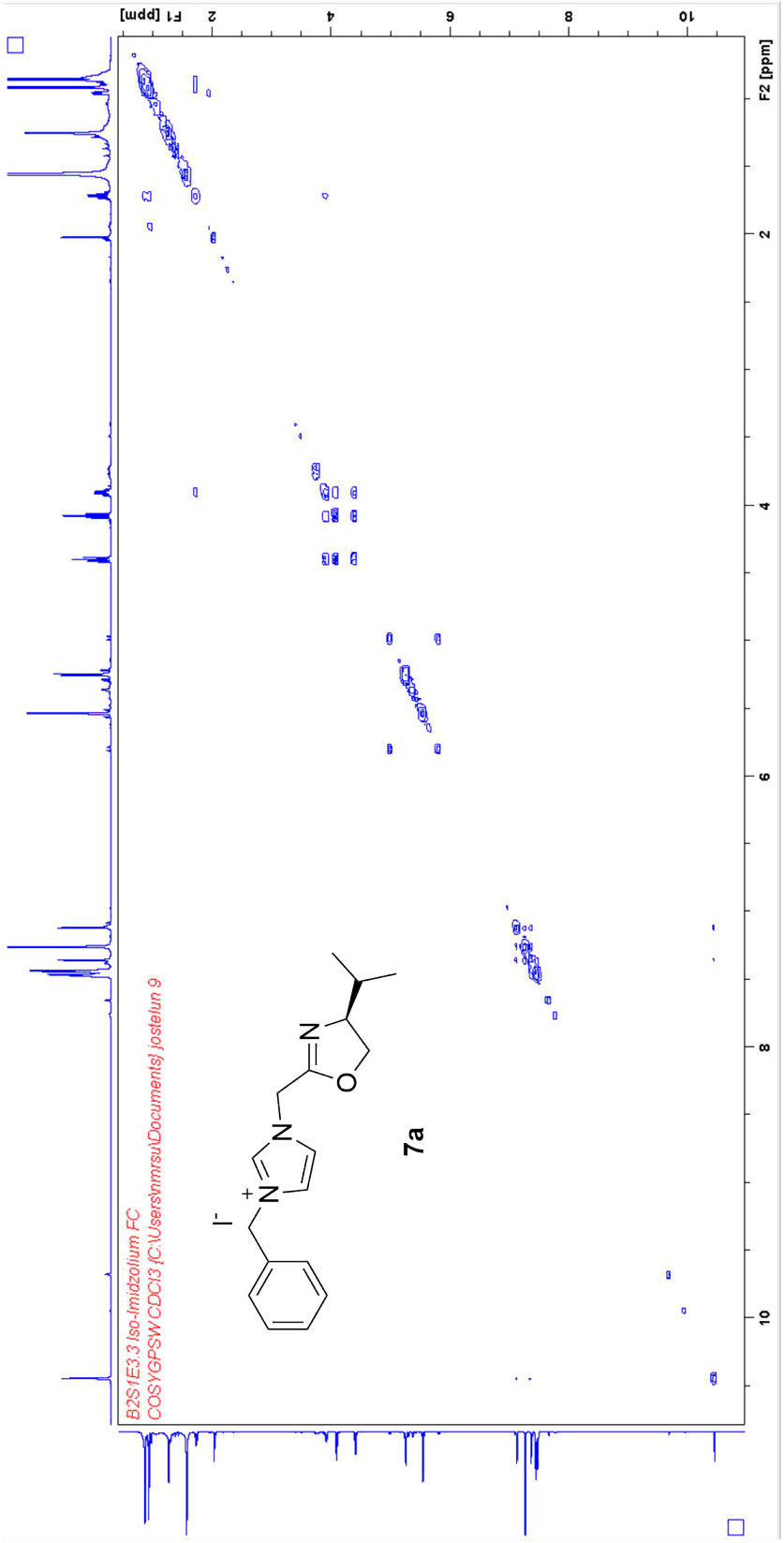

HSQC of Imidazolioum salt 7a

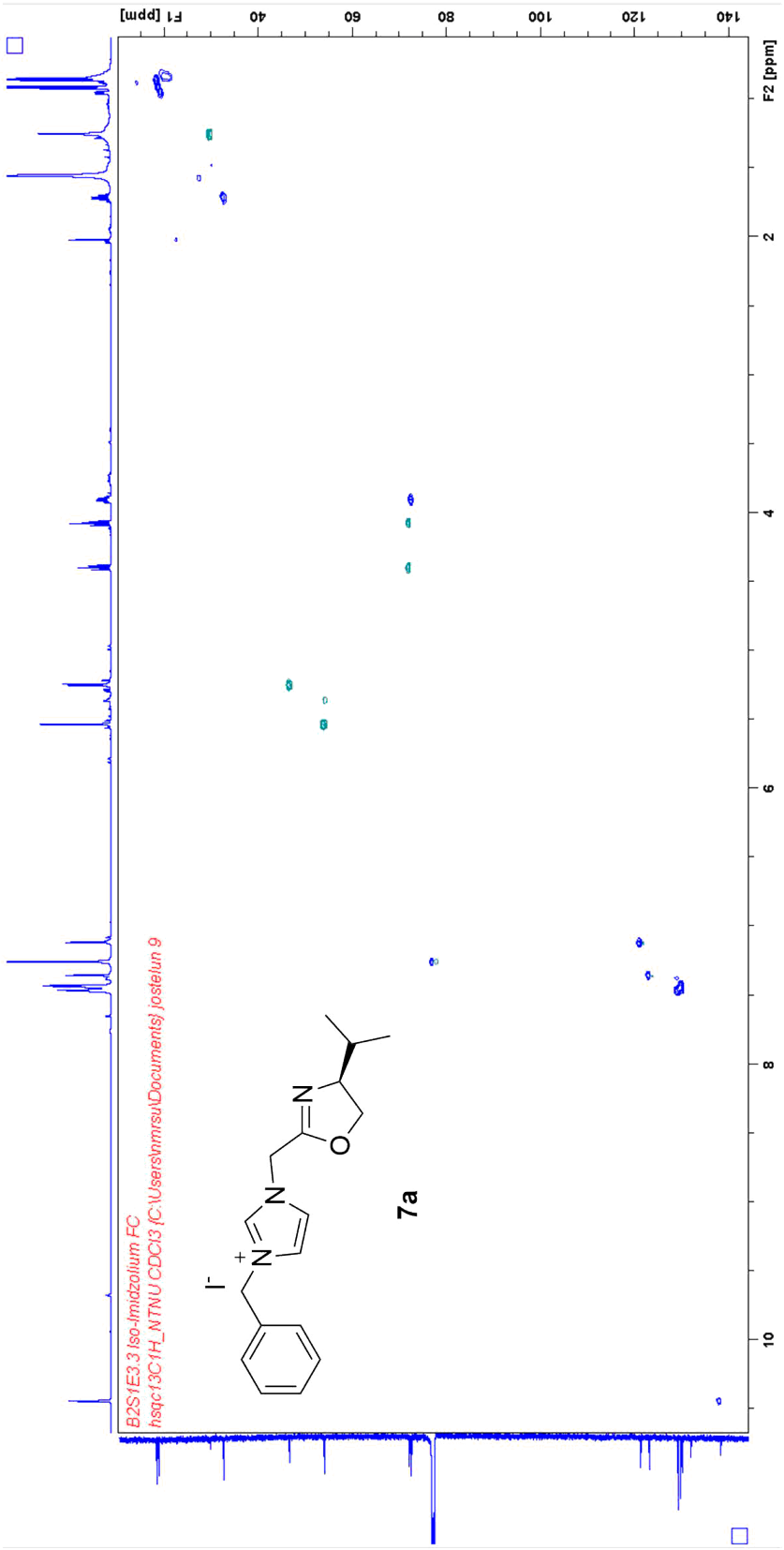

HMBC of Imidazolioum salt 7a

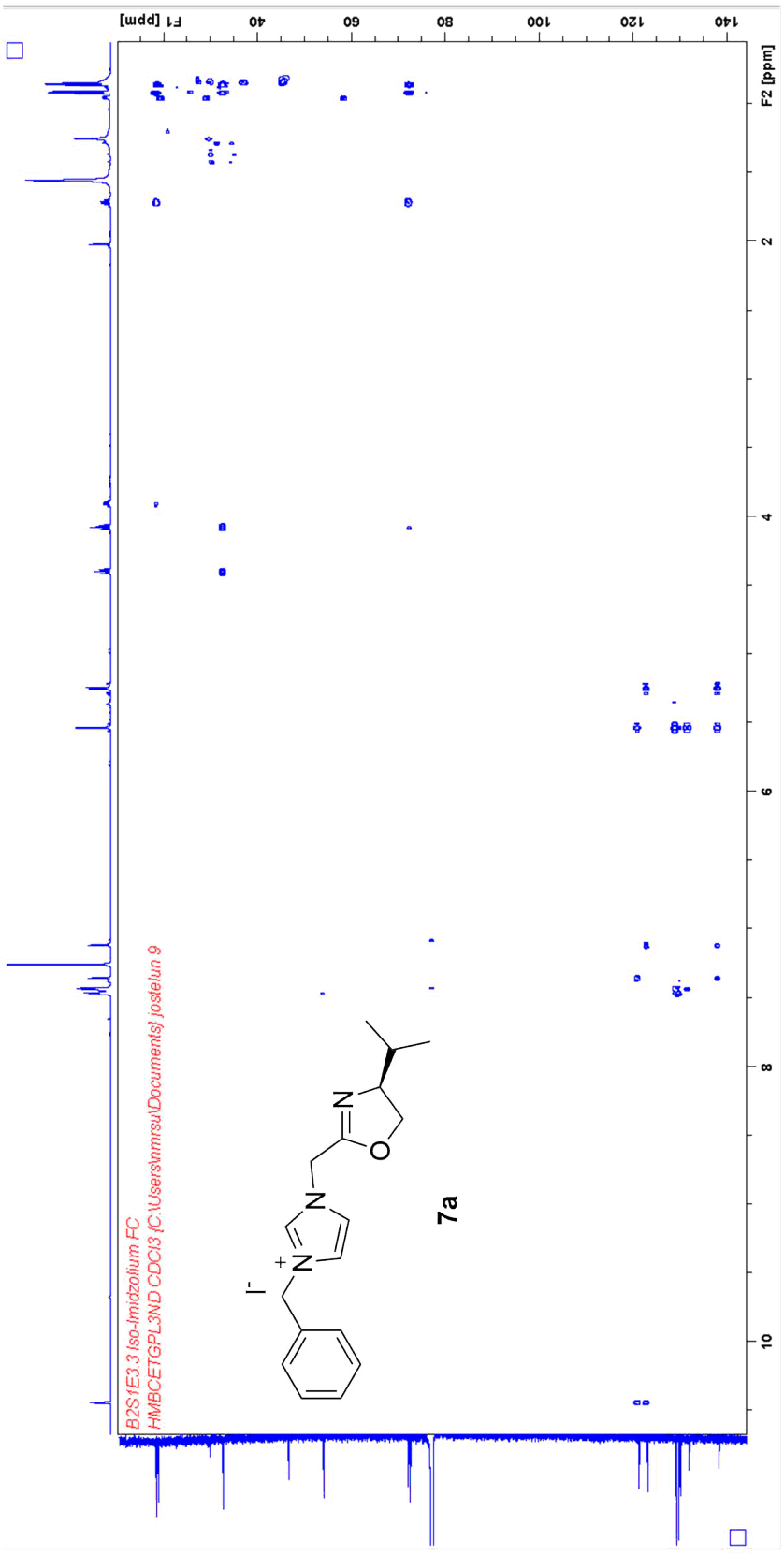

HRMS of Imidazolium salt 7a

Elemental Composition Report **Page 1**

Single Mass Analysis
Tolerance = 2.0 PPM / DBE: min = -5.0, max = 50.0
Element prediction: Off
Number of isotope peaks used for i-FIT = 3

Monoisotopic Mass, Even Electron Ions
347 formula(e) evaluated with 1 results within limits (all results (up to 1000) for each mass)
Elements Used:
C: 0-100 H: 0-100 N: 0-3 O: 0-12 S: 0-1
2020-145 237 (4.617) AM2 (Ar,35000.0,0.00,0.00); Cm (203:239)
1: TOF MS ASAP+

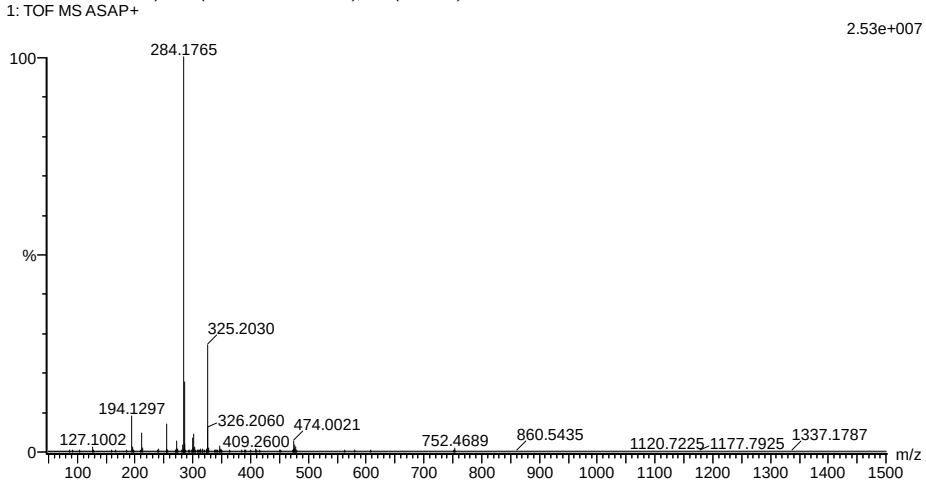

Minimum:				-5.0				
Maximum:		5.0	2.0	50.0				
Mass	Calc. Mass	mDa	PPM	DBE	i-FIT	Norm	Conf(%)	Formula
284.1765	284.1763	0.2	0.7	8.5	1792.6	n/a	n/a	C17 H22 N3 O

IR of Imidazolium salt 7a

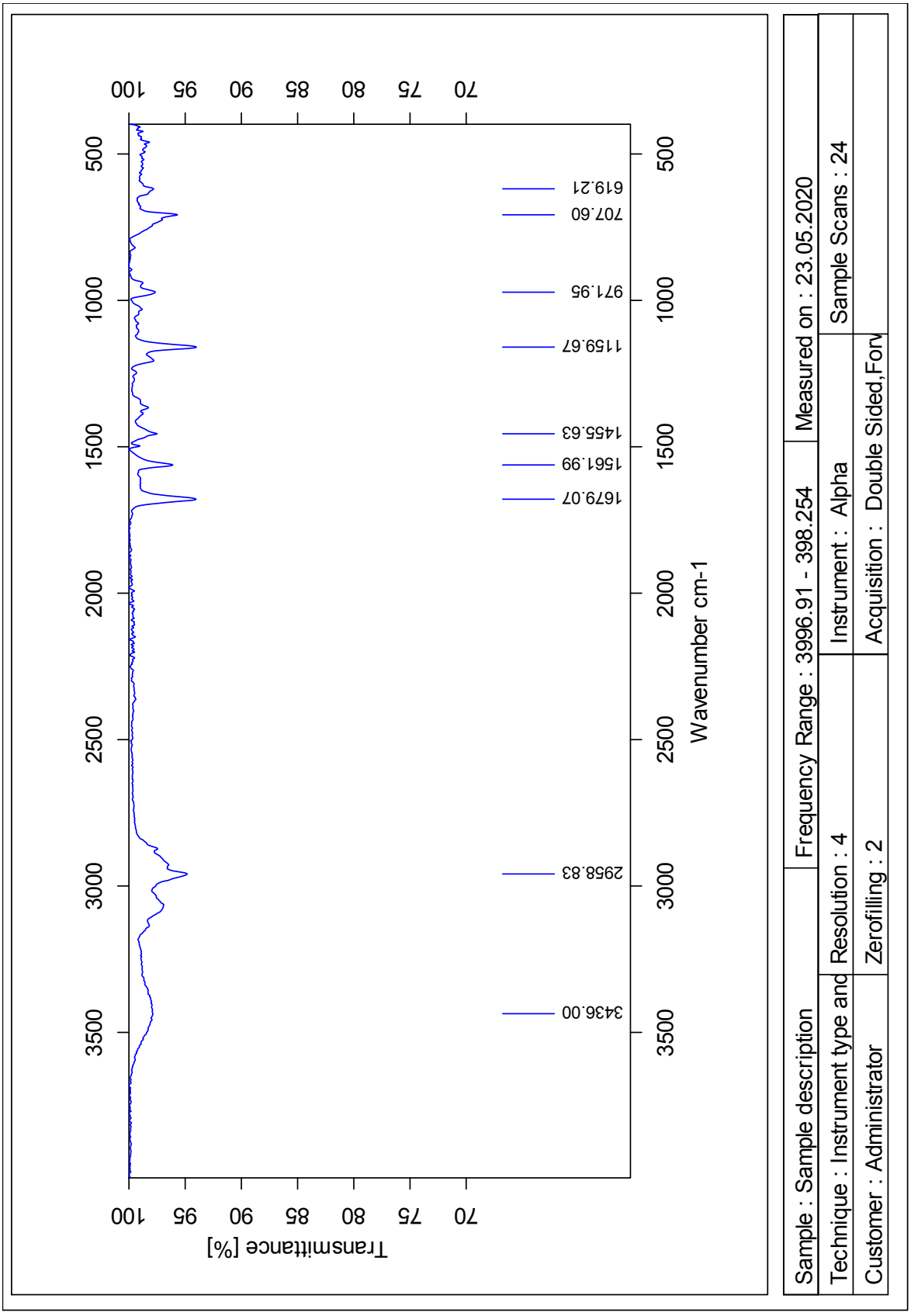

^{1}H-NMR of Imidazolioum salt 7b

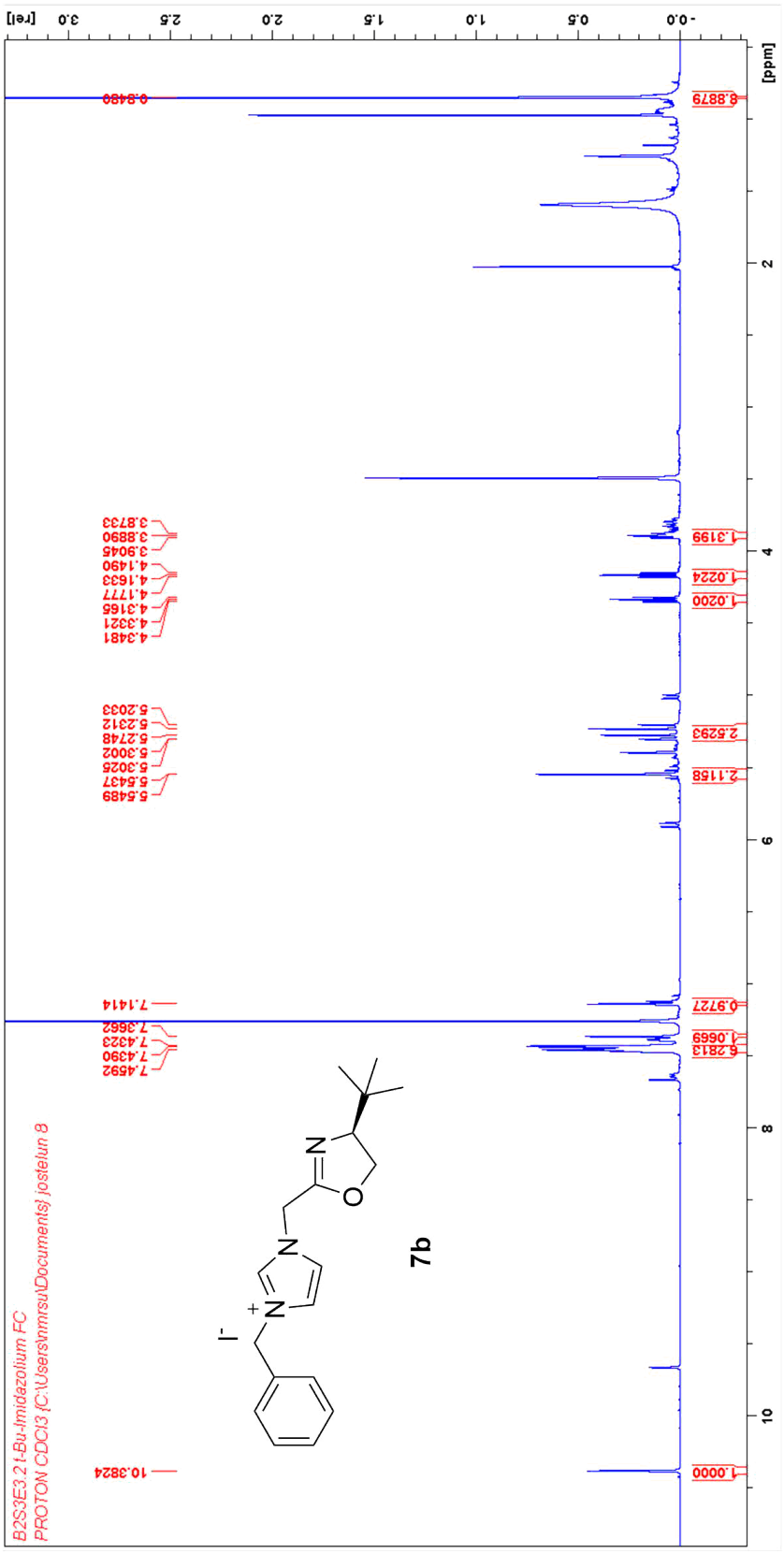

^{13}C-NMR of Imidazolioum salt 7b

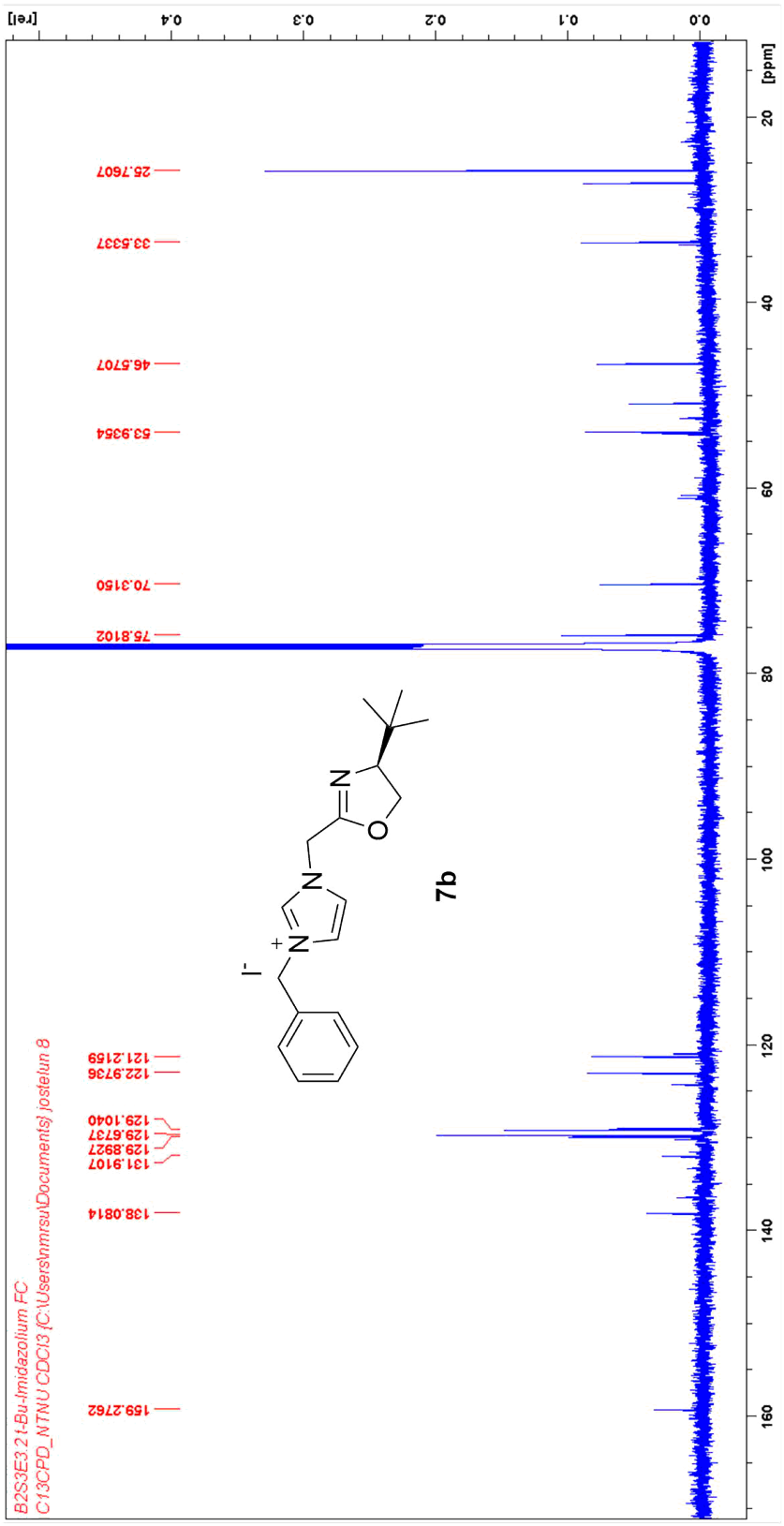

COSY of Imidazolioum salt 7b

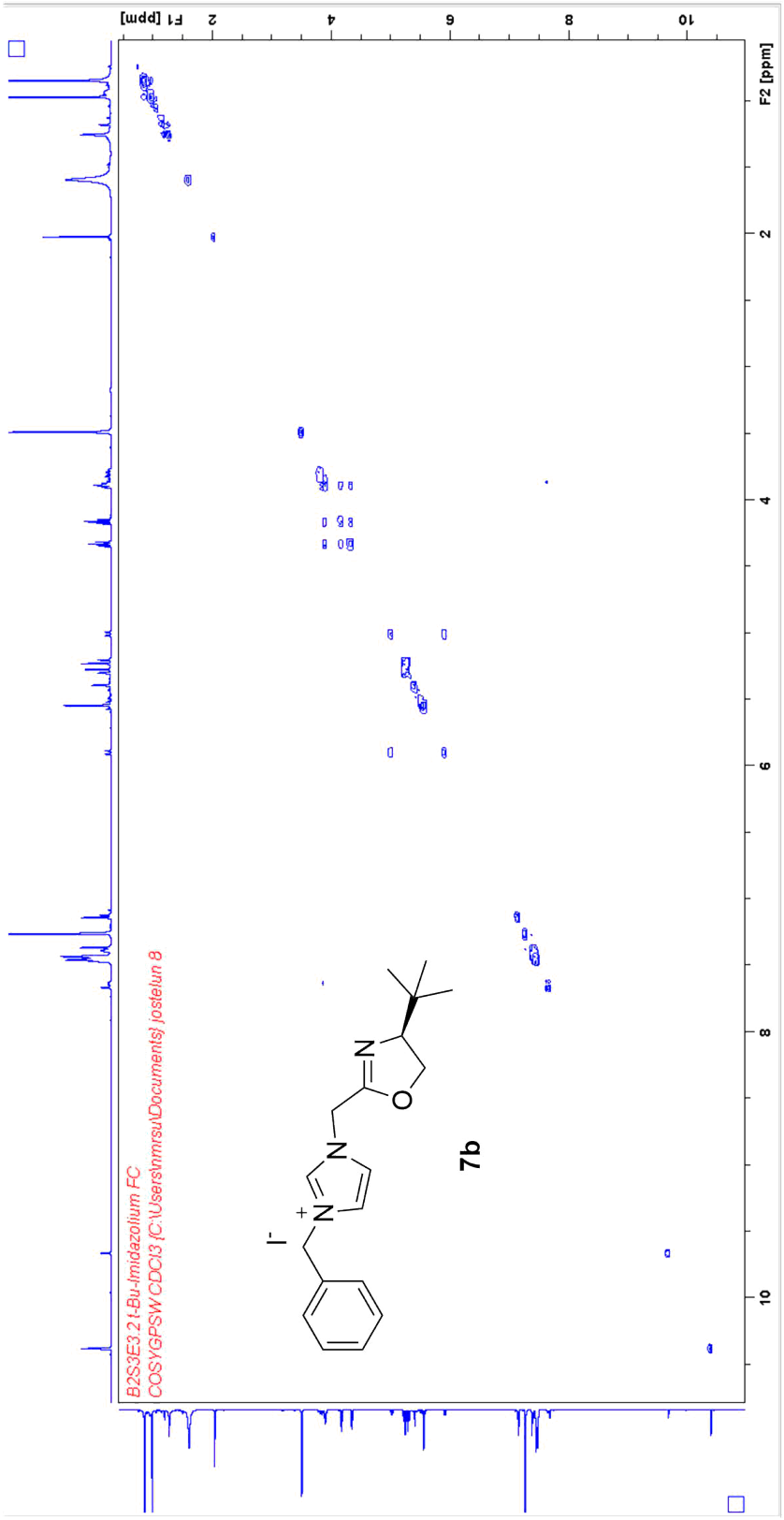

HSQC of Imidazolioum salt 7b

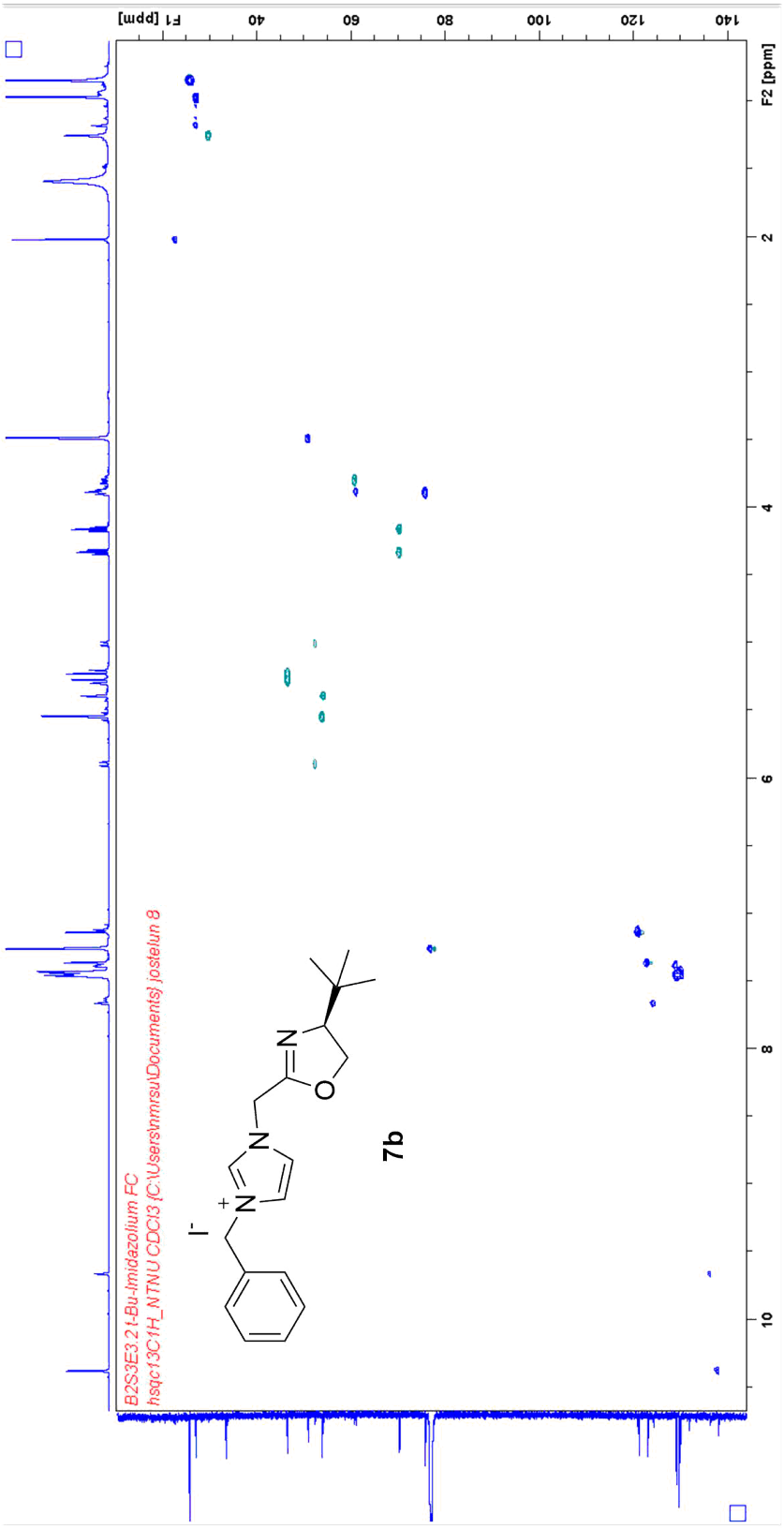

HMBC of Imidazolioum salt 7b

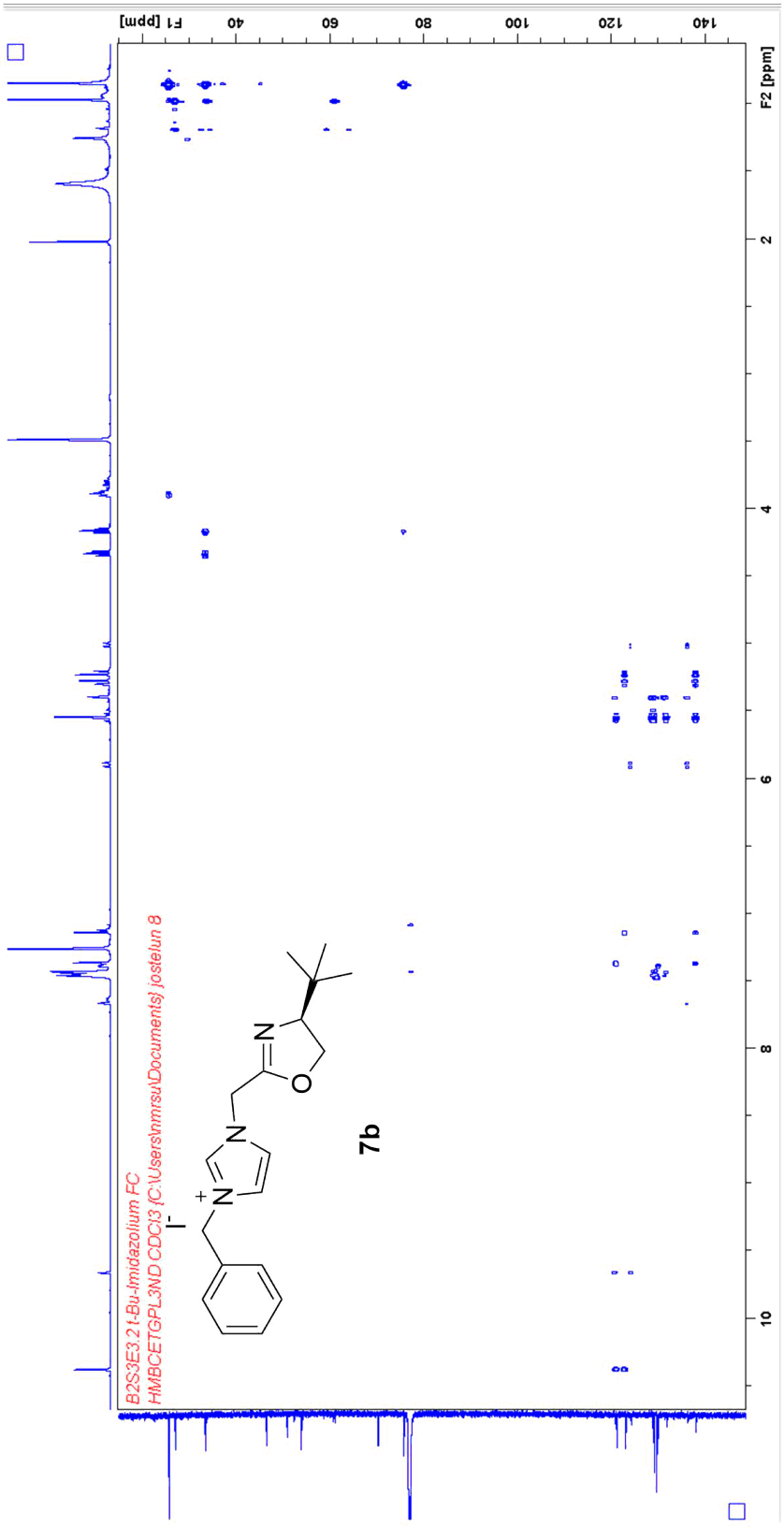

HRMS of Imidazolium salt 7b

Elemental Composition Report **Page 1**

Single Mass Analysis
Tolerance = 5.0 PPM / DBE: min = -5.0, max = 50.0
Element prediction: Off
Number of isotope peaks used for i-FIT = 3

Monoisotopic Mass, Even Electron Ions
136 formula(e) evaluated with 1 results within limits (all results (up to 1000) for each mass)
Elements Used:
C: 0-100 H: 0-100 N: 0-3 O: 0-7
JA_SVG_20200507_146 27 (0.505) AM2 (Ar,35000.0,0.00,0.00); Cm (22:27)
1: TOF MS ES+

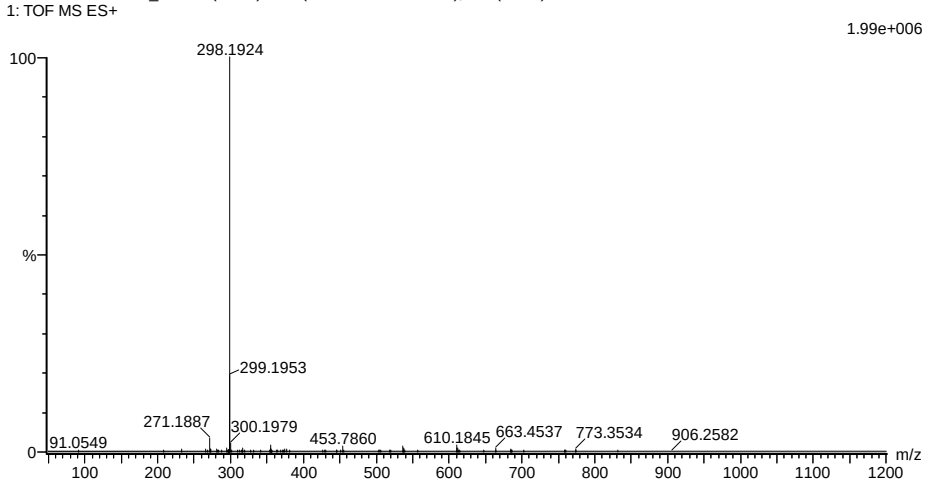

Minimum:				-5.0				
Maximum:		5.0	5.0	50.0				
Mass	Calc. Mass	mDa	PPM	DBE	i-FIT	Norm	Conf(%)	Formula
298.1924	298.1919	0.5	1.7	8.5	1263.0	n/a	n/a	C18 H24 N3 O

IR of Imidazolium salt 7b

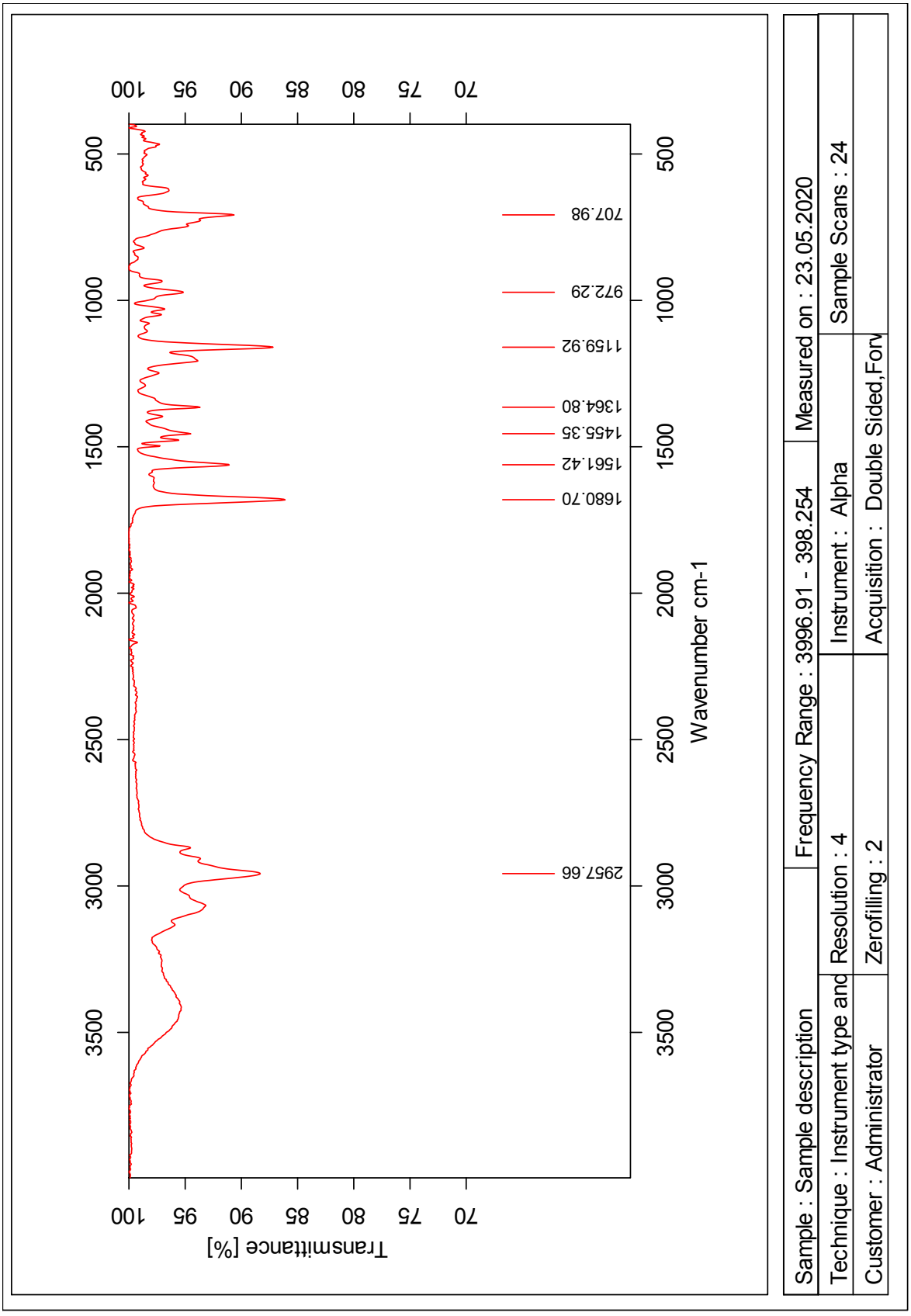

D SPectra of Au(I)-complexes 8a, 8b

^{1}H-NMR of Au(I)-Complex 8a

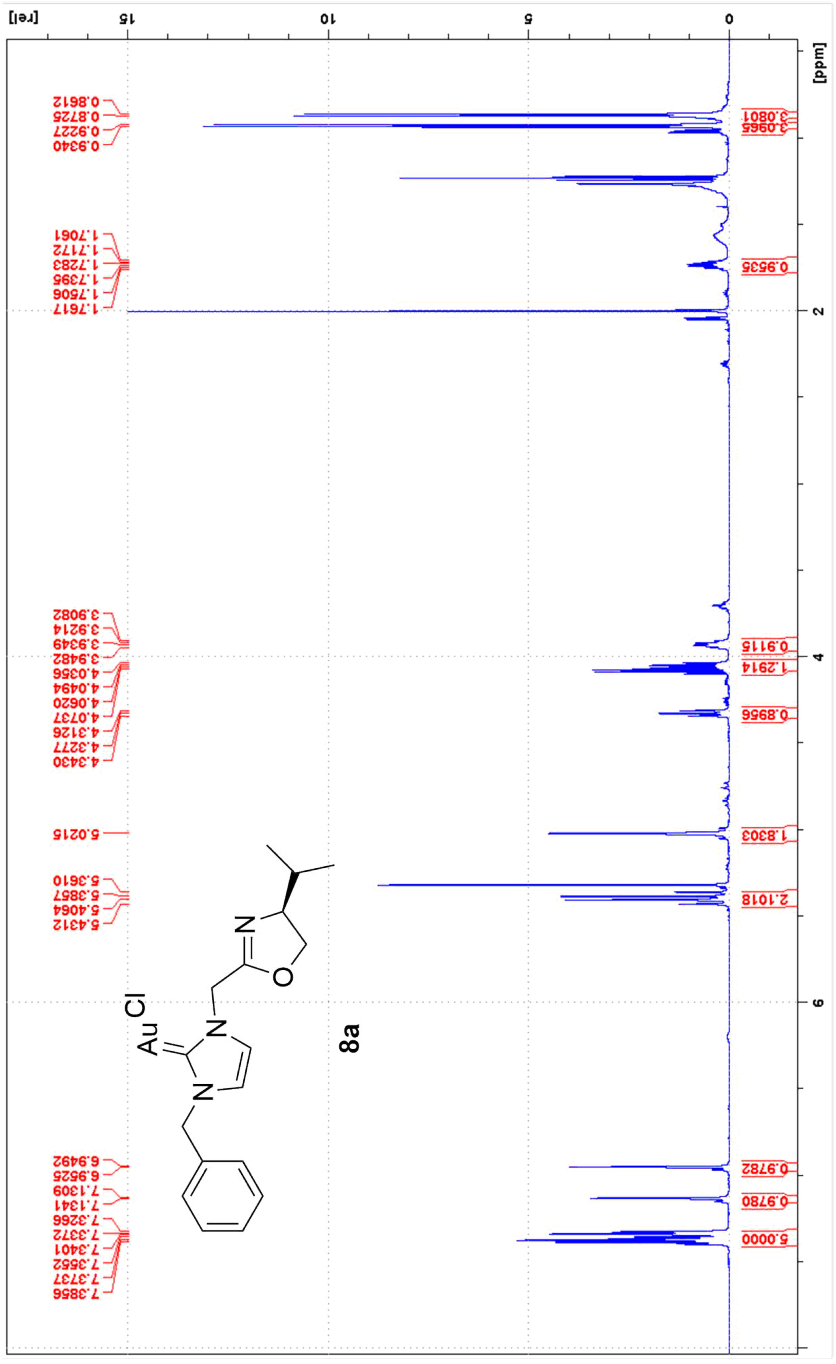

^{13}C-NMR of Au(I)-Complex 8a

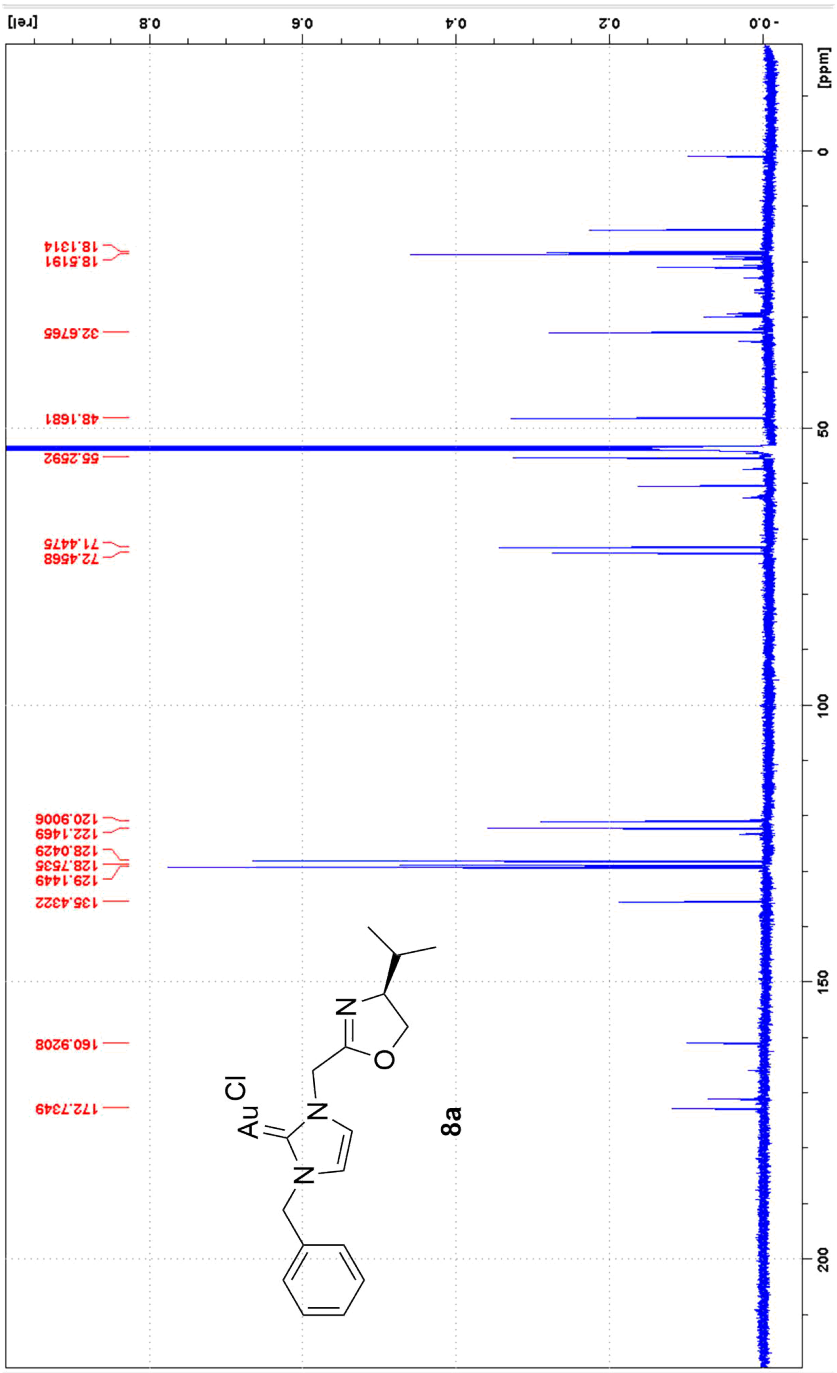

COSY of Au(I)-Complex 8a

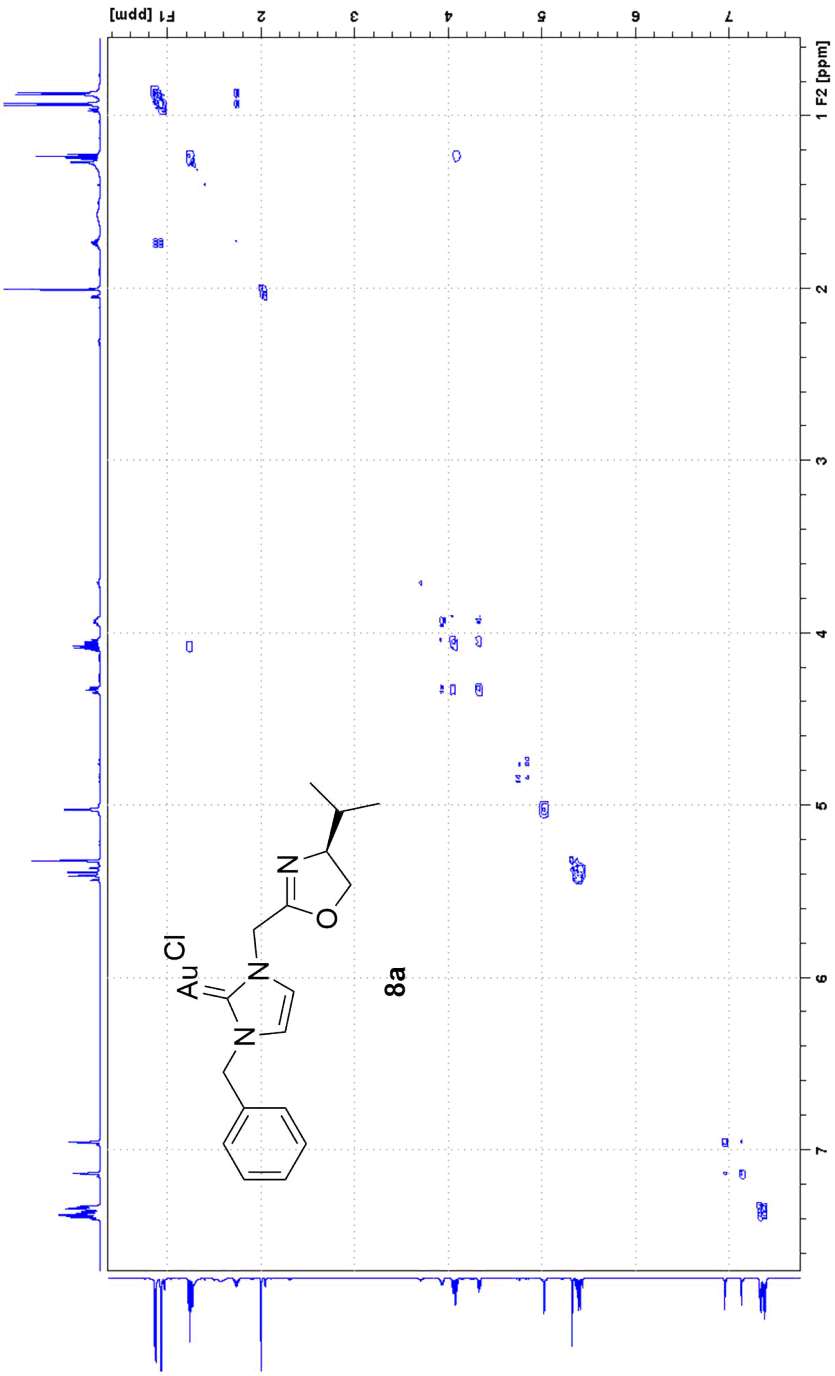

HSQC of Au(I)-Complex 8a

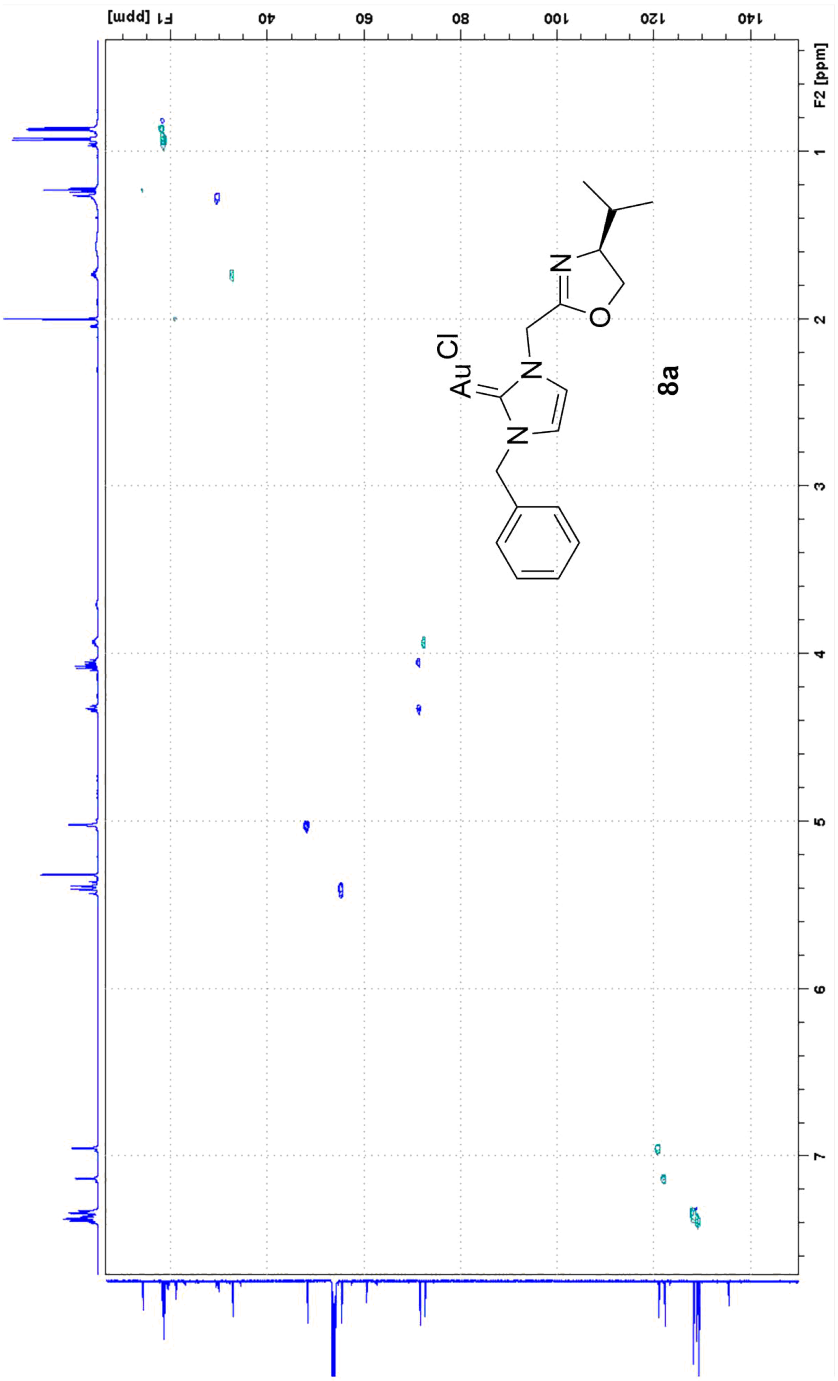

HMBC of Au(I)-Complex 8a

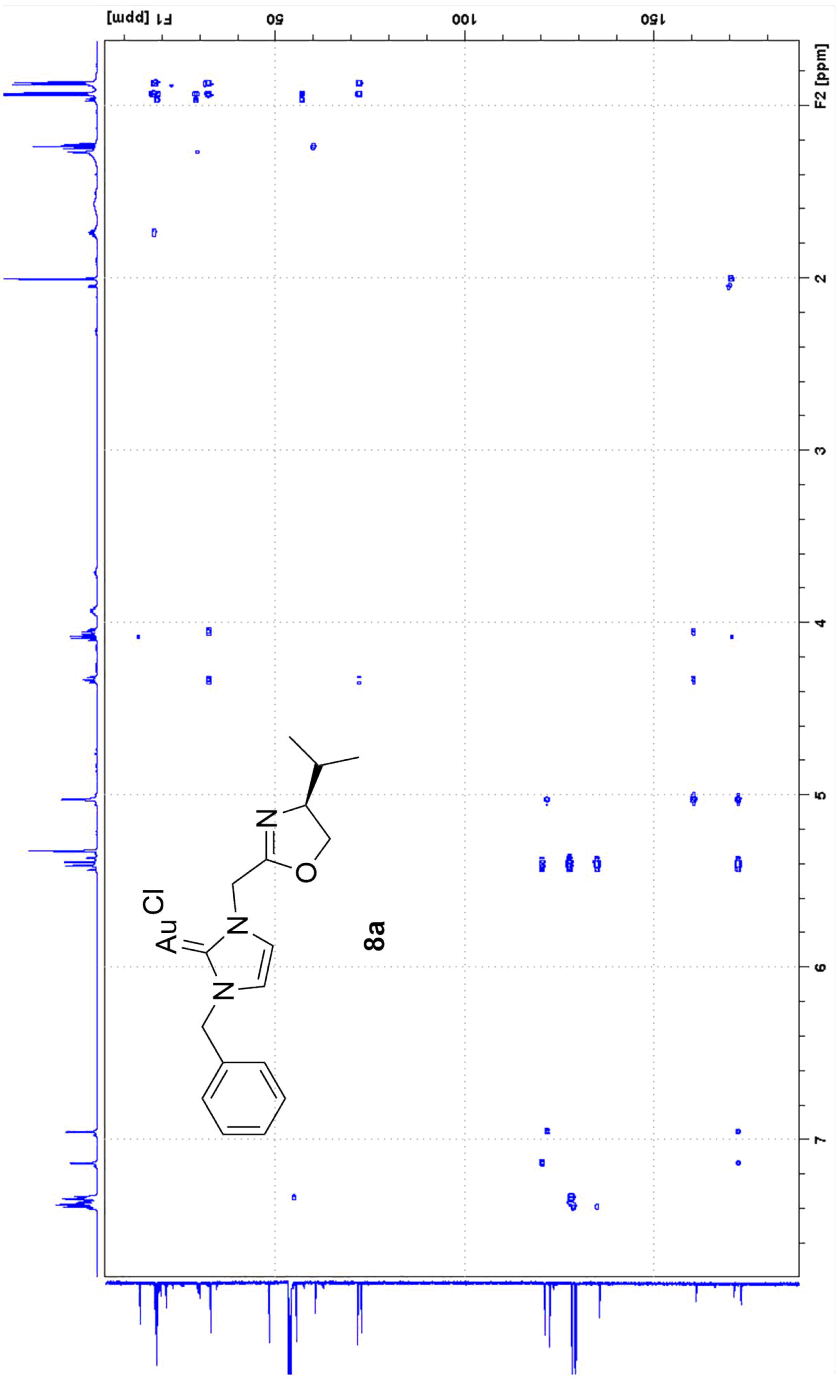

^{1}H,^{15}N-HMBC of Au(I)-Complex 8a

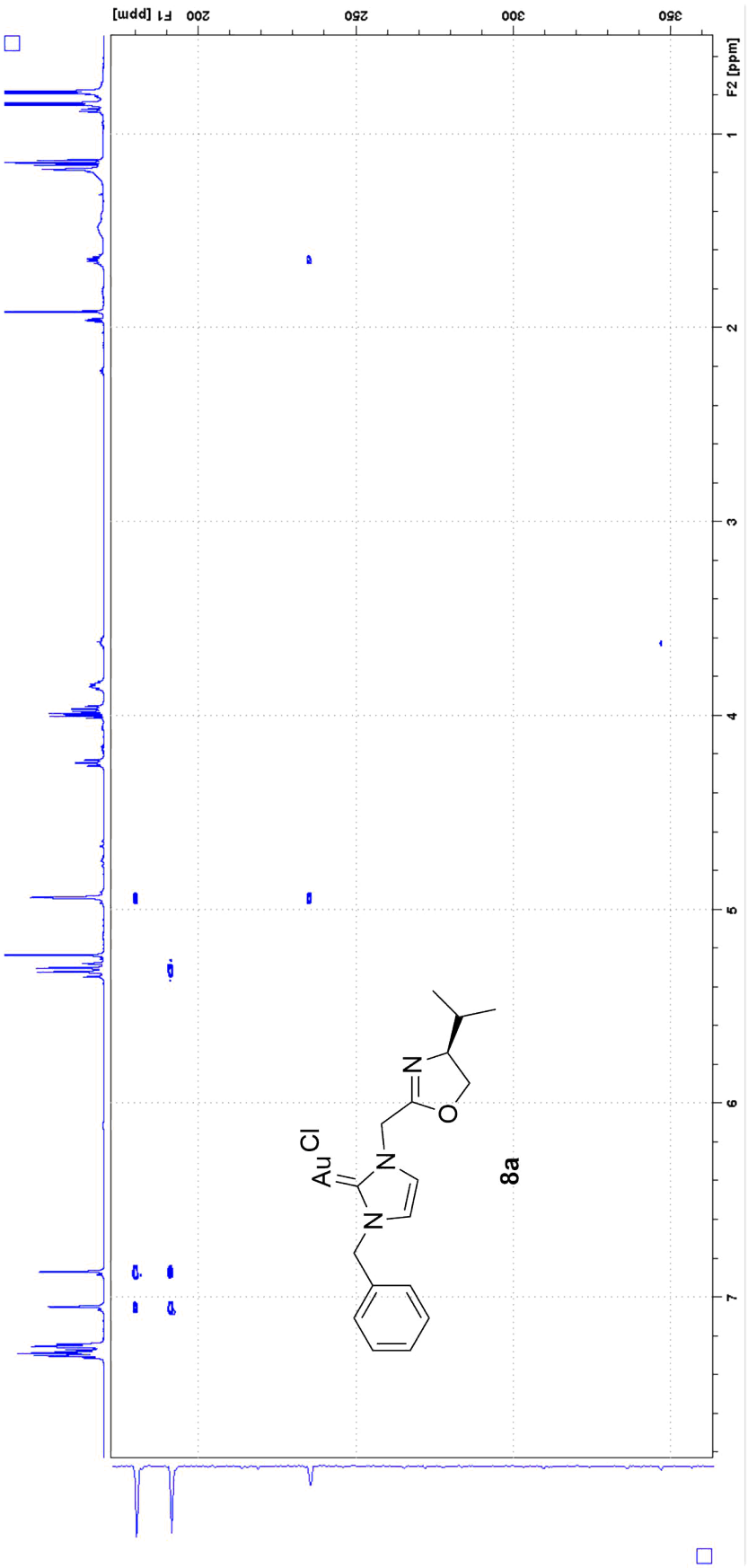

HRMS of Au(I)-complex 8a

Elemental Composition Report **Page 1**

Single Mass Analysis
Tolerance = 2.0 PPM / DBE: min = -5.0, max = 50.0
Element prediction: Off
Number of isotope peaks used for i-FIT = 3

Monoisotopic Mass, Even Electron Ions
265 formula(e) evaluated with 1 results within limits (all results (up to 1000) for each mass)
Elements Used:
C: 0-100 H: 0-100 N: 0-5 O: 0-2 Au: 0-3

2020 149 253 (2.357) AM2 (Ar,35000.0,0.00,0.00); Cm (244:263)
1: TOF MS ES+

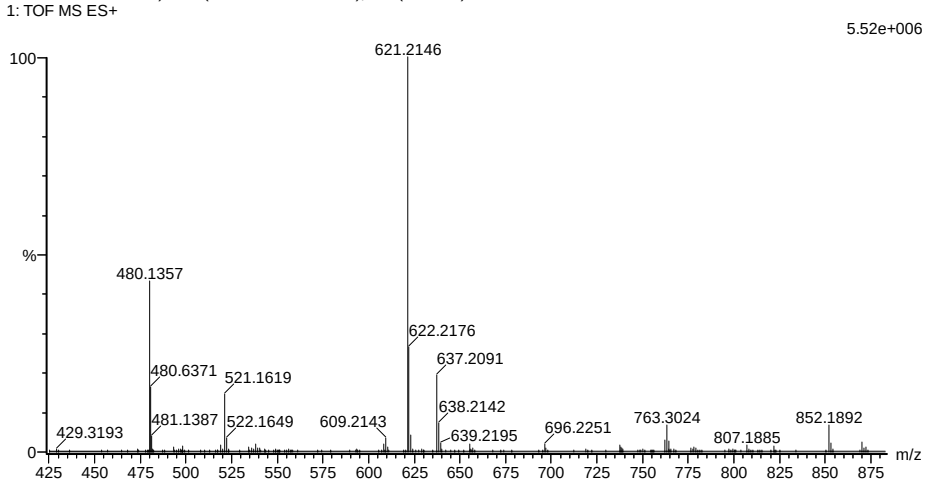

Minimum:				-5.0				
Maximum:		5.0	2.0	50.0				
Mass	Calc. Mass	mDa	PPM	DBE	i-FIT	Norm	Conf(%)	Formula
521.1619	521.1616	0.3	0.6	10.5	878.2	n/a	n/a	C19 H24 N4 O Au

IR of Au(I)-complex 8a

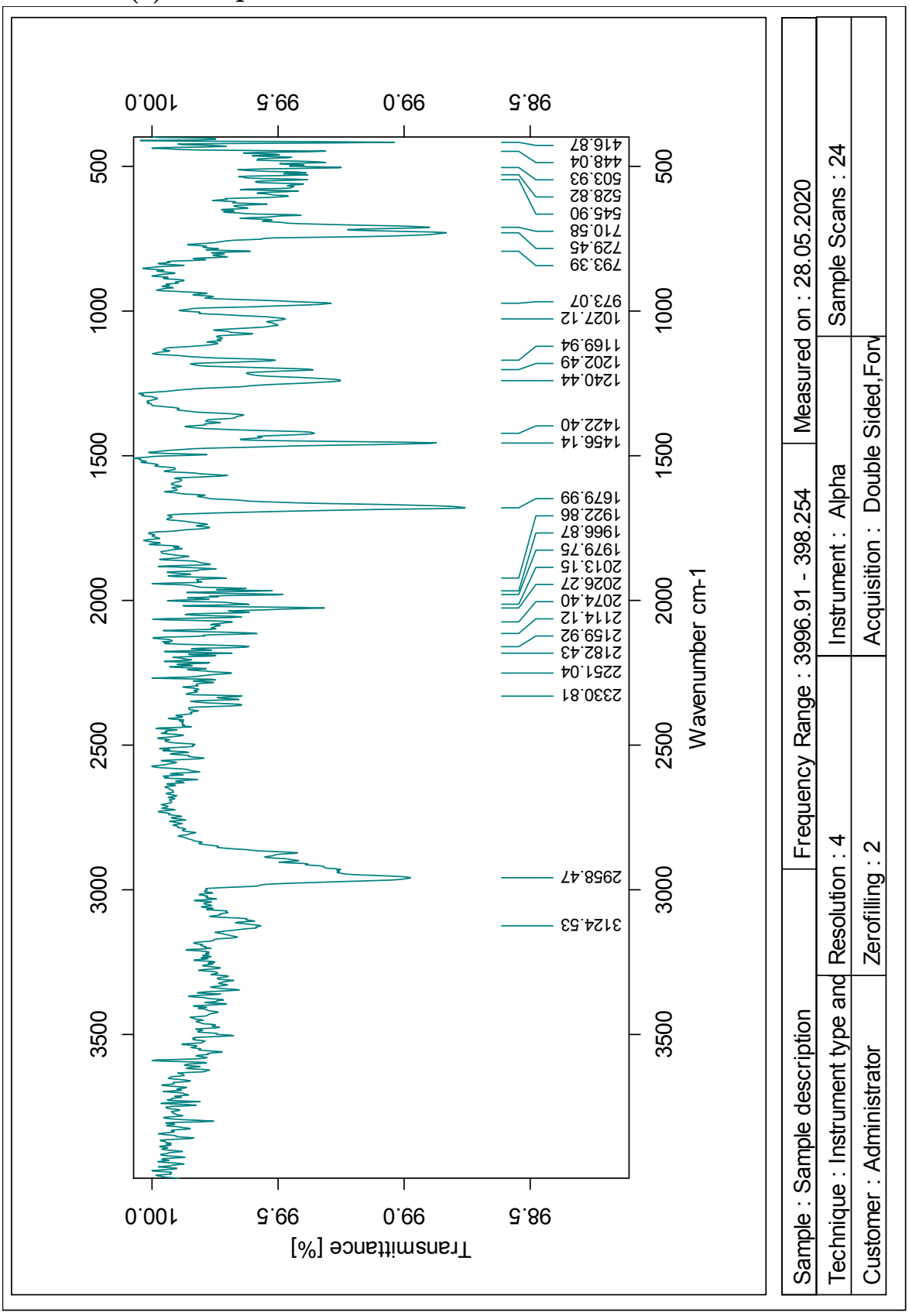

^{1}H-NMR of Au(I)-Complex 8b

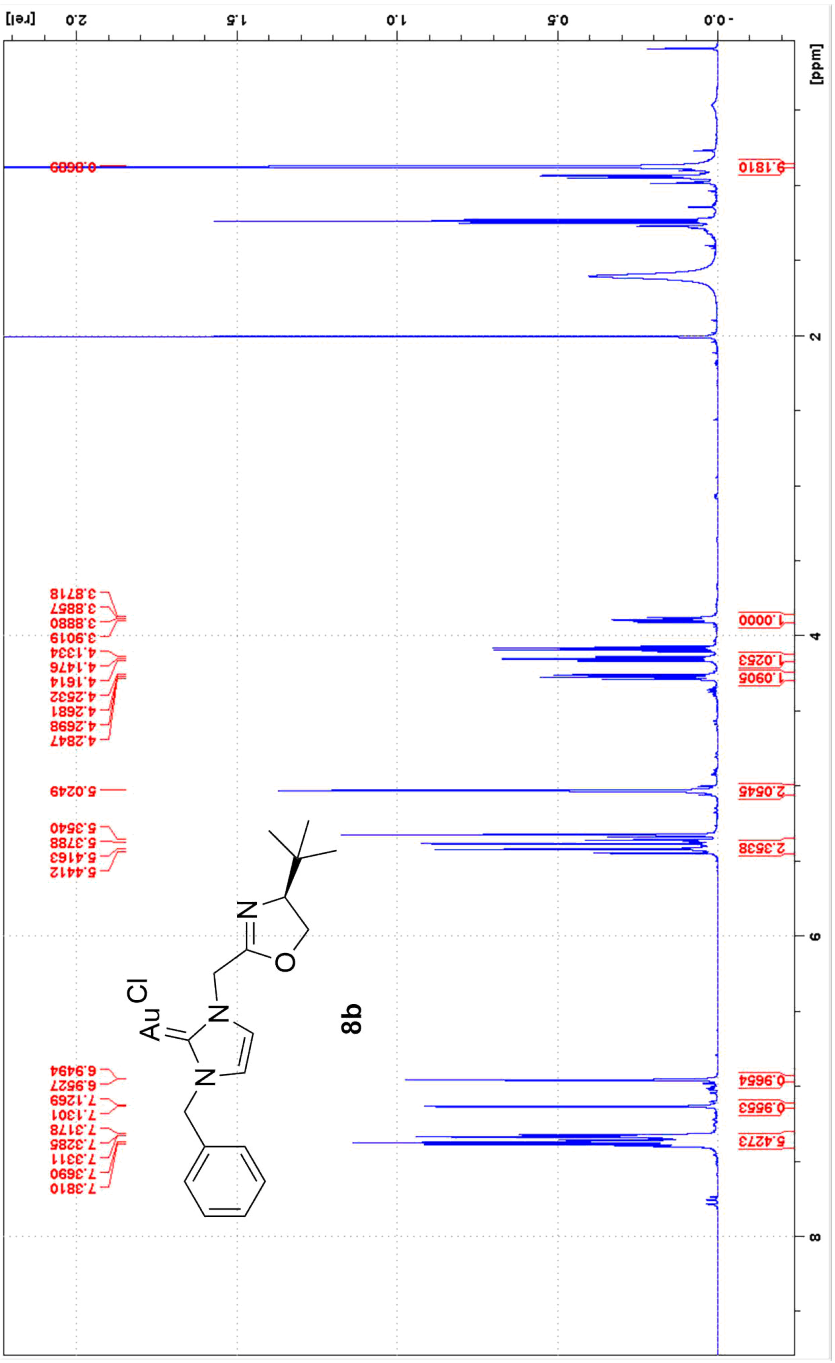

^{13}C-NMR of Au(I)-Complex 8b

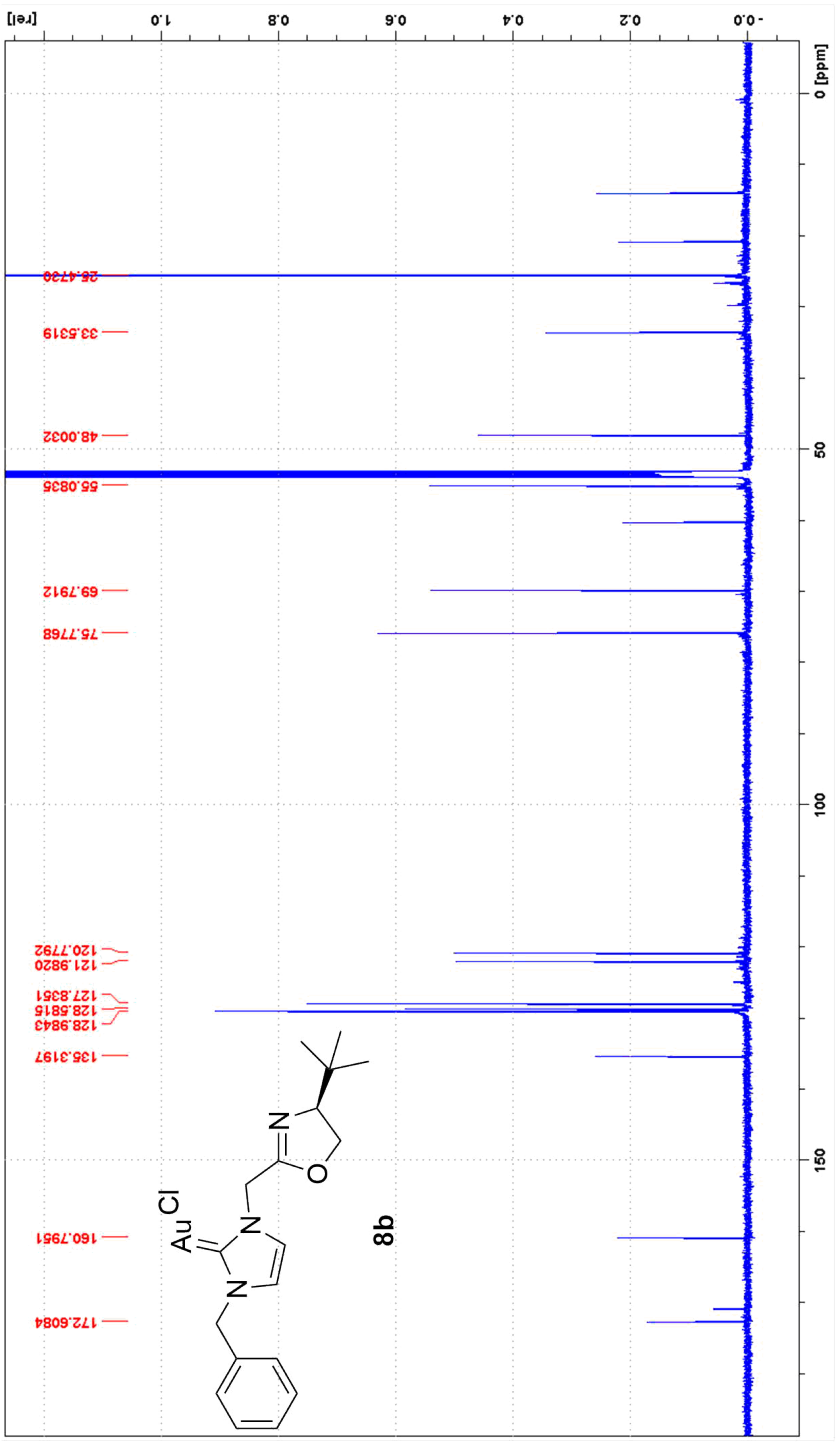

COSY of Au(I)-Complex 8b

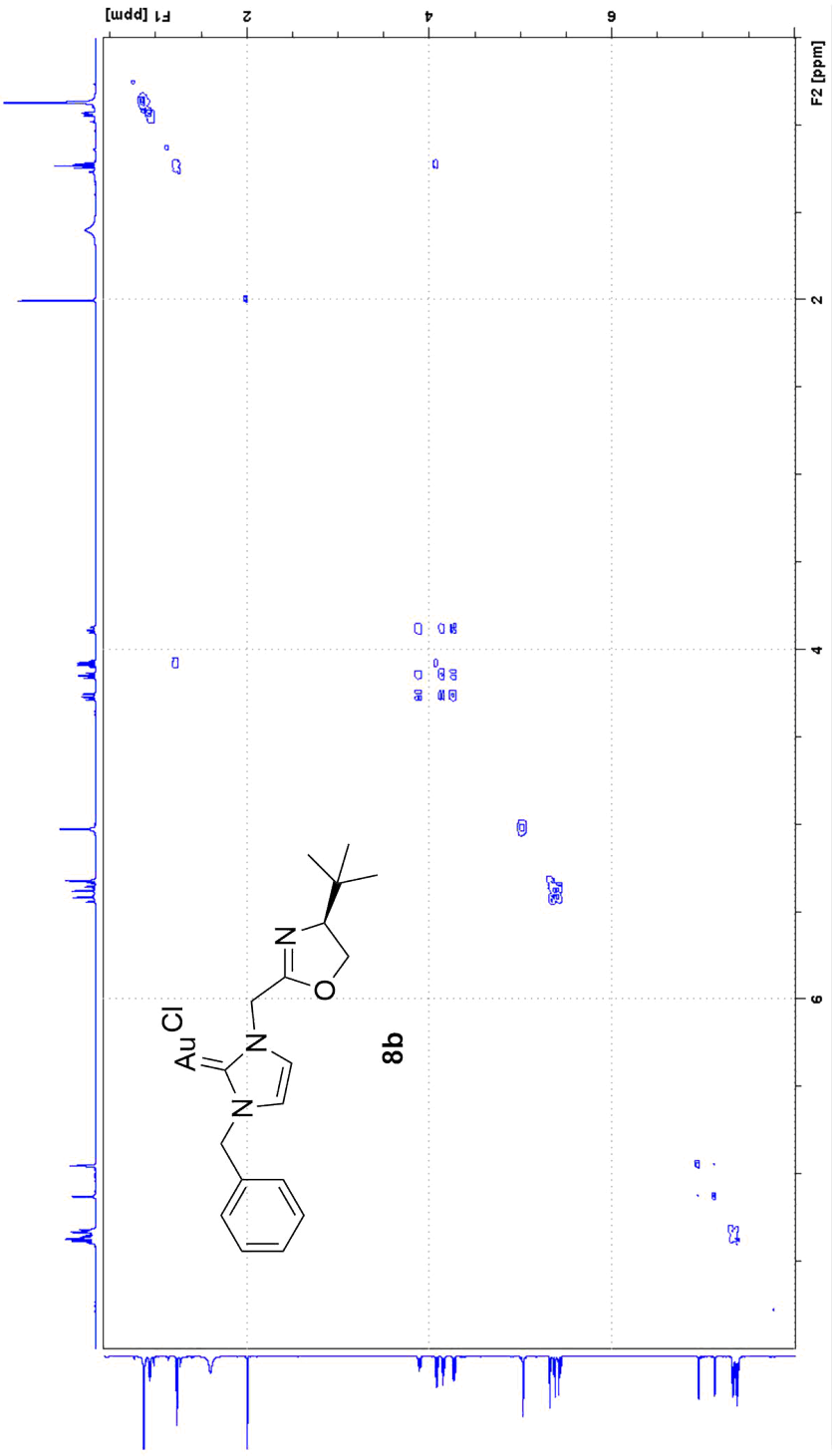

HSQC of Au(I)-Complex 8b

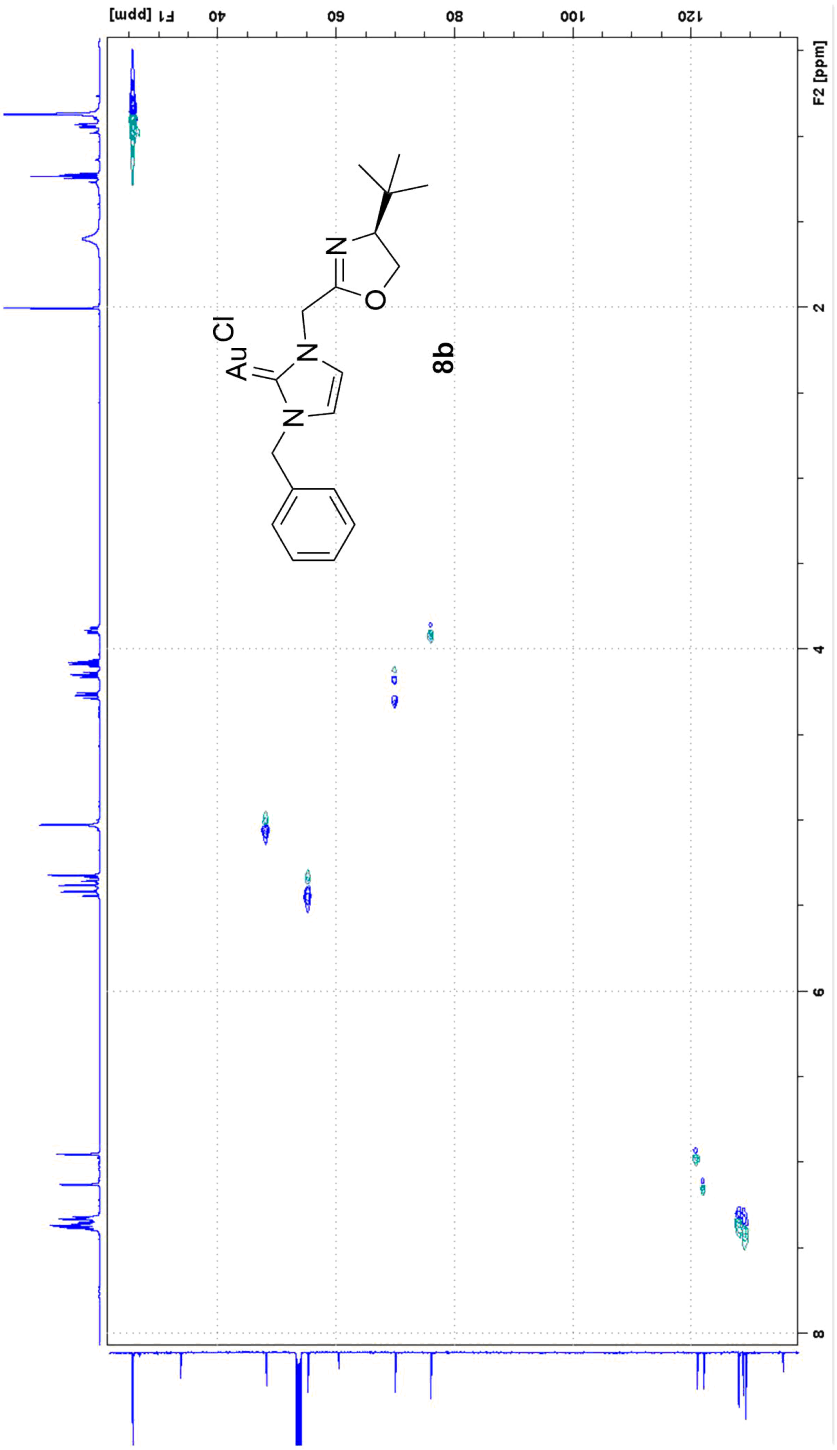

^{1}H,^{13}C-HMBC of Au(I)-Complex 8b

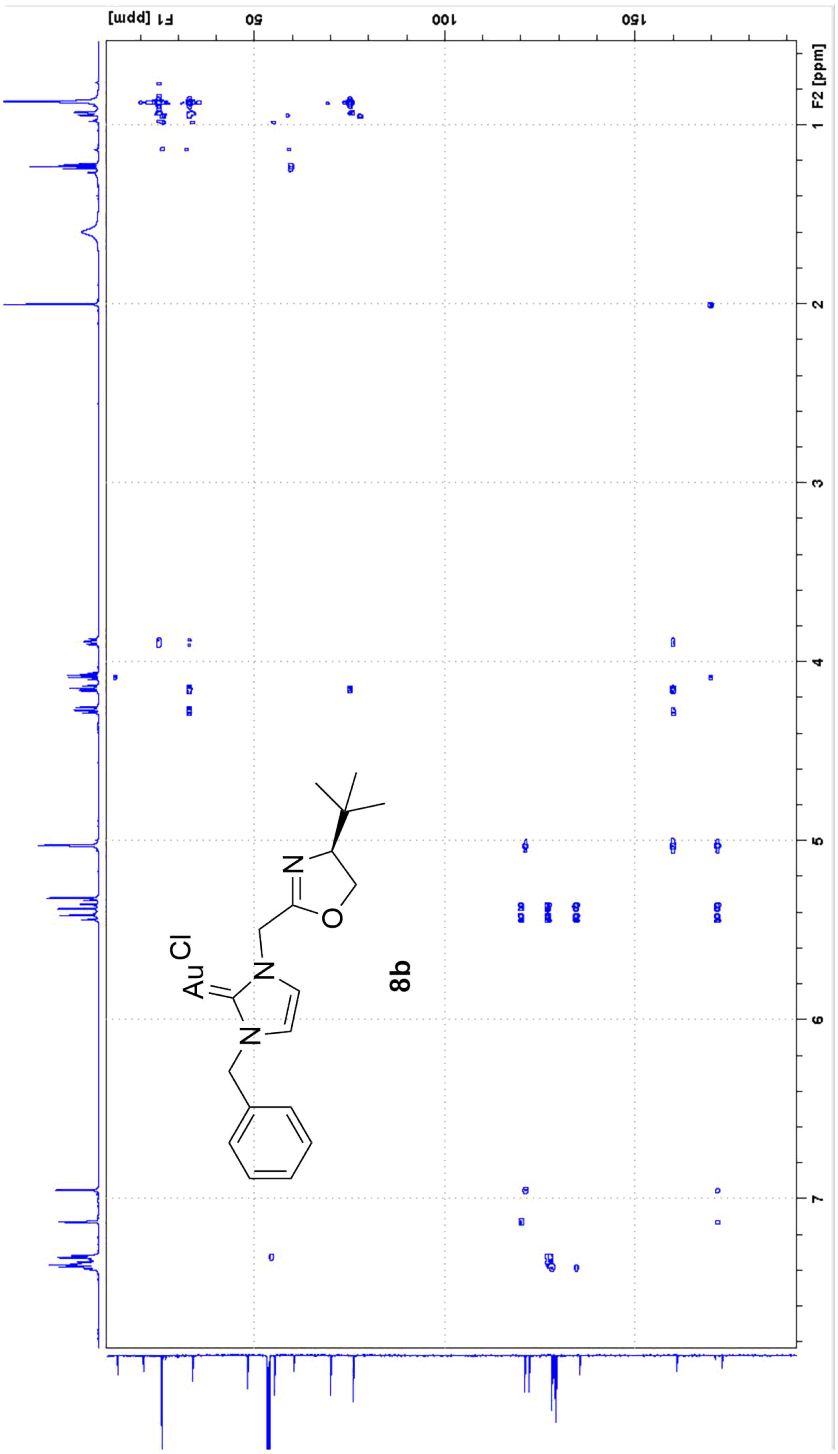

^{1}H,^{15}N-HMBC of Au(I)-Complex 8b

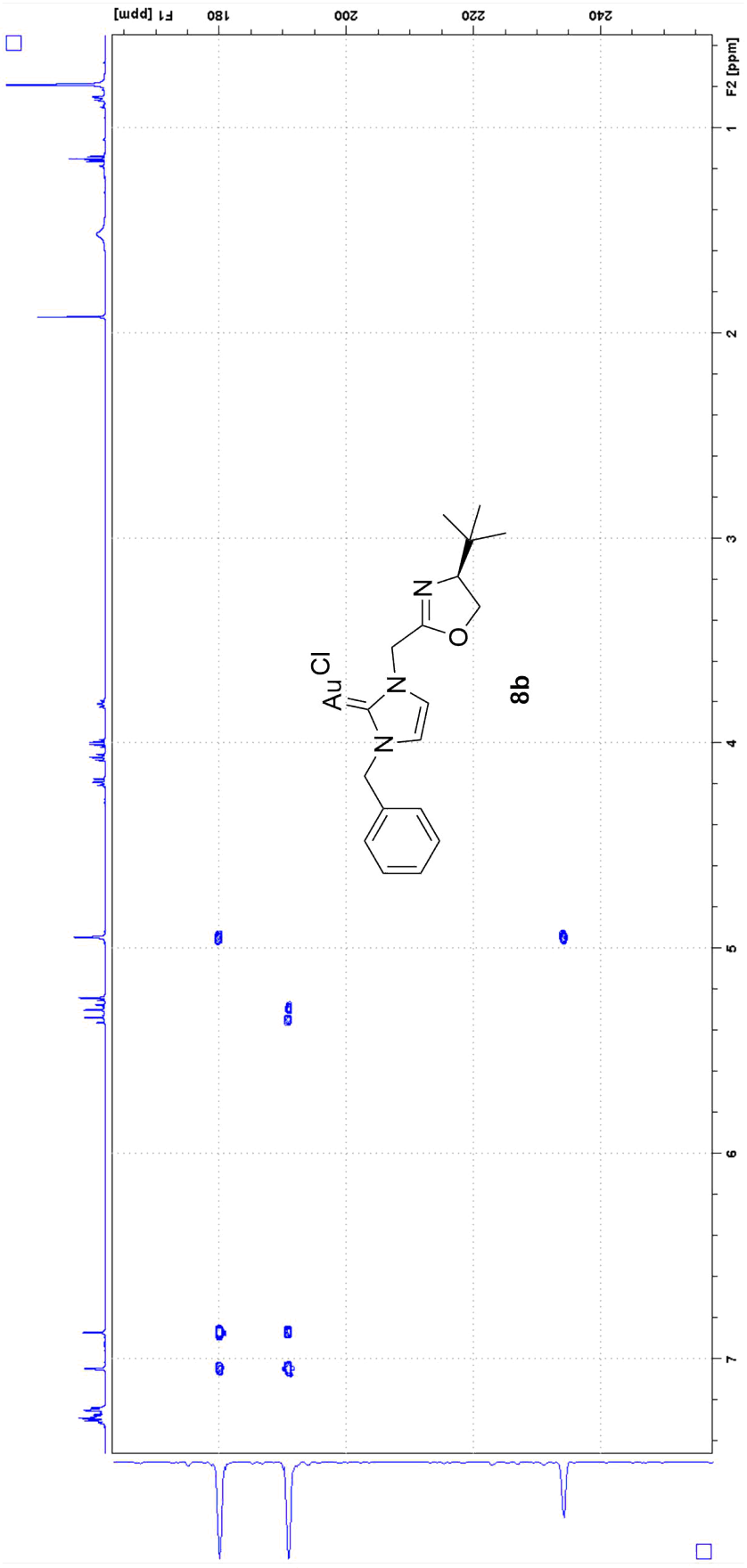

HRMS of Au(I)-complex 8b

Elemental Composition Report **Page 1**

Single Mass Analysis
Tolerance = 2.0 PPM / DBE: min = -5.0, max = 50.0
Element prediction: Off
Number of isotope peaks used for i-FIT = 3

Monoisotopic Mass, Even Electron Ions
274 formula(e) evaluated with 1 results within limits (all results (up to 1000) for each mass)
Elements Used:
C: 0-100 H: 0-100 N: 0-5 O: 0-2 Au: 0-3

2020 148 73 (0.700) AM2 (Ar,35000.0,0.00,0.00); Cm (67:73)
1: TOF MS ES+

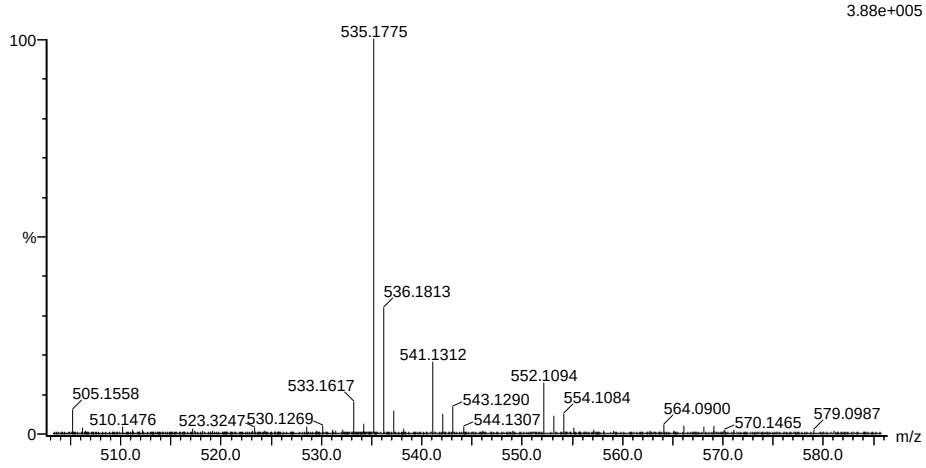

Minimum:				-5.0				
Maximum:		5.0	2.0	50.0				
Mass	Calc. Mass	mDa	PPM	DBE	i-FIT	Norm	Conf(%)	Formula
535.1775	535.1772	0.3	0.6	10.5	832.5	n/a	n/a	C20 H26 N4 O Au

IR of Au(I)-complex 8b

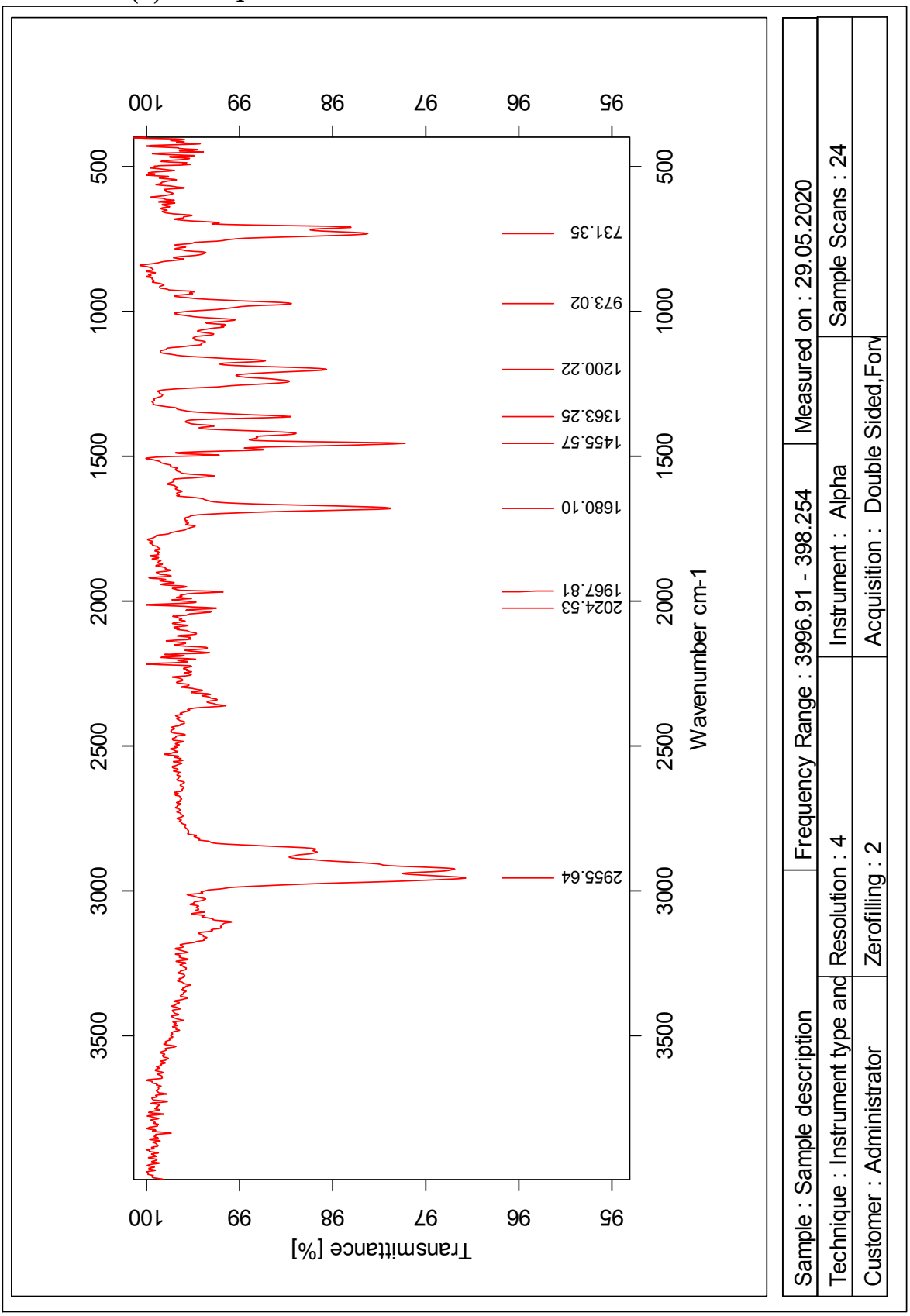

E Spectra of Au(III)[C_3]-complexes 10a, 10b

^{1}H-NMR of Au(III)NHC[Cl_3]-Complex 10a

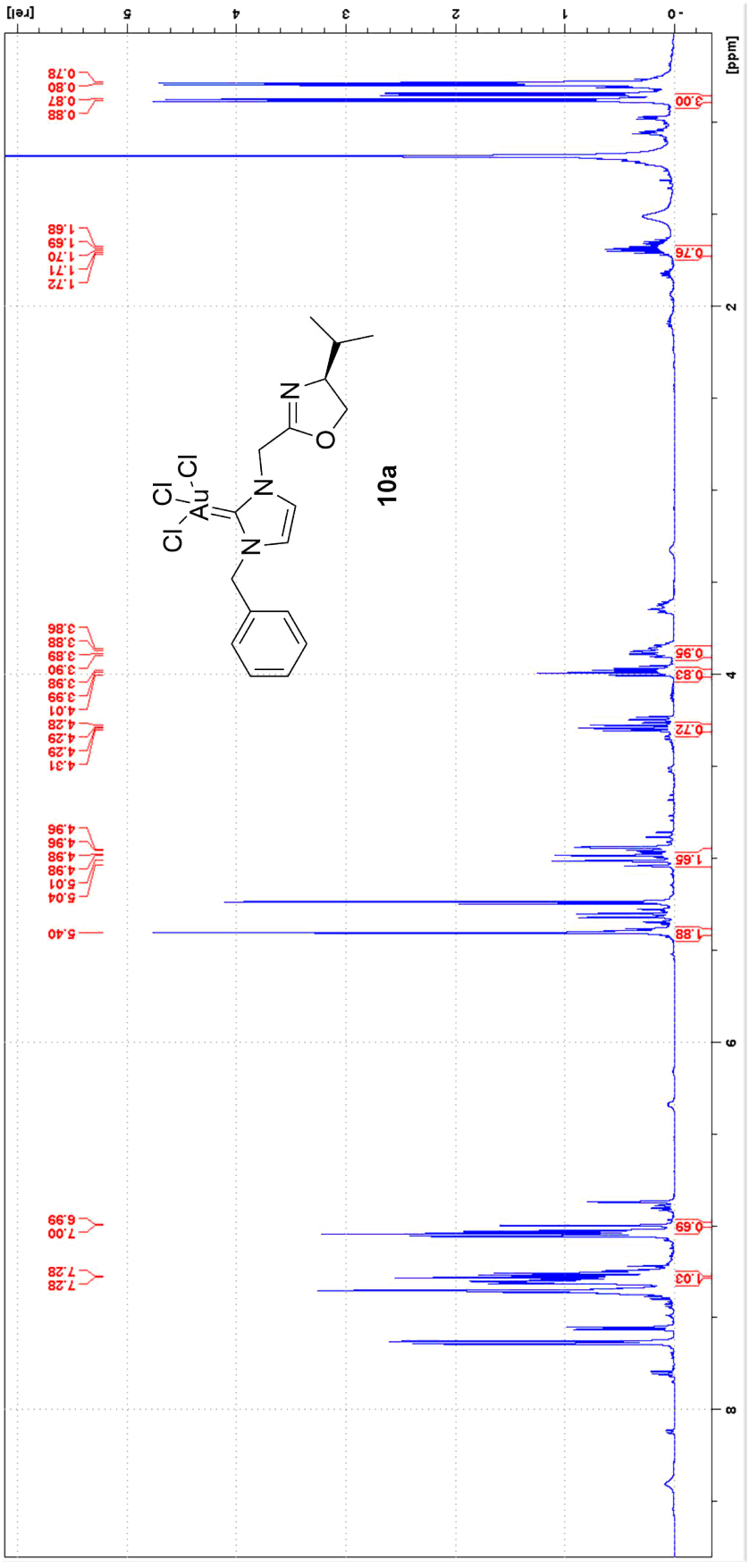

^{1}H,^{15}N-HMBC of Au(III)NHC[Cl_3-Complex 10a

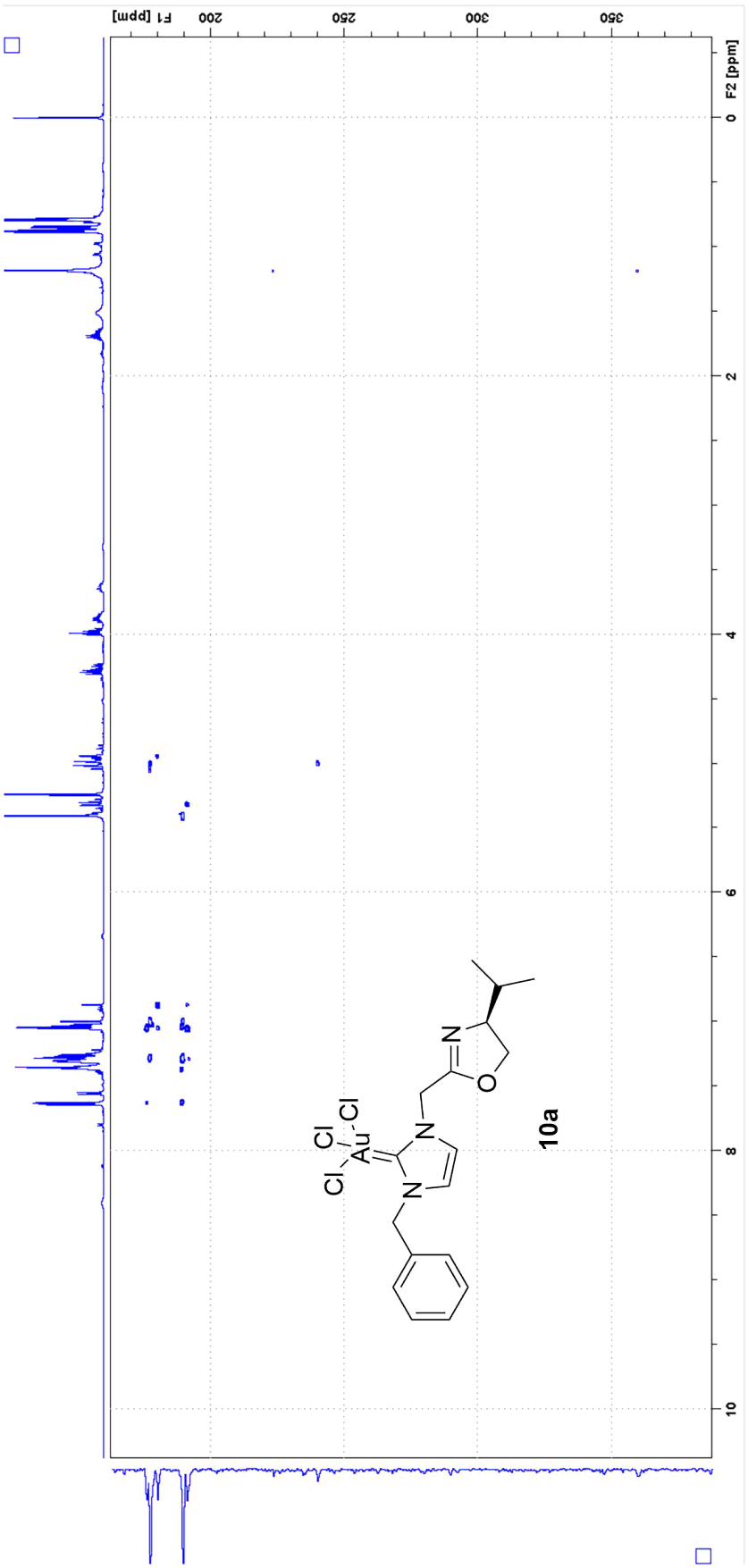

^{1}H-NMR of Au(III)NHC[Cl_3]-Complex 10b

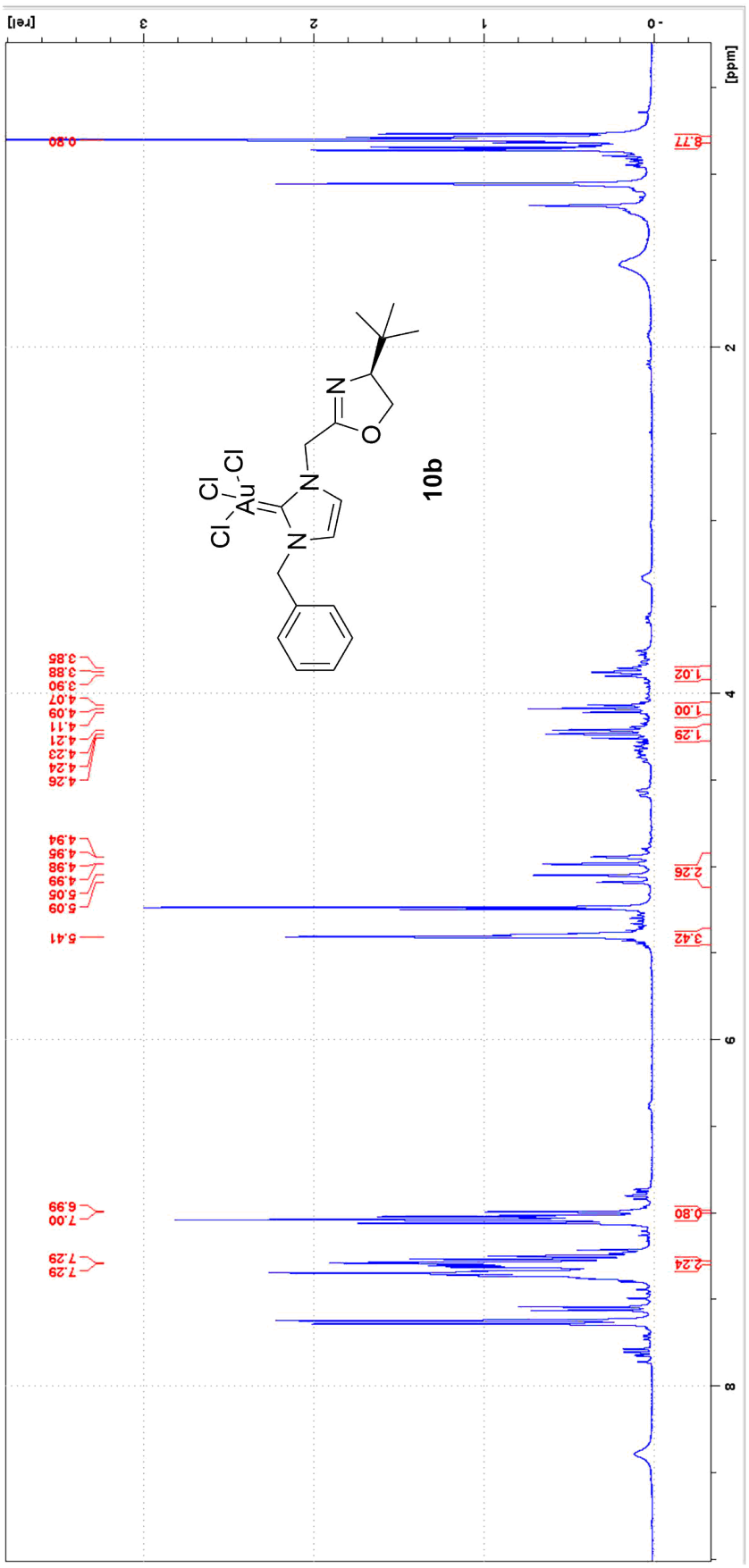

^{1}H,^{15}N-HMBC of Au(III)NHC[Cl_3-Complex 10b

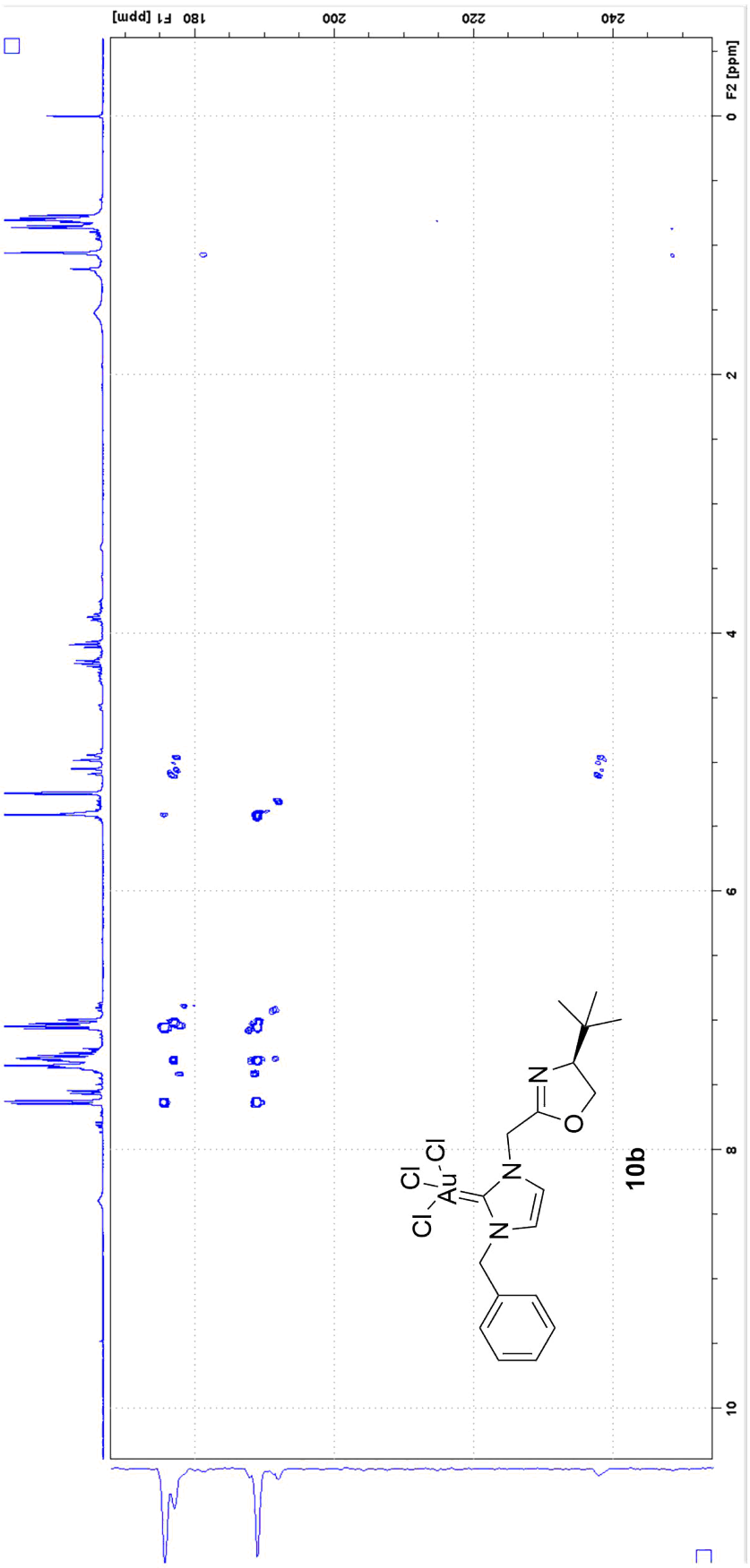

F Spectra of Bidentate C,N-Au(III)NHC[Cl_3 complexes 11a, 11b

^{1}H-NMR of Bidentate C,N-Au(III)NHC[Cl_3 complexes 11a

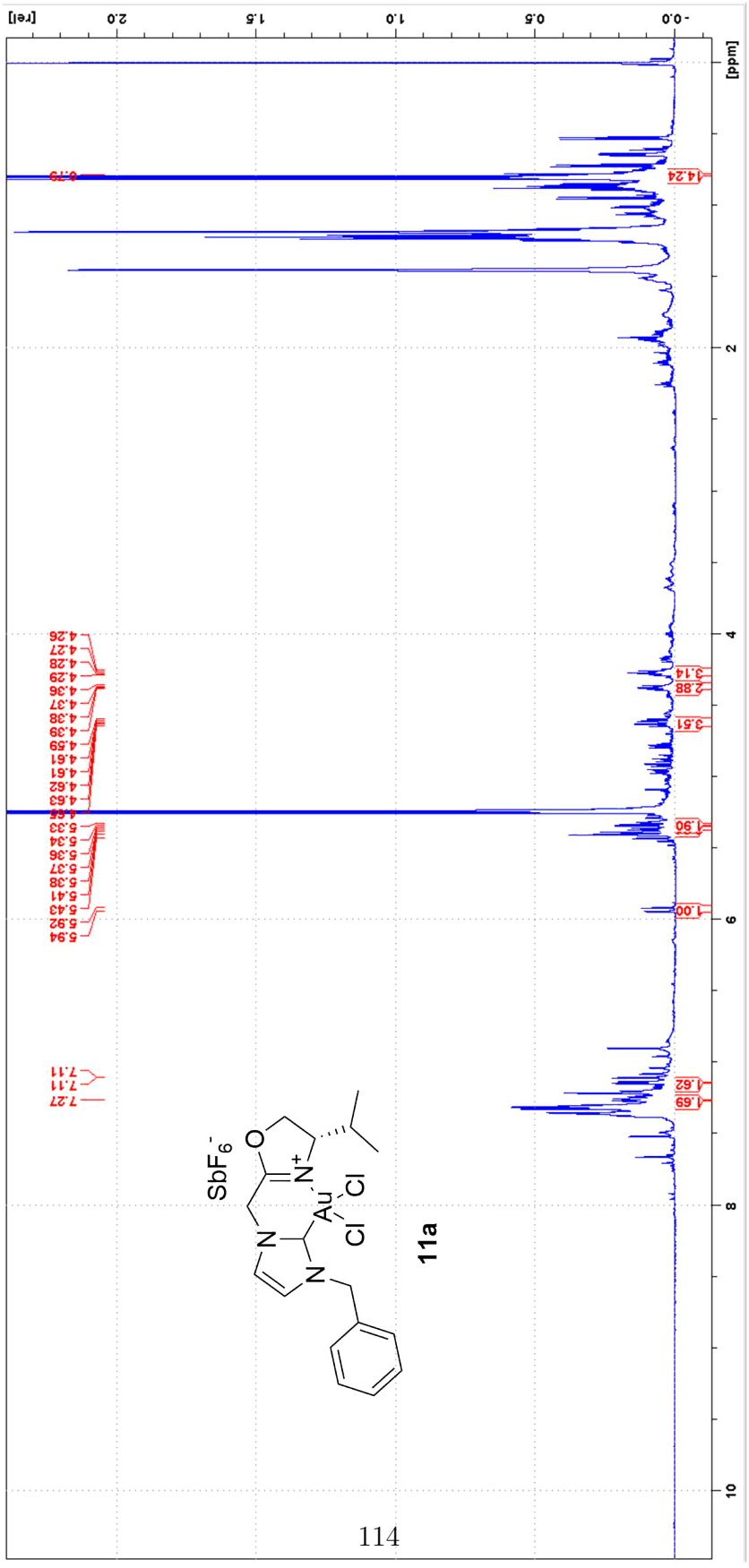

^{1}H,^{15}N-HMBC of Bidentate C,N-Au(III)NHC[Cl$_3$ complexes 11a

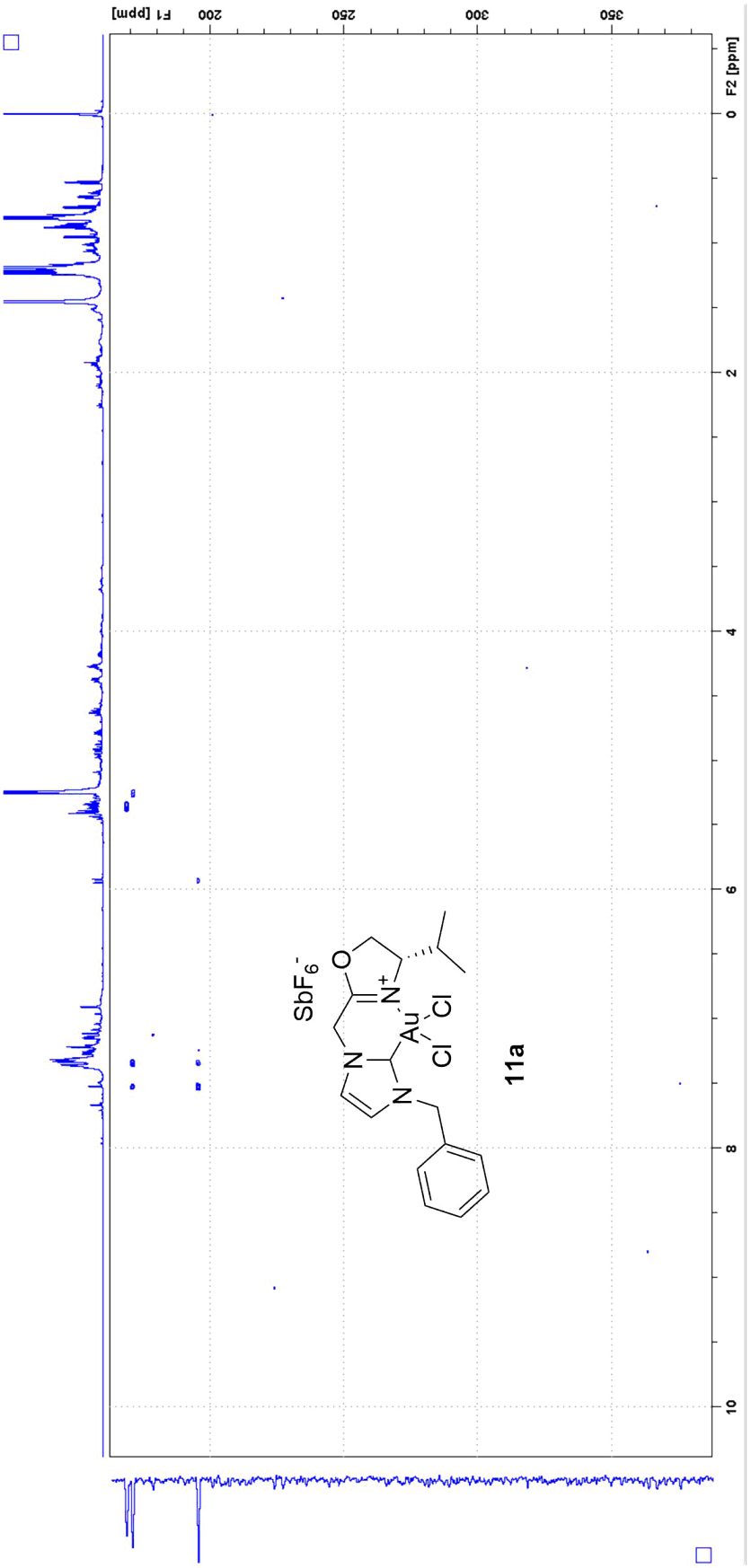

^{1}H-NMR of Bidentate C,N-Au(III)NHC[Cl$_3$ complexes 11b

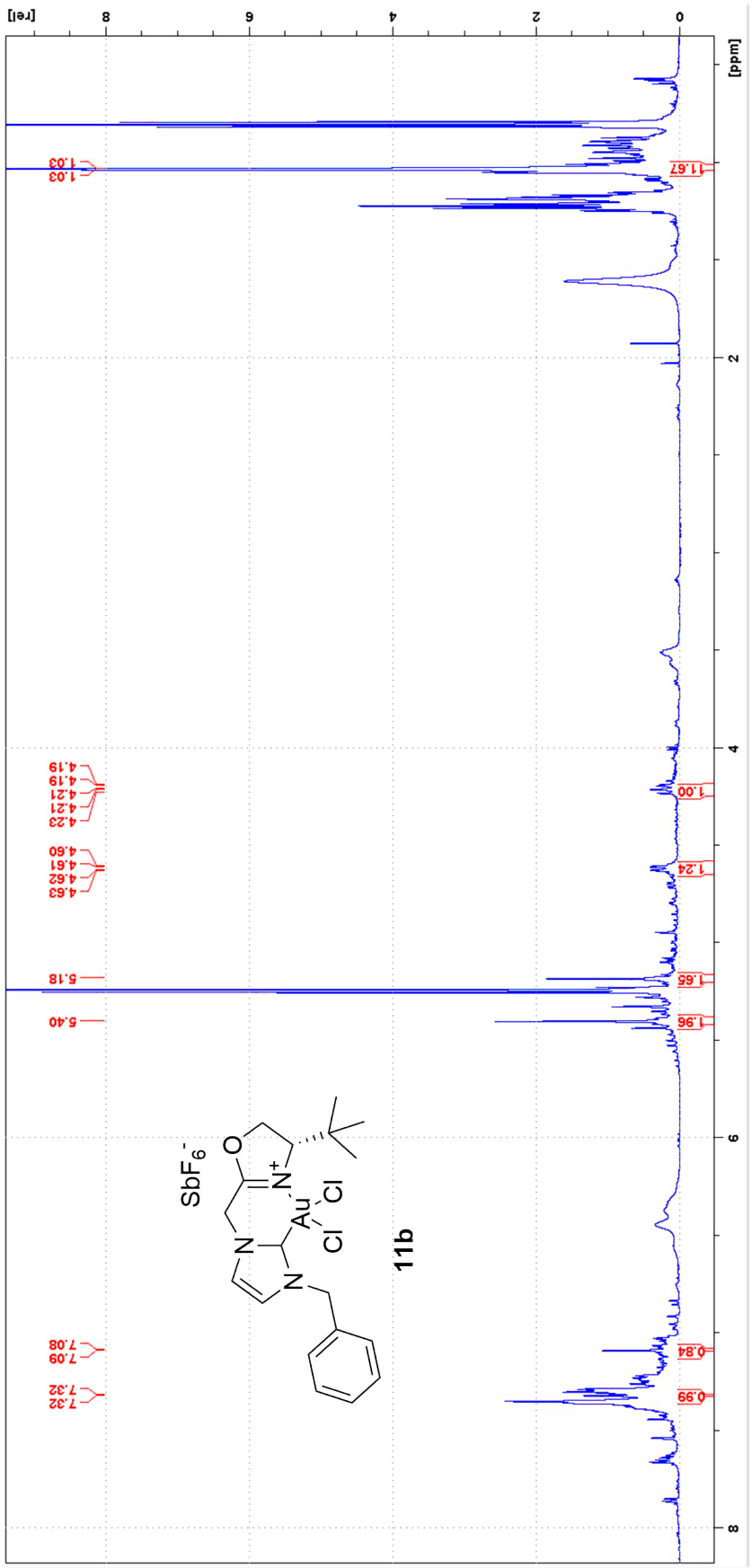

^{1}H,^{15}N-HMBC of Bidentate C,N-Au(III)NHC[Cl$_3$ complexes 11b

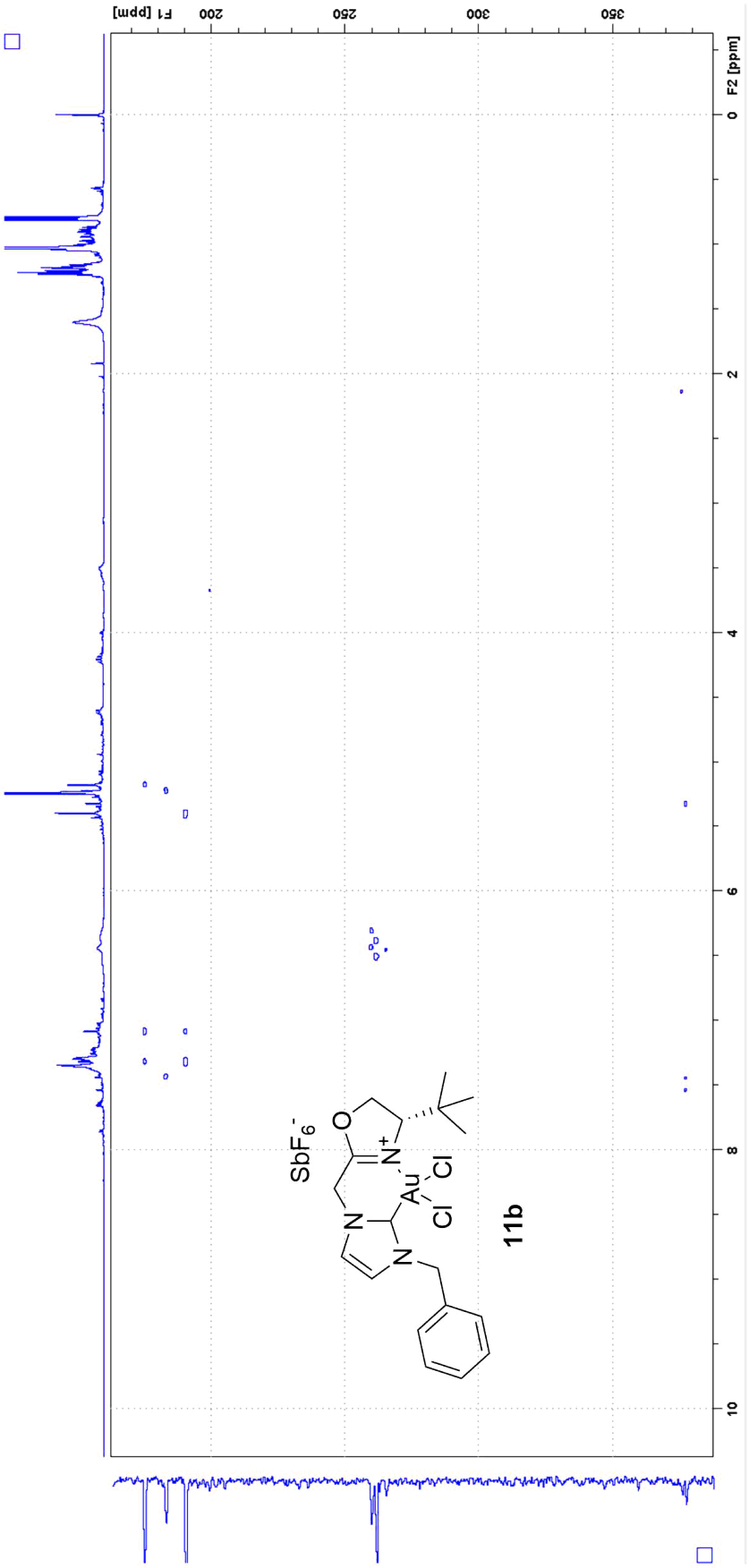

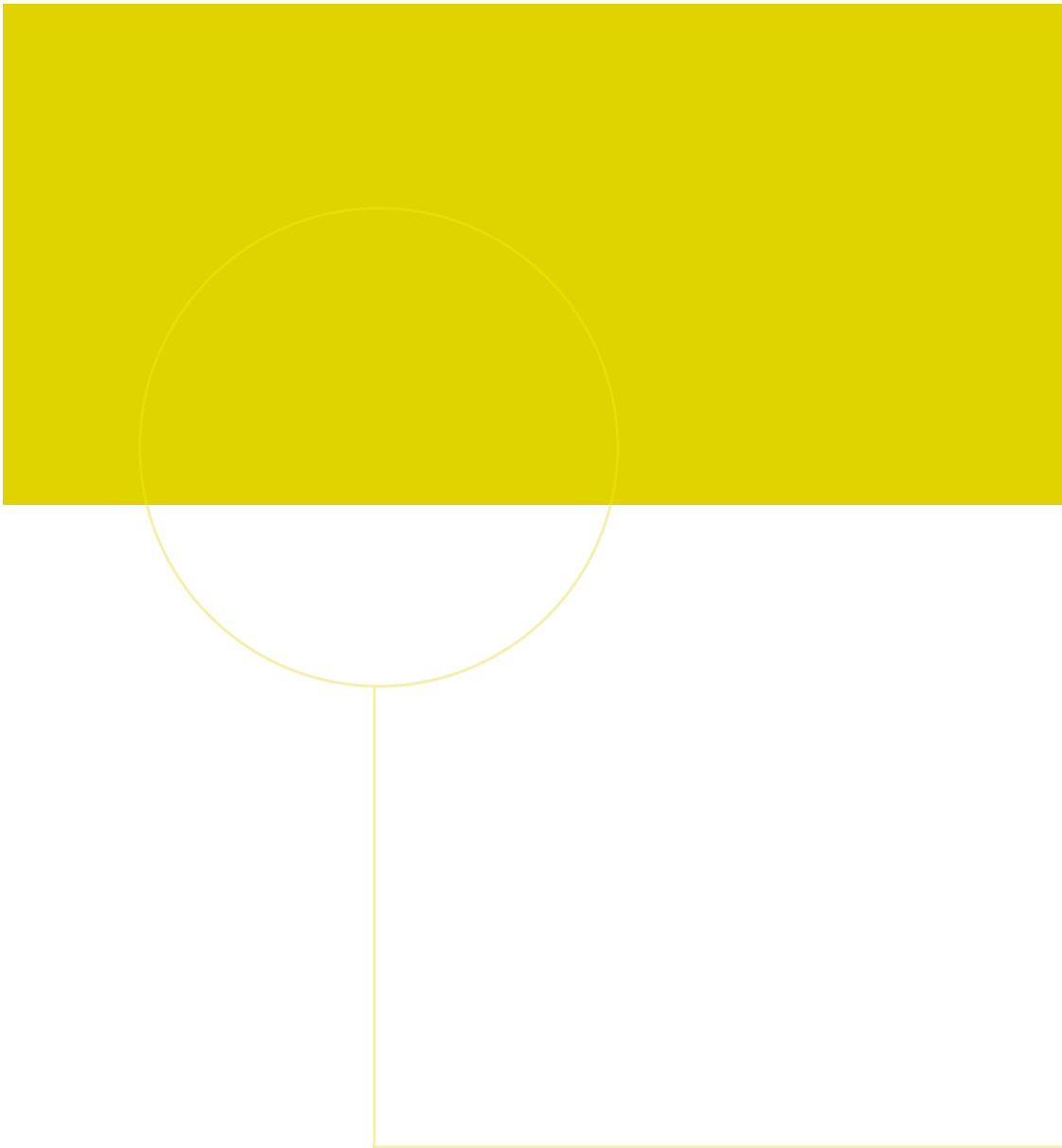

NTNU

Kunnskap for en bedre verden